

# Exploring Human-AI Collaboration in E-Textile Design: A Case Study on Flex Sensor Placement for Shoulder Motion Detection

ZHUCHENYANG LIU\*, Aalto University, Finland

YAO ZHANG\*, Aalto University, Finland

YALAN HE, Fudan University, China

HILLA PAASIO, Aalto University, Finland

CHANGYI LI, Aalto University, Finland

GUNA SEMJONOVA, Riga Stradins University, Latvia

YU XIAO, Aalto University, Finland

Flex sensors are widely used in e-textiles for detecting joint motions and, subsequently, full-body movements. A critical initial step in utilizing these sensors is determining the optimal placement on the body to accurately capture human motions. This task requires a combination of expertise in fields such as anatomy, biomechanics, and textile design, which is seldom found in a single practitioner. Generative AI, such as Large Language Models (LLMs), has recently shown promise in facilitating design. However, to our knowledge, the extent to which LLMs can aid in the e-textile design process remains largely unexplored in the literature. To address this open question, we conducted a case study focusing on shoulder motion detection using flex sensors. We enlisted three human designers to participate in an experiment involving human-AI collaborative design. We examined design efficiency across three scenarios: designs produced by LLMs alone, by humans alone, and through collaboration between LLMs and human designers. Our quantitative and qualitative analyses revealed an intriguing relationship between expertise and outcomes: the least experienced human designer achieved continuous improvement through collaboration, ultimately matching the best performance achieved by humans alone, whereas the most experienced human designer experienced a decline in performance. Additionally, the effectiveness of human-AI collaboration is affected by the granularity of feedback - incremental adjustments outperformed sweeping redesigns - and the level of abstraction, with observation-oriented feedback producing better outcomes than prescriptive anatomical directives. These findings offer valuable insights into the opportunities and challenges associated with human-AI collaborative e-textile design.

CCS Concepts: • **Human-centered computing** → **Empirical studies in HCI**; **User studies**; **Collaborative interaction**; **Empirical studies in ubiquitous and mobile computing**; • **Computing methodologies** → *Natural language processing*; Knowledge representation and reasoning; • **Computer systems organization** → **Sensors and actuators**.

Additional Key Words and Phrases: Electronic Textiles, Sensor Layout Design, Large Language Models, Human-AI Collaboration, Wearable Motion Capture

\*Both authors contributed equally to this research.

---

Authors' Contact Information: Zhuchenyang Liu, Aalto University, Espoo, Finland, zhuchenyang.liu@aalto.fi; Yao Zhang, Aalto University, Espoo, Finland; Yalan He, Fudan University, Shanghai, China; Hilla Paasio, Aalto University, Espoo, Finland; Changyi Li, Aalto University, Espoo, Finland; Guna Semjonova, Riga Stradins University, Riga, Latvia; Yu Xiao, Aalto University, Espoo, Finland.

---

Permission to make digital or hard copies of all or part of this work for personal or classroom use is granted without fee provided that copies are not made or distributed for profit or commercial advantage and that copies bear this notice and the full citation on the first page. Copyrights for components of this work owned by others than the author(s) must be honored. Abstracting with credit is permitted. To copy otherwise, or republish, to post on servers or to redistribute to lists, requires prior specific permission and/or a fee. Request permissions from [permissions@acm.org](mailto:permissions@acm.org).

*Conference acronym 'XX, Woodstock, NY*

© 2018 Copyright held by the owner/author(s). Publication rights licensed to ACM.

ACM ISBN 978-1-4503-XXXX-X/2018/06

<https://doi.org/XXXXXXX.XXXXXXX>

### ACM Reference Format:

Zhuchenyang Liu, Yao Zhang, Yalan He, Hilla Paasio, Changyi Li, Guna Semjonova, and Yu Xiao. 2018. Exploring Human-AI Collaboration in E-Textile Design: A Case Study on Flex Sensor Placement for Shoulder Motion Detection. In *Proceedings of Make sure to enter the correct conference title from your rights confirmation email (Conference acronym 'XX)*. ACM, New York, NY, USA, 78 pages. <https://doi.org/XXXXXXX.XXXXXXX>

## 1 Introduction

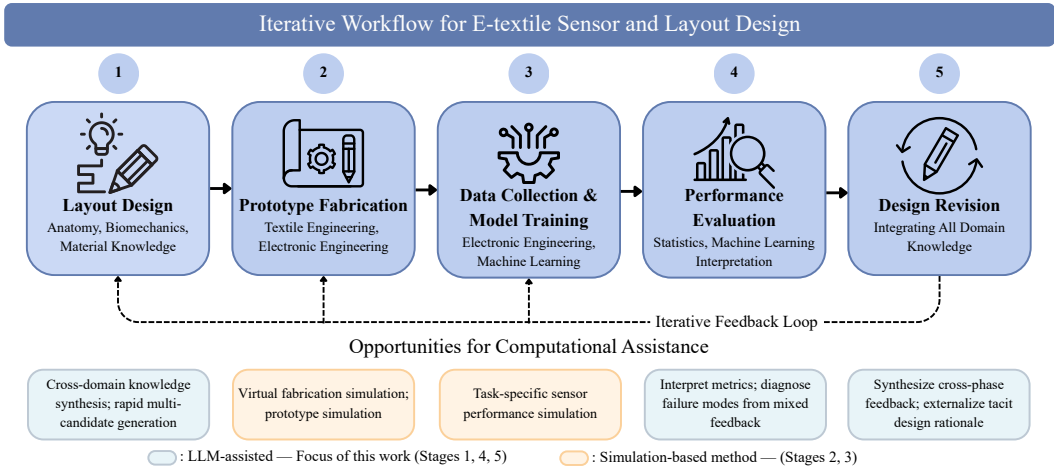


Fig. 1. Iterative design process of e-textile-based motion capture systems. Each phase is annotated with the domain knowledge it requires. Below the workflow, we map opportunities for AI assistance: LLM-based approaches (blue) can support Phases 1, 4, and 5, while simulation-driven approaches (orange) primarily address Phases 2 and 3. This work focuses on the LLM-assisted stages.

Electronic textiles (e-textiles) integrate sensing, computation, and communication directly into fabric, enabling unobtrusive monitoring of human physiology in everyday settings [12, 18, 30]. Among the sensing modalities employed in e-textiles, resistive flex sensors have become a popular choice for capturing joint motions and, by extension, full-body movements: bending a flex sensor along a limb or joint produces a resistance change proportional to the deflection angle, which can be mapped to joint kinematics through machine learning models [7, 20, 28]. Systems built on this principle have been used for hand gesture recognition [16], gait analysis [24], and upper-limb rehabilitation monitoring [5], demonstrating the breadth of applications that flex-sensor-based motion capture can address.

As shown in Fig 1, the design process for e-textile-based motion capture systems typically involves several iterative steps: designing the sensors and their layout on the human body, fabricating hardware prototypes, collecting sensor readings and corresponding motion measurements, training a prediction model, evaluating performance, and refining the design based on evaluation results [6, 19]. For each specific application, selecting sensor types is often straightforward. For instance, flex sensors are commonly utilized for detecting joint movements, while pressure sensors measure the force applied. Projects not focused on developing new sensor designs generally opt for commercially available or pre-evaluated sensors with clearly defined specifications such as sensitivity, sensing range, and resolution.

Given a selection of sensors, determining the optimal placement of sensors on the human body — known as *sensor layout design* [16, 29] — is a complex optimization challenge. The goal is to maximize

the information captured about target movements with a limited number of sensors. Effective sensor placement necessitates integrating knowledge from several fields, including anatomy (identifying which muscles and tendons are involved in the target motion), biomechanics (understanding skin deformation during movement), textile engineering (considering how fabric affects sensor-body coupling), and signal processing (mapping sensor signals to joint angles) [9, 10]. It is challenging for any designer to possess comprehensive expertise in all these areas. Typically, designers adopt a trial-and-error approach, iteratively improving the layout based on evaluation outcomes. This knowledge- and labor-intensive process has spurred efforts to introduce computational assistance to streamline and enhance the design process.

Simulation-driven approaches have made notable progress by enabling virtual prototyping through motion and/or sensor simulation, which reduces the cost of physical fabrication and evaluation [15, 16, 25, 26]. However, in these approaches the design proposals still originate from human designers; the simulation serves primarily to evaluate candidate layouts rather than to generate or refine them.

Large Language Models (LLMs) have recently demonstrated potential as cross-domain knowledge integrators in mechanical and physical design tasks [22, 23]. Their ability to synthesize information from various disciplines suggests they could be well-suited to the e-textile design workflow, particularly in sensor layout design. Nevertheless, how and to what extent LLMs can contribute to sensor layout design remains largely unexplored.

In this study, we aim to explore the opportunities and challenges associated with leveraging LLMs to assist in the e-textile design process, specifically focusing on sensor layout optimization. We selected shoulder motion detection as our case study due to the shoulder's complexity as a joint with three degrees of freedom. This choice reflects the shoulder's role as a representative and clinically significant case in previous e-textile design studies [13, 16, 25]. We engaged three human designers with varying levels of expertise in e-textile design – senior, intermediate, and junior – to participate in a user study aimed at addressing the following research questions:

**RQ1:** Can LLMs generate sensor layouts that match or surpass the quality of initial designs produced by human designers across different experience levels?

**RQ2:** When designs generated by LLMs are iteratively refined through human-AI collaboration, how does their quality compare to that of designs produced through a purely human-driven iterative process?

**RQ3:** How do the human designers' levels of experience, feedback strategies, and interaction patterns affect the effectiveness of human-AI collaboration in the iterative sensor layout optimisation process?

We assess design quality based on the motion detection accuracy attained by each design. The scientific contributions of this paper are threefold. First, we provide an empirical comparison of initial sensor layout designs generated by LLMs with those created by human designers, offering preliminary evidence of LLMs' capability to synthesize cross-disciplinary knowledge in physical design tasks. Second, we compare human-AI collaborative designs with those developed by human designers in subsequent design iterations. This study reveals an intriguing finding: the least experienced designer consistently improved the quality of the design through human-AI collaboration, eventually matching the highest performance achieved by participating human designers working without AI assistance. In contrast, the most experienced designer experienced a decline in final output quality when collaborating with AI. Third, through qualitative analysis, we identify two critical factors influencing the effectiveness of human-AI collaboration – *granularity of feedback* (incremental adjustments outperform sweeping redesigns) and *level of abstraction* (observation-oriented input yields better outcomes than prescriptive anatomical directives). These insights offer practical guidance for facilitating effective human-AI collaboration in design tasks.

## 2 Background and Related Works

This section provides the background and positions our work relative to existing literature.

### 2.1 Shoulder Motion Capture

As the most mobile and complex joint in the human body, the shoulder holds significant clinical importance, since shoulder pathologies are among the most common musculoskeletal conditions. The glenohumeral (GH) joint allows motion in three degrees of freedom through the coordinated action of four articulations [3, 32], producing highly heterogeneous skin deformation patterns across large, overlapping muscle groups with distinct fiber orientations [11, 13].

Current measurement tools for shoulder motion are limited to subjective clinical scales or lab-bound optical tracking systems [5, 31, 38]. E-textile-based motion capture offers a promising path toward continuous, ambulatory shoulder motion monitoring. However, significant challenges persist in optimally placing sensors on this anatomically complex region.

Recently, the shoulder has consequently emerged as the primary evaluation site in the simulation-driven e-textile design work closely related to this paper. For instance, Laytex [25] validated its layout generation tool with participants performing shoulder motions, while OptiSense [16] optimized strain sensor placement for shoulder angle prediction. Jin et al. [13] and Zhang et al. [36] developed textile sensor systems specifically targeting shoulder kinematics. By selecting the same body site, our case study allows for direct methodological comparison with these prior approaches while exploring a complementary axis of innovation – LLM-assisted sensor layout design.

### 2.2 LLMs in Physical Design and Sensing

LLMs have demonstrated emergent capabilities in reasoning about physical systems. Makatura et al. [22] evaluated LLMs on engineering design tasks and found that they can generate plausible design proposals by synthesizing information across disciplines, though they noted limitations in precise geometric reasoning. Mustapha et al. [23] surveyed LLM applications in engineering and highlighted their strength in integrating heterogeneous domain knowledge. In the Internet of Things domain, Xu et al. [33] showed that LLMs possess considerable proficiency in employing world knowledge to interpret IoT sensor data and reason about physical tasks, demonstrating their ability to bridge the gap between raw sensor signals and meaningful physical interpretation. Kaneko and Inoue [14] demonstrated that ChatGPT can suggest sensor locations for human activity recognition (HAR), achieving comparable classification accuracy with fewer sensors. Their study represents an initial exploration of LLMs for sensor placement, particularly focusing on inertial measurement unit (IMU)-based systems for classifying discrete activity categories using open datasets. In contrast, our case study extends beyond LLM-based design to evaluate the effectiveness of human-AI collaboration in the design process. Additionally, our research specifically targets the layout design of resistive flex sensors for continuous, fine-grained joint angle prediction.

### 2.3 Human-AI Collaborative Design

A growing body of work has examined how humans and AI systems collaborate in design tasks. In digital design domains, studies have explored human-AI co-creation in code generation [37], UI prototyping [17], and creative content production [27], identifying factors such as user trust, feedback modality, and the balance between directive and open-ended interaction as key determinants of collaboration quality. Gmeiner et al. [8] studied AI-assisted design in engineering contexts and found that overly prescriptive human input can suppress the complementary reasoning that makes AI assistance valuable, while observation-level feedback tends to enable more synergistic outcomes. Brynjolfsson et al. [2] reported that generative AI productivity gains among customer

support agents accrued primarily to novice workers, suggesting that AI can effectively disseminate expert-level knowledge to less experienced practitioners.

However, the majority of this work has focused on purely digital design tasks where iteration is fast and feedback is immediate. Physical design introduces embodied constraints—fabric behavior, body mechanics, sensor–surface coupling—that may be difficult for LLMs to reason about without direct physical experience [22]. Whether insights from digital human–AI collaboration transfer to physical prototyping contexts, and how expertise level mediates the effectiveness of such collaboration, remain open questions that our study aims to address.

### 3 User Study Design

This section describes the design of our case study. We first present the overall study protocol and explain how each phase addresses our research questions (§3.1). We then detail the technical implementation that supports the implementation of the protocol (§3.2), and finally describe participant recruitment (§3.3).

#### 3.1 User Study Protocol

To address our three research questions, we designed a within-subject user study in which three human designers each completed the same design task under different experimental conditions. The design task required placing  $k=4$  commercially available resistive flex sensors on a garment to predict three clinical shoulder joint angles (flexion/extension, abduction/adduction, and internal/external rotation). The number of sensors was limited to  $k=4$ , as this configuration offers a balanced trade-off between prediction accuracy and garment complexity for shoulder kinematics, as established in prior studies [16, 25]. Keeping  $k$  constant also ensures a fair comparison across all conditions; designers were not allowed to use fewer or more sensors.

The study comprised three sequential phases—*Onboarding*, *Experiment 1* (initial design comparison), and *Experiment 2* (iterative design refinement comparison)—structured to progressively address the research questions (Figure 2). In Experiment 1, we compare the achieved motion sensing performance of initial sensor layouts produced independently by the LLM and by each human designer, respectively, directly addressing **RQ1**. Experiment 2 involves two conditions for each human designer: the *H-Series* where the human designer iteratively refines their own initial design without AI assistance, and the *LH-Series*, where the human designer collaborates with the LLM to iteratively refine the LLM-generated initial design. Comparing the iteration trajectories between these two conditions addresses **RQ2**, while the records of structured feedback from human designers and human-AI interaction logs collected during the LH-Series provide the qualitative evidence needed to address **RQ3**.

The user study was conducted collaboratively by a researcher and a research assistant. To quickly validate the quality of the design, a test subject was recruited to immediately perform pre-defined shoulder movements while wearing a garment equipped with flex sensors arranged according to the layout design. The entire user study lasted approximately two hours per designer, encompassing all three phases.

**3.1.1 Onboarding (~20 min).** An onboarding session was conducted for each participating human designer prior to the start of the experiments. The session consisted of three parts. First, a *task briefing* presented the design challenge—placing  $k=4$  flex sensors on a garment to detect three clinical shoulder joint angles (flexion/extension, abduction/adduction, internal/external rotation)—along with physical constraints such as pre-selected sensor dimensions and attachment mechanisms. Second, a *metrics walkthrough* acquainted each participant with the performance dashboard, which

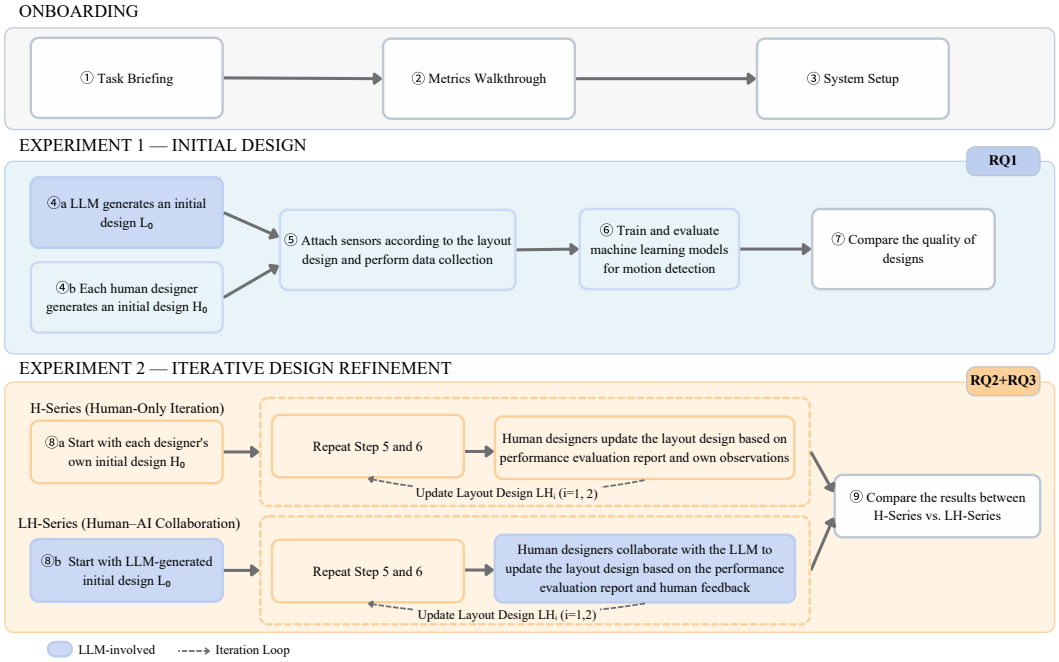


Fig. 2. Overview of the user study protocol. The study proceeds through three phases: Onboarding, Experiment 1 (initial design comparison, addressing RQ1), and Experiment 2 (iterative design refinement comparison across H-Series and LH-Series, addressing RQ2 and RQ3). Within Experiment 2, the H-Series (amber) follows a human-only iteration loop, while the LH-Series (blue) introduces human-AI collaborative design refinements.

displays the quantitative evaluation results of their designs. This includes the key performance indicator, Mean Per-Joint Angular Error (MPJAE), along with other metrics such as Pearson Correlation Coefficient and average mean percentage error. More details about these metrics are presented in Section 3.2.5. Human designers practiced reading a sample report of these metrics to confirm comprehension. Third, a *system calibration* step fitted the garment on a test subject, synchronized the sensor acquisition and reference tracking systems, and established a neutral-pose baseline.

**3.1.2 Experiment 1: Initial Design Comparison (~30 min per designer).** Experiment 1 was designed to address **RQ1**: *Can LLMs generate sensor layouts that match or surpass the quality of initial designs produced by human designers across different experience levels?*

We compared the quality of the four sensor layout designs:

- $L_0$  (LLM-created initial design): Generated prior to the workshop session via a divergent-convergent prompting strategy (detailed in §3.2.1), without any input from human designers.
- $H_0^A, H_0^B, H_0^C$  (Human designer created initial designs): Each human designer independently proposed a 4-sensor layout, drawing on their own domain knowledge. Designers received no information about  $L_0$  or each other's designs. They specified sensor locations using anatomical landmarks and garment reference points. The resulting layouts ( $H_0^A, H_0^B, H_0^C$ ) serve as initial designs from human designers in Experiment 1 and as starting points for the H-Series in Experiment 2.

**3.1.3 Experiment 2: Iterative Design Refinement and Comparison between H-Series and LH-Series (~2 hrs per human designer).** Experiment 2 was designed to address **RQ2** (*When designs generated by LLMs are iteratively refined through human-AI collaboration, how does their quality compare to that of designs produced through a purely human-driven iterative process?*) and **RQ3** (*How do the human designers' levels of experience, feedback strategies, and interaction patterns affect the effectiveness of human-AI collaboration in the iterative sensor layout optimisation process?*).

Each human designer completed the H-Series first, and then the LH-Series in Experiment 2. This fixed ordering was a practical constraint of our workshop format: the H-Series allowed designers to familiarize themselves with the evaluation pipeline before introducing the LLM-mediated component. Crucially, this ordering creates a *conservative test* for H-Series superiority: any knowledge gained during independent iteration could carry over to benefit LH-Series performance, meaning that if the H-Series still outperforms the LH-Series, the advantage is likely genuine. Conversely, LH-Series improvements should be interpreted with the caveat that designers had prior iteration experience. We return to this point when discussing the results of the experiment (§5.2).

*H-Series (Human-Only).* Starting from their own initial design ( $H_0$ ) produced in Experiment 1, each human designer independently refined the layout through up to two iteration cycles. In each cycle, the human designer: (1) inspected the deployed prototype and reviewed the performance evaluation report on the feedback dashboard (~10 min); (2) decided what to modify based on their own analysis and physically repositioned sensors on the garment (~5 min); and (3) ran another data collection and evaluation round (~10 min, covering data collection, model training, and performance metric computation). The human designer could stop early if satisfied with the result. This condition captures the conventional iterative design process driven entirely by human expertise.

*LH-Series (Human-AI Collaboration).* Starting with the LLM-generated initial layout design ( $L_0$ ), each human designer collaborated with LLMs (Figure 3) over two iteration cycles at most. In each cycle, the human designer: (1) inspected the deployed prototype and reviewed the performance evaluation report; (2) completed a structured feedback template, documenting both quantitative performance evaluation (e.g., identifying underperforming sensors) and personal observations (e.g., fabric bunching, poor fit), which was submitted to the LLM along with performance metrics (~10 min); (3) reviewed the LLM-generated refined layout design along with its explicit rationale, and then deployed and tested the refined layout (~10 min).

The layout design generated in each iteration in both Experiment 1 and 2 was evaluated following a consistent procedure which involved three steps: (1) the human designer attached sensors to the garment according to the specified layout (~ 5 minutes); (2) the test subject executed a predefined series of shoulder movements (~ 5 minutes); and (3) a machine learning model was trained from the collected sensor measurements and corresponding labels (i.e. ground-truth motion data extracted from video) to detect joint angles and the relevant performance indicators were calculated (~ 5 minutes). Each layout required roughly 30 minutes from deployment to evaluation. Since all four layouts were tested on the same subject performing identical motions using the same machine learning model architecture, any observed performance differences can be attributed to the layout design rather than external confounding factors. The technical implementation for rapid design evaluation will be presented in Section 3.2.2.

### 3.2 Technical Implementation

Figure 3 gives an overview of the technical implementation of the system needed for implementing the study protocol, including: *Initial Design Generation (Experiment 1)* (left), *Rapid Validation (Experiment 1 and 2)* (center) and *Feedback & Refinement (Experiment 2)* (right).

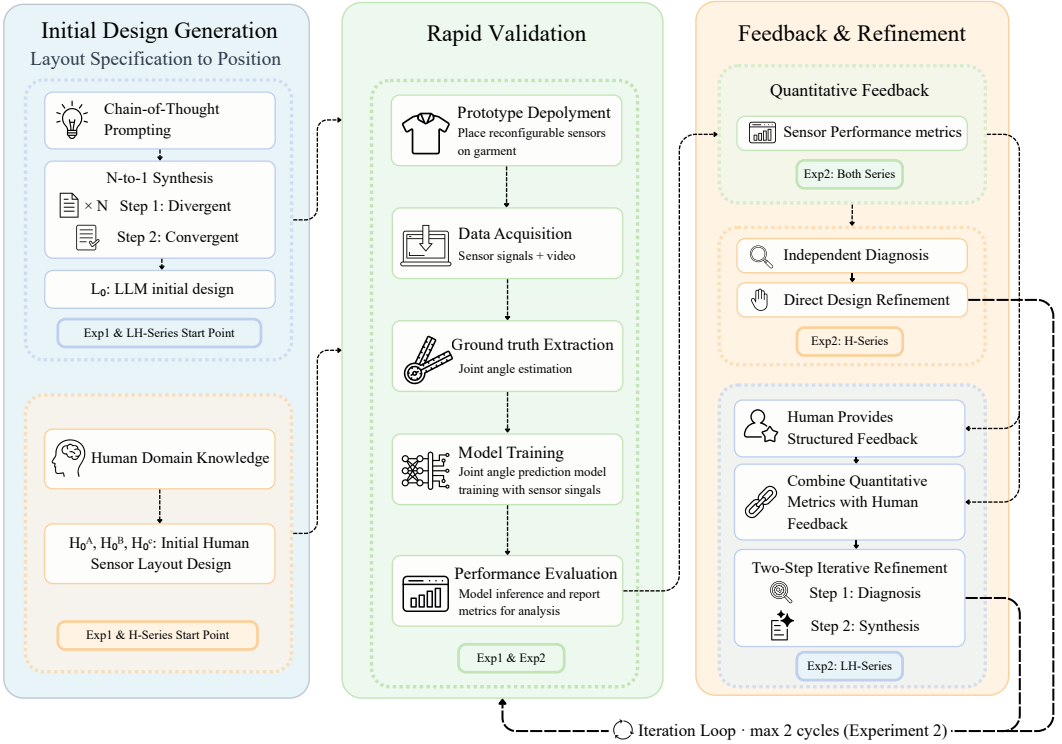


Fig. 3. Overview of the technical implementation: LLM-based N-to-1 synthesis (blue) produces  $L_0$  during Experiment 1. Within the Feedback & Refinement module, there are two pathways: human designer-only diagnosis and direct design refinement (amber; H-Series), and LLM-mediated two-step refinement informed by structured human feedback (blue; LH-Series). Dashed arrows indicate the iteration loop (up to two cycles). The Rapid Validation pipeline (green) is utilized for evaluating both initial designs and refined ones.

**3.2.1 LLM-driven Initial Design Generation.** We applied structured prompting to generate  $L_0$ . The output consisted of a specification detailing the positions of four flex sensors relative to anatomical landmarks. To mitigate single-generation randomness, we employed GPT-4 as the core reasoning engine with a divergent-convergent strategy. In the divergent phase, we generated five independent candidate proposals, each using chain-of-thought prompting. The following step repeated five times: Firstly, we elicited relative knowledge from LLM by itself with the prompt design shown in the Appendix: Figure 11. Secondly, LLM generated a design based on the knowledge following the prompt shown in Appendix: Figure 12. In the convergent phase, a meta-synthesis prompt filtered biomechanically implausible configurations and consolidated robust design principles into a unified initial layout ( $L_0$ ). The detailed prompt design is shown in Appendix: Figure 13.

**3.2.2 Rapid Validation.** The Rapid Validation pipeline translates each candidate sensor layout into a deployable prototype and produces a standardized performance evaluation within approximately 15 minutes per layout. As shown in Figure 3, this pipeline is shared identically across all experimental conditions, ensuring that any observed performance differences can be attributed to the layout design rather than to external confounding factors. The pipeline comprises five sequential stages: prototype deployment, data acquisition, ground-truth extraction, model training, and performance reporting. Below we describe each stage in detail.

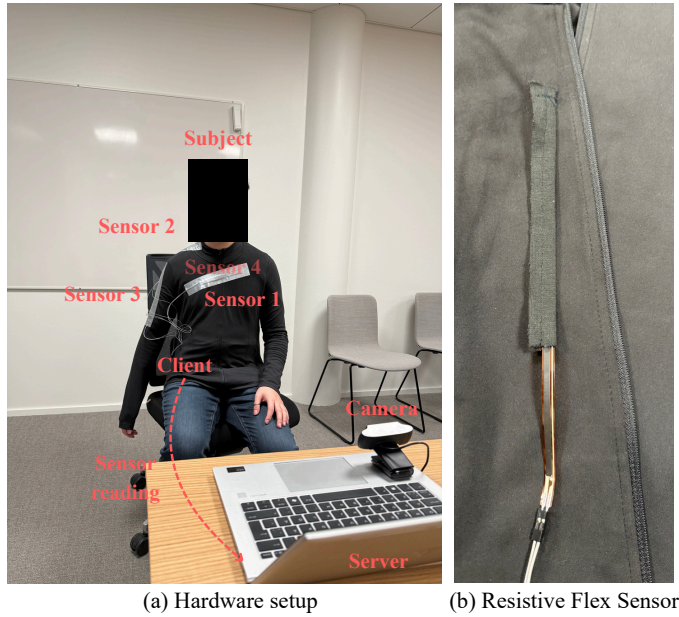


Fig. 4. Data collection setup. (a) Hardware overview: four resistive flex sensors are attached to a compression shirt worn by the subject; a client microcontroller reads the sensor signals and transmits them to a server laptop, while an RGB webcam captures reference video. (b) Close-up of a SpectraFlex™ flex sensor with a custom-fitted fabric container.

As shown in Fig. 4, the physical prototype consists of a tight-fitting compression shirt that conforms closely to the body surface, ensuring consistent sensor–skin coupling across postures. Four resistive SpectraFlex™ Flex Sensors<sup>1</sup> (95 mm active length, 10 k $\Omega$  nominal resistance) serve as the sensing elements. Resistive flex sensors were selected for their high signal stability and low drift over repeated bending cycles [28], which is critical for an iterative prototyping study. A custom-fitted fabric container was prepared for each sensor (Fig. 4(b)) to prevent direct contact between the sensor and the adhesive tape, avoiding residue buildup on the sensing surface and enabling rapid removal and reattachment across layout iterations. The containers were secured to the garment surface using elastic antistatic tape, pressing each sensor against the fabric to capture bending dynamics during motion. Given a layout specification, the four sensor containers can be attached to the designated positions on the garment in approximately five minutes.

**Data acquisition** Two data streams were recorded simultaneously during each evaluation: sensor readings and reference video. An Arduino-based acquisition board samples the four flex sensors at 40 Hz, while a single RGB webcam captures reference video at 60 fps (Fig. 4(a)). An online world clock provides a shared epoch-time reference to synchronize the two recording systems. Note that all raw data containing personally identifiable information—including video recordings of the motion participant and photographs of the garment during fitting—were destroyed after the relevant features (joint angles, sensor coordinates) had been extracted and anonymized. Only the derived, de-identified data are retained for analysis.

To ensure a fair comparison across layouts and conditions, the same data collection process was used in each iteration. This began with a neutral-pose calibration phase lasting 15 seconds.

<sup>1</sup><https://www.spectrasymbol.com/resistive-flex-sensors/spectraflex-flex-sensors>

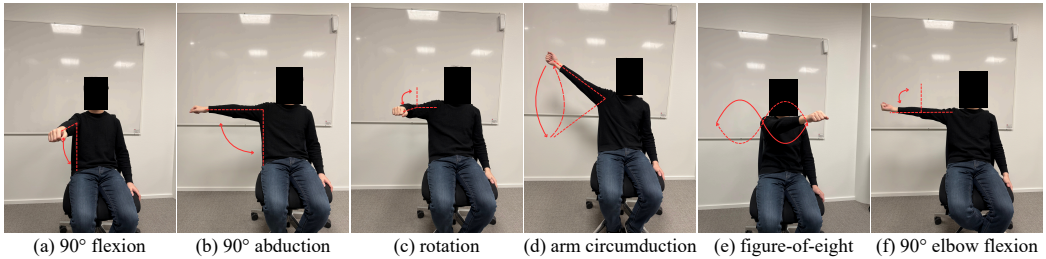


Fig. 5. Illustration of the six standardized motions used for performance evaluation.

Subsequently, a training set (~3 minutes) was gathered, consisting of six standardized motions adapted from the shoulder movement protocol defined by Qu et al. [25]—90° flexion, 90° abduction, internal–external rotation, arm circumduction, figure-of-eight, and 90° elbow flexion (Fig. 5)—, with each motion repeated five times. A separate test set (~45 s) used the same six motions performed once in reversed order for generalization assessment. The training set was used to fit the prediction model; the test set was utilized for generating reported performance metrics.

**Ground-truth extraction from video:** Raw video frames were processed through SMPLest-X [34], a foundation model for expressive human pose and shape estimation based on SMPL-X parametric fitting, to extract per-frame shoulder joint angles for three clinical degrees of freedom: flexion/extension, abduction/adduction, and internal/external rotation. The resulting pose sequences were further refined using SmoothNet [35], a temporal-only network that mitigates frame-to-frame jitter while preserving motion detail, yielding temporally smooth ground-truth angle trajectories stored as per-frame arrays of shape  $(N, 3)$ .

Because the sensor and video streams operate at different sampling rates (40 Hz vs. 60 fps), a temporal alignment procedure is required before model training. First, both streams were cropped to their overlapping interval. The per-frame joint angle labels were then aligned to the cropped video frames using frame indices. Next, the joint angle time series was linearly interpolated from the video-frame timestamps to the sensor sampling timestamps, effectively downsampling the labels to 40 Hz. Then, the sensor readings were normalized to zero mean and unit variance using a standard scaler fitted on the training set only; the same scaler parameters were applied to the test set to prevent information leakage. Finally, a sliding window with a length of 40 samples (approximately one second) with a stride of one was applied to construct input–output pairs: each input window comprises 40 consecutive readings across all four sensor channels, and the corresponding output is the three-dimensional joint angle vector at the last timestep of the window.

**Machine learning models for joint angle estimate** A hybrid 1D-CNN + LSTM architecture was designed [4, 21] to ensure the robustness of model training. The spatial feature extraction stage consists of two stacked one-dimensional convolutional layers: the first applies 32 filters of kernel size 3 with zero-padding of 1 to the four input sensor channels, followed by batch normalization, ReLU activation, and dropout ( $p=0.1$ ); the second expands to 64 filters with the same kernel and padding configuration. The resulting feature maps are then passed to a single-layer LSTM with 64 hidden units for temporal modeling. Only the final hidden state is forwarded to a regression head comprising a fully connected layer ( $64 \rightarrow 32$  units) with ReLU and dropout ( $p=0.1$ ), followed by a linear output layer ( $32 \rightarrow 3$ ) that produces the predicted flexion, abduction, and rotation angles in degrees. The model was trained from scratch for every layout configuration using the Adam optimizer with a learning rate of  $10^{-3}$ , mean squared error loss, a batch size of 32, and gradient clipping at a maximum norm of 1.0. Training runs for 50 epochs, and the checkpoint with the lowest

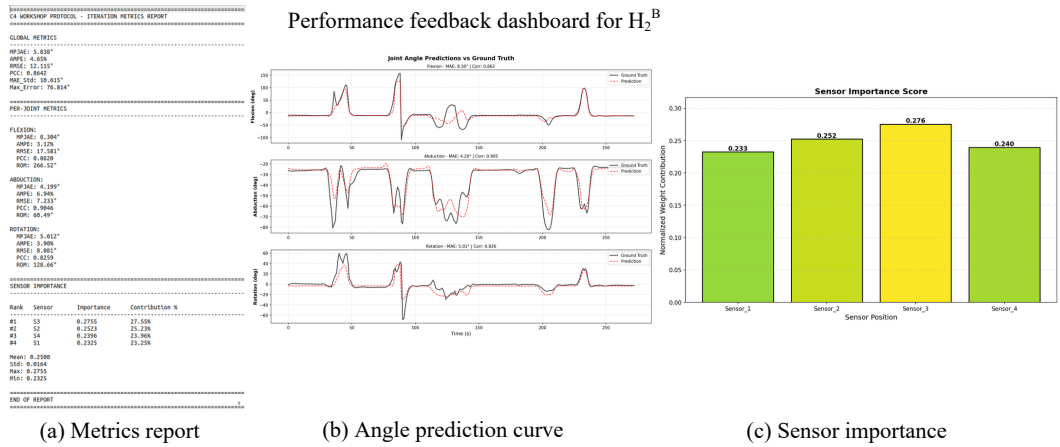


Fig. 6. Screenshots of the Quantitative Feedback dashboard. (a) a metrics report lists global and per-joint prediction errors (MPJAE, AMPE, RMSE, PCC) and sensor importance rankings, (b) joint angle prediction curves versus ground truth for flexion, abduction, and rotation, respectively and (c) a bar chart of normalized sensor importance scores across four sensors.

training loss was retained for evaluation. The complete training and evaluation cycle completed within approximately five minutes, enabling rapid turnaround during the iterative design workshop. Finally, a performance dashboard was generated by applying trained model to the test set, which will be introduced in Section 3.2.3.

**3.2.3 Feedback & Refinement.** At the conclusion of each Rapid Validation cycle in Experiment 2, the performance evaluation results were presented to the designers via a Quantitative Feedback dashboard (see Figure 6). The dashboard presents global metrics, per-joint error decomposition, and sensor contribution rankings based on feature importance scores. The definition for each metric will be presented in Section 3.2.5. In the H-Series and LH-Series, the feedback was interpreted and translated into design refinements using different approaches. In the H-Series, the human designer follows an independent diagnosis-to-revision pathway. They inspected both the quantitative evaluation results and the physical prototype, independently diagnosed performance issues—drawing on their own domain expertise to connect observed errors to physical causes—and directly repositioned sensors on the garment.

In the LH-Series, feedback integration and design Refinement proceed through a three-stage process that combines human physical observations with LLM-driven analytical reasoning (Figure 3, right).

**Stage 1: Structured Human Feedback.** Rather than directly revising the layout, the human designer provided structured feedback following the template shown in Figure 7. These per-sensor and global observations capture information that is inaccessible to the LLM from quantitative data alone: physical phenomena observed during motion, sensor-body coupling quality, positional adjustment suggestions based on hands-on inspection, and priority judgments indicating which sensors or issues the human designer considers most critical.

**Stage 2: Diagnostic Integration.** The structured human designer observations from Stage 1 are combined with the quantitative performance metrics from the dashboard into an integrated diagnostic prompt. This prompt is submitted to the LLM, which performs a diagnosis step: analyzing the

### Structure

Each expert provides feedback per round using the following JSON schema. Fields marked in *gray italic* are to be filled by the expert.

#### Template Schema

```

expert [K]:
Round [N]: {
  "expert_id": [to be filled]
  "expert_domain": [to be filled]
  "iteration": [N]
  "base_design": L0
  "feedback_date": [YYYY-MM-DD]
  "start_time": [HH:MM]
  "end_time": [HH:MM]
  "sensor_feedback": {
    "S1": { "comment": [expert comment] },
    "S2": { "comment": [expert comment] },
    "S3": { "comment": [expert comment] },
    "S4": { "comment": [expert comment] }
  },
  "global_observations": [overall observations]
  "suggested_focus": [focus for next iteration]
}

```

#### Field Descriptions

- `expert_id`: Unique identifier for the expert
- `expert_domain`: Expert's area of specialization
- `iteration`: Design iteration number being reviewed
- `base_design`: Base design version (e.g., L0)
- `sensor_feedback.S1-S4`: Per-sensor comments on placement, orientation, and effectiveness
- `global_observations`: Overall observations about the design
- `suggested_focus`: Recommended focus areas for next iteration

Fig. 7. Template for Structured Human Feedback. Note that only feedback information is used for LLM prompting to avoid misleading.

current design's failure modes by cross-referencing the quantitative indicators (e.g., low sensor importance, high per-joint error) with the human designer's physical observations (e.g., poor coupling, misalignment with motion axes). The LLM explicitly identifies root causes before proposing any changes, reasoning across biomechanical, material, and signal processing considerations to connect symptoms to underlying design issues. The detailed prompt is shown in Appendix: Figure 14.

*Stage 3: Synthesis and Refinement.* Building on the diagnosis, the LLM generates a refined layout specification in which each proposed modification is explicitly traced to a finding from the diagnosis step. The output is a JSON specification containing updated sensor coordinates (relative to anatomical landmarks), orientations, and a structured design rationale that links each change to the identified root cause. It creates an auditable record of design evolution across iterations. The detailed prompt is shown in Appendix: Figure 15.

The refined layout is then evaluated following the Rapid Validation pipeline. This three-stage structure enforces a separation between observation (human), diagnosis (LLM with human input), and synthesis (LLM with traceability), ensuring that human embodied knowledge and LLM cross-domain reasoning are integrated systematically.

During the user study, besides quantitative performance metrics, we recorded complete LLM interaction logs (prompt-response chains), human designer's structured feedback, design evolution trajectories (sensor coordinate changes across iterations), and photographs of the garment at each iteration.

**3.2.4 LLM Configuration.** All LLM interactions used gpt-4.1-2025-04-14 accessed through the Azure OpenAI API. For text generation temperature setting, in Experiment 1, two different temperature is used for N-to-1 generation. The first divergent phase uses a higher temperature ( $T=0.7$ ) to encourage diversity across the five independent candidate proposals; the convergent synthesis phase uses a lower temperature ( $T=0.2$ ) to favor deterministic consolidation; In Experiment 2, we used an intermediate temperature ( $T=0.4$ ) to balance creative and consistent generation.

**3.2.5 Quantitative Performance Metrics.** We employed four complementary metrics to assess the quality of the layout design. We denote the total number of time samples as  $N$ , the number of degrees of freedom as  $J$ , the ground-truth joint angle at time  $t$  for joint  $j$  as  $y_{t,j}$ , and the predicted joint angle as  $\hat{y}_{t,j}$ .

*Mean Per-Joint Angular Error (MPJAE).* The primary metric, representing the average absolute deviation in degrees:

$$\text{MPJAE} = \frac{1}{J} \sum_{j=1}^J \left( \frac{1}{N} \sum_{t=1}^N |\hat{y}_{t,j} - y_{t,j}| \right) \quad (1)$$

*Root Mean Square Error (RMSE).* Penalizes large deviations more heavily, highlighting occasional spikes:

$$\text{RMSE}_j = \sqrt{\frac{1}{N} \sum_{t=1}^N (\hat{y}_{t,j} - y_{t,j})^2} \quad (2)$$

*Pearson Correlation Coefficient (PCC).* Evaluates how well the predicted signal tracks the shape and temporal dynamics of the ground truth, independent of offset or scaling:

$$\text{PCC}_j = \frac{\sum_{t=1}^N (y_{t,j} - \bar{y}_j)(\hat{y}_{t,j} - \bar{\hat{y}}_j)}{\sqrt{\sum_{t=1}^N (y_{t,j} - \bar{y}_j)^2} \sqrt{\sum_{t=1}^N (\hat{y}_{t,j} - \bar{\hat{y}}_j)^2}} \quad (3)$$

*Average Mean Percentage Error (AMPE).* A scale-independent measure normalized by the range of motion, enabling comparison across joints with different movement ranges:

$$\text{AMPE}_j = \frac{1}{N} \sum_{t=1}^N \left( \frac{|\hat{y}_{t,j} - y_{t,j}|}{\max(y_j) - \min(y_j)} \right) \times 100\% \quad (4)$$

*Sensor Importance Score (SIS).* Quantifies each sensor's contribution to the prediction based on the learned weights of the first convolutional layer in the prediction model. Let  $\mathbf{W} \in \mathbb{R}^{F \times K \times M}$  denote the weight tensor of the first Conv1d layer, where  $F$  is the number of output filters,  $K$  is the number of input channels (one per sensor), and  $M$  is the kernel size. The importance of sensor  $i$  is defined as:

$$\text{SIS}_i = \frac{\sum_{f=1}^F \sum_{m=1}^M |W_{f,i,m}|}{\sum_{k=1}^K \sum_{f=1}^F \sum_{m=1}^M |W_{f,k,m}|} \quad (5)$$

The resulting scores sum to one across all sensors. A higher score indicates that the model relies more heavily on the corresponding sensor's signal for prediction. Ideally, equal SIS values for each sensor reflect a balanced design for joint-angle prediction.

Overall, we define the design quality as the combined measure of the final prediction performance—primarily represented by MPJAE—supplemented by the additional metrics discussed above.

### 3.3 Participant Recruitment

Test subject for sensing performance evaluation: we employed a single-subject design (male, age 28, athletic build, no shoulder pathologies). This choice was motivated by two considerations: (1) holding biomechanical variation constant isolates the effect of layout design methodology, enabling direct comparison across conditions; and (2) a single participant enables more iteration cycles within practical time constraints. The participant performed standardized motions only and did not participate in design decisions.

Human designers: we recruited three designers with distinct domain backgrounds to explore how expertise influences both H-Series and LH-Series, Recruitment criteria included: (1) prior experience of designing and implementing e-textile-based motion sensing systems; (2) willingness to participate in both H-Series and LH-Series.

Table 1. Human Designer Profiles

Human Designer	Background	Experience
A	Kinesiology Research	8 years (Senior)
B	E-Textile Engineering	4 years (Intermediate)
C	Electrical Engineering	2 years (Junior)

The three human designers have diverse knowledge backgrounds and varying levels of experience. They all have prior experience using LLMs; however, they have not used LLMs specifically for sensor layout design generation. This provides a suitable foundation for understanding general LLM usage practices while ensuring that their feedback is not biased toward this particular task.

## 4 Results

### 4.1 Experiment 1: Initial Design Comparison

To address **RQ1**, we compared the quality of the four initial designs including the LLM-generated layout ( $L_0$ ) and the three human designer-generated layouts ( $H_0^A$ ,  $H_0^B$ ,  $H_0^C$ ), as illustrated in Figure 8. The detailed LLM generated outputs using divergent-convergent strategy can be found in Appendix B. Following the results in Table 2, the LLM-generated layout achieved the lowest MPJAE of 10.94°, compared to 15.58° (Designer A), 14.82° (Designer B), and 19.21° (Designer C).  $L_0$  also achieved the highest PCC and the lowest AMPE and RMSE.

Table 2. Initial Design Performance Metrics. Bold values indicate best performance per metric.

Design	MPJAE (°)	PCC	AMPE (%)	RMSE (°)
$L_0$ (LLM)	<b>10.94</b>	<b>0.794</b>	<b>8.75</b>	<b>17.03</b>
$H_0^A$ (Senior)	15.58	0.566	9.28	27.31
$H_0^B$ (Intermediate)	14.82	0.390	9.66	25.42
$H_0^C$ (Junior)	19.21	0.340	13.58	28.02

We also analysed the per-joint error decomposition as shown in Table 3.  $L_0$  achieved the lowest error for flexion and rotation. For abduction, Designer A's design  $H_0^A$  achieved the best performance.

Table 3. Per-Joint MPJAE in degrees. Bold indicates the best per degree of freedom.

Degree of Freedom	$L_0$	$H_0^A$	$H_0^B$	$H_0^C$
Flexion	<b>18.01</b>	30.21	25.36	30.98
Abduction	9.62	<b>7.76</b>	9.91	13.77
Rotation	<b>5.20</b>	8.78	9.20	12.88

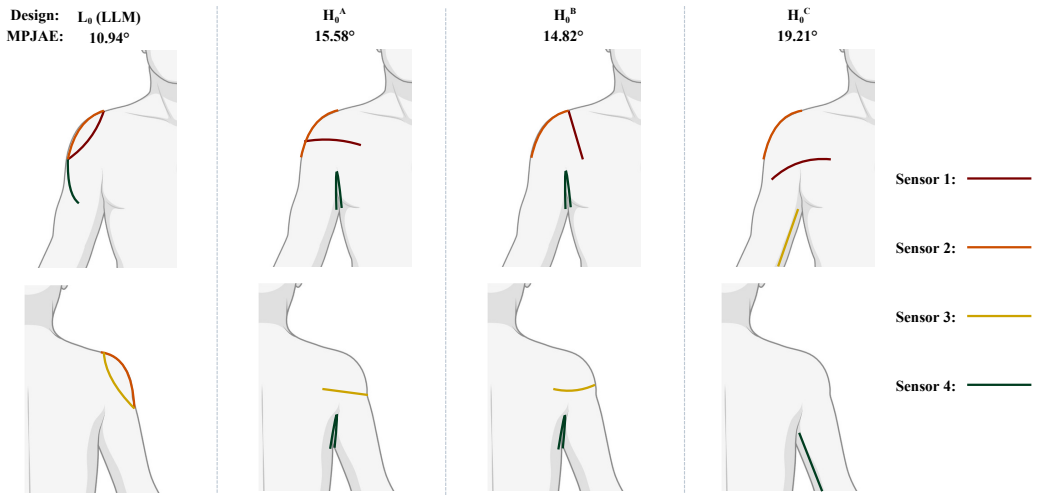


Fig. 8. Initial sensor layouts proposed by LLM and human designers, shown on a standardized shoulder model. Each layout comprises 4 flex sensors (colored rectangles).

## 4.2 Experiment 2: Iterative Design Refinement

To address **RQ2**, we compared iteration trajectories across H-Series and LH-Series for all three designers over two iteration cycles. The detailed sensor layout design (Appendix C), performance dashboard (Appendix D), structured human designer feedback logs (Appendix E) and LLM outputs (Appendix F) for different iteration conditions can be found in the Appendix.

As listed in Table 4, in the H-Series, Designer A (Senior) achieved consistent performance improvement over two iterations, reaching the second-lowest MPJAE overall. Designer B (Intermediate) improved the design quality steadily across both iterations, achieving the lowest MPJAE in the H-Series and LH-Series. Designer C (Junior) improved substantially in iteration 1 but regressed in iteration 2.

In the LH-Series, designers modified sensor positions based on the evaluation results of  $L_0$  in the first iteration. Designer A modified all four sensor positions, resulting in an increase of MPJAE from  $10.94^\circ$  to  $12.75^\circ$ . Designer A chose to discontinue the LH-Series after Iteration 1. Designer B achieved a 28.4% improvement in Iteration 1 but regressed in Iteration 2. Designer C was the only participant who achieved consistent improvement over the two iterations. Compared with the best design Designer C achieved in the H-Series, Designer C achieved better design with the assistance of LLM.

Figure 9 illustrates Designer C’s layout design evolution in the LH-Series. Designer C suggested moving sensors “a bit to chest side” in Iteration 1, and placing sensors to “follow the muscle direction” in Iteration 2. Each iteration involved incremental adjustments to one or two sensors rather than comprehensive redesign, and the LLM translated these directional observations into concrete coordinate updates.

**4.2.1 Human Designers’ Structured Feedback.** To address **RQ3**, we examined the feedback records from LH-Series iterations. Table 5 presents representative excerpts from each designer, the observation column is concluded from the corresponding feedback excerpt. We further observe the following patterns across the three cases:

Table 4. MPJAE in each iteration.

Condition	Initial	Iter 1	Iter 2	Pattern
<i>H-Series (Independent Human Iteration)</i>				
Designer A	15.58°	6.49°	<b>6.33°</b>	↘↘
Designer B	14.82°	7.80°	<b>5.84°</b>	↘↘
Designer C	19.21°	10.08°	13.03°	↘↗
<i>LH-Series (LLM-Human Collaboration)</i>				
Designer A	10.94°	12.75°	— <sup>†</sup>	↗
Designer B	10.94°	7.83°	10.18°	↘↗
Designer C	10.94°	8.17°	<b>6.86°</b>	↘↘

↘ = improvement; ↗ = regression. <sup>†</sup>Designer A terminated after iteration 1.

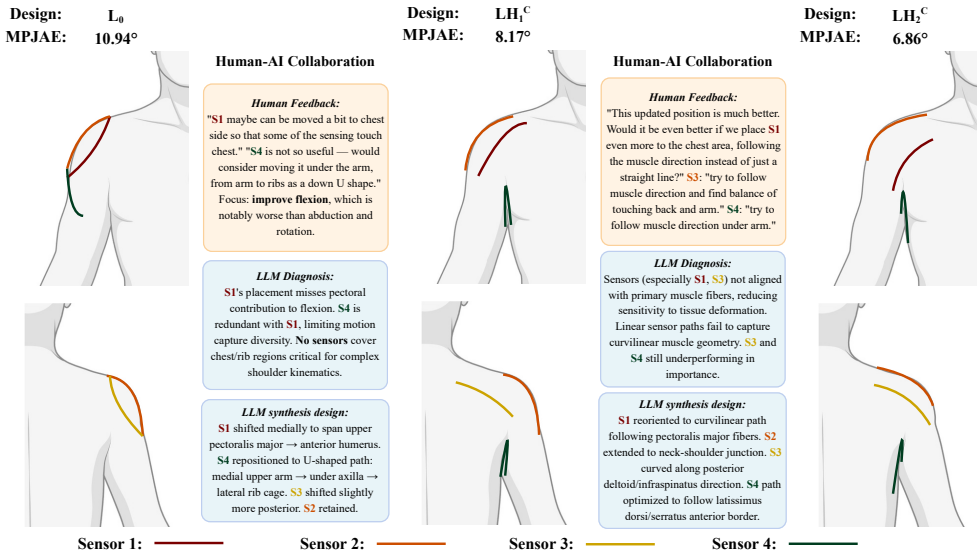


Fig. 9. Designer C's LH-Series layout evolution. Annotations show corresponding feedback excerpts.

*Feedback framing differed across designers.* Designer A framed feedback in terms of anatomical principles, prescribing specific positions based on muscle anatomy. For instance, Designer A identified each sensor position by its corresponding muscle (e.g., “m.deltoides anterior part,” “m.deltoides middle part”) and consistently recommended that sensors “should touch or pass the GH joint.” Designer A also noted that certain placements “will not detect IR/ER rotations of the shoulder.” Designer B referenced quantitative metrics and sensor physical constraints. In Iteration 1, Designer B observed that “the sensors bend only in one direction” and highlighted that sensors are “placed on clothes” rather than directly on the body, requesting the system to “compensate for that.” In Iteration 2, Designer B noted that “S2 importance is quite low” and that “rotation detection got worse.” Designer C described observations from physical interaction with the prototype, using tentative language (“maybe,” “I am wondering”). Designer C grounded suggestions in personal testing experience (e.g., “this suggestion is especially based on my own testing results”) and referred

to perceived sensor behavior during movement, such as suggesting a sensor be moved “a bit to chest side so that some of the sensing are touch chest.”

*Scope of proposed changes varied.* Designer A proposed modifications to all four sensors with detailed per-sensor anatomical reasoning. Designer B provided only global feedback without targeting specific sensors in either of the two iterations, offering directives such as “move it so that the sensors better move with the joint” and “distributing them a bit wider” around the shoulder seam. Designer C proposed two to three incremental adjustments per iteration with global observations, building on the previous iteration’s outcome. In Iteration 2, Designer C acknowledged that “the flexion has improved and is much better now” and noted that “the importance of sensors are more equal and balanced”, while referencing current metric values (e.g., “MPJAE is around 11.7, 6.7 and 6.1 for flexion, abduction and rotation”) to guide further refinement.

*Observed relationship between feedback style and outcome.* In this case study, the human designer who proposed fewer changes per round and described physical observations (Designer C) achieved the best LH-Series outcome. Designer C completed two iterations, progressively refining sensor positions while retaining effective placements from the previous iteration. The designer who proposed the most changes grounded in domain theory (Designer A) completed only one iteration and experienced performance degradation. Designer B also completed two iterations with global-level suggestions and achieved intermediate results.

## 5 Discussion

### 5.1 LLM as a Cross-Domain Knowledge Integrator (RQ1)

RQ1 asked whether LLMs can generate sensor layouts that match or exceed the quality of initial designs produced by human designers. Our results indicate that, the answer is yes:  $L_0$  outperformed all three human designs across every evaluation metric.

A closer look at the designs helps explain why. Each designer approached placement through the lens of their own discipline. Designer A, drawing on kinesiology training, concentrated sensors on anatomically meaningful muscle groups—a strategy that yielded the best abduction prediction among all initial designs ( $7.76^\circ$ ) but left anterior–posterior coverage gaps that penalized flexion and rotation. Designer B distributed sensors along garment structural features, reflecting an e-textile engineering perspective, while Designer C clustered sensors around the most visibly mobile region of the shoulder. Each design thus bore the imprint of its creator’s disciplinary focus, capturing some motion axes well but underserving others.

$L_0$ , by contrast, spread sensors across both the anterior and posterior shoulder—a broader spatial strategy that none of the three designers adopted independently. This pattern is consistent with the hypothesis that LLMs can act as cross-domain knowledge integrators, simultaneously drawing on anatomy, biomechanics, and textile–skin coupling in ways that are difficult for a single practitioner [22, 33]. The per-joint error decomposition reinforces this interpretation:  $L_0$  achieved the lowest errors for flexion and rotation—the two axes that benefit most from spatially distributed sensing—while Designer A’s anatomically focused layout retained an advantage for abduction, a motion well captured by localized deltoid placement alone.

The N-to-1 divergent–convergent prompting strategy also contributed to  $L_0$ ’s robustness. Our synthesis analysis (Appendix B) revealed that while all five independent LLM proposals converged on lateral and posterior deltoid coverage, they diverged most on the fourth sensor’s path and on flexion sensor orientation. The meta-synthesis step filtered implausible configurations and consolidated the most robust principles into a balanced layout.

Table 5. Representative Designer Feedback Excerpts from the LH-Series

Designer	Iter.	Feedback Excerpt	Observation
A	1	“This sensor position mimics the m.deltoideus anterior part placement/location in the body. The flex sensor should touch or pass the GH joint.”	References specific anatomy to prescribe sensor positions
	1	“If the sensor is placed like in the description, there will be curves (waves) that the sensor will make, which will not align with the human body surface during flexion and abduction movement.”	Predicts physical behavior from anatomical reasoning
B	1	“The detection results have a lot of error. Move it so that the sensors better move with the joint. Note that the sensors bend only in one direction, so orient the sensors accordingly.”	References error metrics and sensor physics
	2	“S2 importance is quite low... the orientation of the sensor is not aligned well enough to the direction of bending of the joints. Currently the three sensors are placed quite close to one another, maybe distributing them a bit wider would capture different movements.”	References computed importance; suggests spatial redistribution
C	1	“Maybe can be moved a bit to chest side so that some of the sensing touch chest... This suggestion is especially based on my own testing results.”	Reports observation from physical testing
	2	“This updated position is much better. I am wondering would it be even better if we place the sensor even more to the chest area? Maybe we could place the sensor to be more following the muscle direction instead of just a straight line.”	Builds on previous round; uses exploratory language

## 5.2 Iterative Refinement: When Does Collaboration Help? (RQ2)

RQ2 asked how human–AI collaborative iteration compares to purely human-driven iteration. Our data reveal that the answer depends critically on the designer’s experience level—a pattern we did not anticipate when designing the study.

In the H-Series, the two more experienced designers (A and B) steadily improved their layouts across both cycles, with Designer B ultimately reaching the lowest MPJAE of any condition. Designer C, the least experienced, improved initially but regressed in the second cycle. The LH-Series told a strikingly different story: Designer C was the only participant to achieve consistent improvement throughout, while Designer A experienced degradation after a single round and chose to discontinue.

This inverted expertise–outcome relationship resonates with recent findings on AI-assisted work in other domains. Brynjolfsson et al. [2] observed that generative AI productivity gains among customer support agents accrued primarily to novice workers, arguing that AI effectively disseminates the tacit knowledge of high performers. A similar dynamic appears at play here:

the LLM’s cross-domain reasoning compensated for Designer C’s limited biomechanical background, while Designer A’s well-established domain models left less room for complementary AI contributions—and may have even introduced friction when the LLM’s suggestions conflicted with their existing mental models. From a practical standpoint, this skill-leveling effect is notable: through collaboration, Designer C (2 years of experience) achieved performance comparable to what Designer B (4 years) reached through fully independent effort.

It is worth noting that the fixed condition ordering (H-Series before LH-Series) makes this finding complex. Any experience accumulated during the H-Series could have carried over to benefit subsequent LH-Series performance, meaning the Designer C’s strong performance on the LH-Series may also stem from tacit knowledge gained during the H-series experiments. Another consideration regarding the experimental design is the starting point for the LH-Series. Instead of using the standard LLM-generated initial design ( $L_0$ ), a potential alternative is to use a human designer’s initial design ( $H_0$ ). While  $L_0$  provides a fair baseline for comparison, using  $H_0$  might offer better insights into how LLMs assist designers in cross-domain knowledge integration by addressing missing layout concerns.

An intriguing piece of convergent evidence further supports this interpretation. The two best-performing layouts— $H_2^B$  (5.84°, human-only) and  $LH_2^C$  (6.86°, human-AI)—arrived at remarkably similar tri-zonal configurations (Figure 10): a superior sensor crossing the acromion, posterior coverage spanning the infraspinatus and posterior deltoid, and an inferior sensor anchored near the axilla. That two independent paths—one guided entirely by an experienced human, the other by a novice collaborating with an LLM—converged on the same spatial solution suggests both a relatively constrained optimum for this task and, more importantly, that LLM-assisted collaboration can guide less experienced designers toward that optimum.

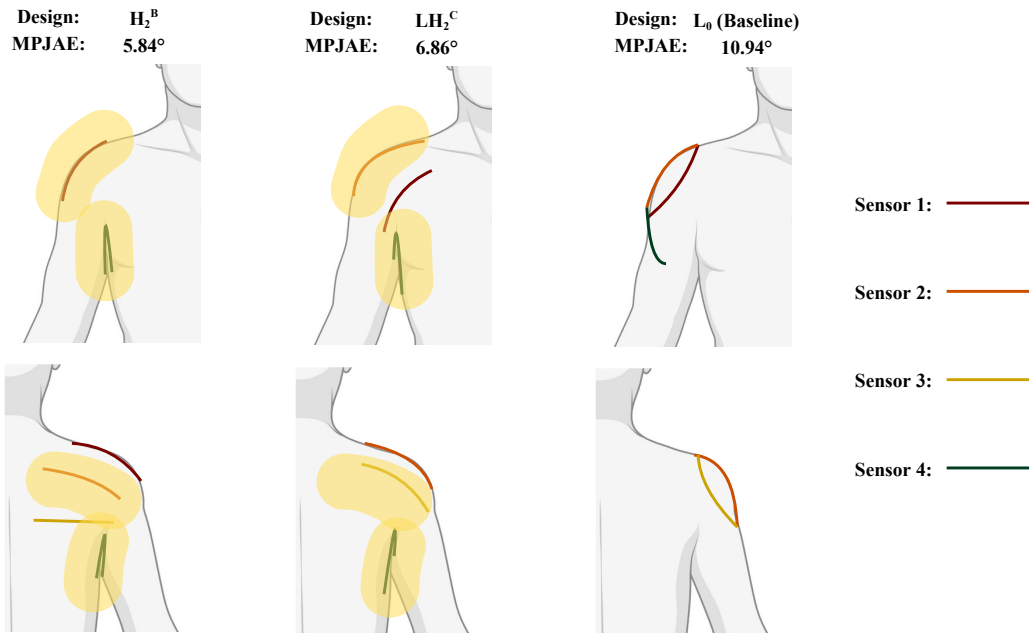


Fig. 10. Best-performing layouts. (a)  $H_2^B$  and (b)  $LH_2^C$  show convergent placement across the acromion, posterior scapula, and axilla, outperforming the (c)  $L_0$  baseline. Highlighted zones indicate these common sensing regions.

### 5.3 What Shapes Collaboration Effectiveness? (RQ3)

RQ3 aimed to identify factors that influence the effectiveness of human–AI collaboration. Our qualitative analysis of the LH-Series feedback records points to three interrelated factors: the granularity and abstraction level of human feedback, and the way domain background shapes both.

*Granularity: incremental adjustments outperform sweeping redesigns.* The contrast between Designer A and Designer C is instructive. Designer A proposed modifications to all four sensors simultaneously, each backed by detailed anatomical reasoning, yet the resulting layout performed worse. Designer C adjusted only one or two sensors per round, preserving what had worked and building on it incrementally. This pattern is consistent with classical iterative experimental design principles: small changes make it possible to attribute performance shifts to specific decisions, while sweeping modifications conflate effects and raise the risk of regression [1]. In the human–AI context, this principle has an additional dimension—targeted feedback constrains each LLM reasoning step to a manageable subproblem, whereas coordinating simultaneous changes across all sensors may stretch the model’s capacity for maintaining internal consistency.

Designer C’s feedback trajectory illustrates this progressive strategy. In Iteration 1, after hands-on inspection of the prototype, Designer C suggested shifting S1 (Sensor 1) toward the chest and repositioning S4 into a U-shaped path under the arm—targeted changes that produced a substantial flexion improvement. In Iteration 2, Designer C explicitly acknowledged the prior gains (“the flexion has improved and is much better now”) and turned attention to finer adjustments, asking sensors to “follow the muscle direction.” Each round thus built on the last rather than starting from scratch.

*Abstraction: observations outperform prescriptions.* How designers framed their feedback proved equally consequential. Designer A communicated in prescriptive anatomical terms—specifying muscle names and insisting that sensors “should touch or pass the GH joint”—effectively dictating exact placements and leaving the LLM to serve as a coordinate translator. Designer C described what they observed and wondered about (“maybe can be moved a bit to chest side”; “I am wondering would it be even better if we place the sensor even more to the chest area?”), giving the LLM space to integrate these observations with the quantitative metrics and its own biomechanical knowledge.

This distinction echoes a broader pattern in human–AI co-creative systems: overly directive instructions tend to suppress complementary AI reasoning, while observation-level prompts enable synergistic outcomes in which each party contributes its distinct strengths [8, 27]. Designer B’s experience occupies a middle ground—global observations (“sensors bend only in one direction”; “distributing them a bit wider”) without per-sensor specificity—and produced intermediate results, reinforcing the idea that collaboration effectiveness varies along a continuum from directive to observational feedback.

## 6 Limitations

Our study has several limitations. First, the single-subject design ensures controlled comparison across layout conditions but limits the generalizability of absolute performance values to other body types and anatomical variations. Second, with only three human designer participants, our findings capture preliminary patterns in feedback diversity and collaboration dynamics but do not support statistical inference; a larger designer panel is needed to validate the observed relationships between domain background and collaboration effectiveness. Third, although markerless motion capture has been widely adopted as a practical reference system and offers acceptable measurement error in prior work [34], its inherent uncertainty means that the lowest reported errors may partially reflect reference noise. Fourth, considering the rapid development and diversity of LLM technologies, a broader range of models needs to be evaluated.

To address these limitations, our next step is to conduct a large-scale multi-subject study with diverse body types and a broader human designer panel, enabling statistical validation of the design patterns and collaboration dynamics observed in the current case study. Additionally, we plan to integrate simulation-based methods into the iterative design pipeline to examine whether combining LLM-driven reasoning with simulation feedback can improve generalizability and reduce reliance on costly physical prototyping and testing. In the future, we will explore more diverse and advanced LLMs to investigate the potential effects of human–AI collaboration on sensor layout design.

## 7 Conclusion

This paper investigated LLMs as cross-domain knowledge integrators for e-textile sensor layout design through a case study on shoulder joint angle prediction involving three human designers with different technical backgrounds. In an initial design comparison, the LLM-generated layout outperformed all three human designers initial designs, demonstrating the potential of LLMs to synthesize cross-domain knowledge. In iterative refinement, comparing human-only iteration with human–AI collaboration revealed an intriguing relationship: the least experienced designer achieved improvement through collaboration, reaching performance comparable to the best human-only result, while the most experienced designer experienced performance degradation. Qualitative analysis identified two critical factors governing collaboration effectiveness: feedback granularity, where incremental adjustments outperformed sweeping redesigns by enabling focused LLM reasoning, and feedback abstraction, where observation-oriented input yielded better outcomes than prescriptive directives by preserving space for complementary AI reasoning. These findings suggest that LLMs can effectively democratize access to cross-domain design expertise in physical prototyping tasks, provided that human feedback is structured to complement rather than constrain AI reasoning. Future work should validate these patterns with larger human designer panels, diverse body types, and integration of simulation-based virtual prototyping and evaluation to further reduce reliance on costly physical prototyping and tests.

## References

- [1] George EP Box, J Stuart Hunter, and William G Hunter. 2005. *Statistics for experimenters: design, innovation, and discovery*. John Wiley & Sons.
- [2] Erik Brynjolfsson, Danielle Li, and Lindsey Raymond. 2025. Generative AI at work. *The Quarterly Journal of Economics* 140, 2 (2025), 889–942.
- [3] Arianna Carnevale, Umile Giuseppe Longo, Emiliano Schena, Carlo Massaroni, Daniela Lo Presti, Andrea Berton, Vincenzo Candela, and Vincenzo Denaro. 2019. Wearable systems for shoulder kinematics assessment: a systematic review. *BMC Musculoskeletal Disorders* 20, 1 (2019), 546. doi:10.1186/s12891-019-2930-4
- [4] Jian Chen et al. 2022. Analyzing Human Muscle State with Flexible Sensors. *Journal of Sensors* 2022 (2022), 5227955.
- [5] Yu-Pin Chen, Chung-Ying Lin, Ming-Jr Tsai, Tai-Yuan Chuang, and Oscar Kuang-Sheng Lee. 2020. Wearable motion sensor device to facilitate rehabilitation in patients with shoulder adhesive capsulitis: pilot study to assess feasibility. *Journal of medical Internet research* 22, 7 (2020), e17032.
- [6] Leire Francés-Morcillo, Paz Morer-Camo, María Isabel Rodríguez-Ferradas, and Aitor Cazón-Martín. 2020. Wearable design requirements identification and evaluation. *Sensors* 20, 9 (2020), 2599.
- [7] Mohsen Gholami, Ahmad Rezaei, Tyler J. Cuthbert, Christopher Napier, and Carlo Menon. 2019. Lower body kinematics monitoring in running using fabric-based wearable sensors and deep convolutional neural networks. *Sensors* 19, 23 (2019), 5325.
- [8] Frederic Gmeiner, Humphrey Yang, Lining Yao, Kenneth Holstein, and Nikolas Martelaro. 2023. Exploring challenges and opportunities to support designers in learning to co-create with AI-based manufacturing design tools. In *Proceedings of the 2023 CHI Conference on Human Factors in Computing Systems*. 1–20.
- [9] Cristóvão Gonçalves, Alexandre Ferreira da Silva, José Gomes, and Ricardo Simões. 2018. Wearable E-Textile Technologies: A Review on Sensors, Actuators and Control Elements. *Inventions* 3, 1 (2018), 14. doi:10.3390/inventions3010014

- [10] Roya Haratian. 2022. Motion capture sensing technologies and techniques: A sensor agnostic approach to address wearability challenges. *Sensing and Imaging* 23, 1 (2022), 25.
- [11] Xinxin Huang, Yunan Xue, and Shuyun Ren. 2023. Sensor-Based Wearable Systems for Monitoring Human Motion and Posture: A Review. *Sensors* 23, 22 (2023), 9047. doi:10.3390/s23229047
- [12] Ezgi Ismar, Senem Kurşun Bahadır, Fatma Kalaoglu, and Vladan Koncar. 2020. Futuristic clothes: electronic textiles and wearable technologies. *Global Challenges* 4, 7 (2020), 1900092.
- [13] Yichu Jin, Christina M. Glover, Haedo Cho, Oluwaseun A. Araromi, Moritz A. Graule, Na Li, Robert J. Wood, and Conor J. Walsh. 2020. Soft Sensing Shirt for Shoulder Kinematics Estimation. In *2020 IEEE International Conference on Robotics and Automation (ICRA)*. IEEE, 4863–4869. doi:10.1109/ICRA40945.2020.9196586
- [14] Haru Kaneko and Sozo Inoue. 2023. Toward pioneering sensors and features using large language models in human activity recognition. In *Adjunct Proceedings of the 2023 ACM International Joint Conference on Pervasive and Ubiquitous Computing & the 2023 ACM International Symposium on Wearable Computing*. 475–479.
- [15] DongWook Kim, Seunghoon Kang, and Yong-Lae Park. 2024. Optimal Sensor Placement for Motion Tracking of Soft Wearables Using Bayesian Sampling. *Soft Robotics* (2024).
- [16] Minu Kim, Juhyung Ahn, Jieun Seo, Steve Park, and Joo Yong Sim. 2025. Optisense: Computational Optimization for Strain Sensor Placement in Wearable Motion Tracking Systems. *Advanced Intelligent Systems* (2025), e202500892.
- [17] Kristian Kolthoff, Felix Kretzer, Christian Bartelt, Alexander Maedche, and Simone Paolo Ponzetto. 2025. GUIDE: LLM-Driven GUI Generation Decomposition for Automated Prototyping. In *2025 IEEE/ACM 47th International Conference on Software Engineering: Companion Proceedings (ICSE-Companion)*. IEEE, 1–4.
- [18] Abiodun Komolafe, Bahareh Zaghari, Russel Torah, Alex S Weddell, Hamideh Khanbareh, Zois Michail Tsikriteas, Mark Vousden, Mahmoud Wagih, Ulises Tronco Jurado, Junjie Shi, et al. 2021. E-textile technology review—from materials to application. *Ieee Access* 9 (2021), 97152–97179.
- [19] Huanhuan Liu, Yuyuan Shi, You Pan, Zhaoxue Wang, and Bingjie Wang. 2025. Sensory interactive fibers and textiles. *NPJ Flexible Electronics* 9, 1 (2025), 23.
- [20] Ruibo Liu, Qijia Shao, Siqi Wang, Christina Ru, Devin Balkcom, and Xia Zhou. 2019. Reconstructing human joint motion with computational fabrics. *Proceedings of the ACM on Interactive, Mobile, Wearable and Ubiquitous Technologies* 3, 1 (2019), 1–26.
- [21] Roberto López Morales et al. 2025. Upper Limb Joint Angle Estimation Using a Reduced Number of IMU Sensors and Recurrent Neural Networks. *Electronics* 14, 15 (2025), 3039.
- [22] Liane Makatura, Michael Ye, et al. 2024. How Can Large Language Models Help Humans in Design and Manufacturing? *arXiv preprint arXiv:2307.14377* (2024). MIT CSAIL.
- [23] KB Mustapha. 2025. A survey of emerging applications of large language models for problems in mechanics, product design, and manufacturing. *Advanced Engineering Informatics* 64 (2025), 103066.
- [24] Wesley Niswander, Wei Wang, and Kimberly Kontson. 2020. Optimization of IMU sensor placement for the measurement of lower limb joint kinematics. *Sensors* 20, 21 (2020), 5993.
- [25] Nianchong Qu, Jiaqi Mo, Yueyao Zhang, Leheng Chen, Yan Zhang, Guanyun Wang, Ye Tao, Yanan Wang, Qi Wang, and Teng Han. 2025. Laytex: A Data-Driven Tool for Automated and Customized Textile Sensor Layout Design in Motion Capture. *Proceedings of the ACM on Interactive, Mobile, Wearable and Ubiquitous Technologies* 9, 3 (2025), 1–42.
- [26] Lala Shakti Swarup Ray, Bo Zhou, and Paul Lukowicz. 2025. W2W: A Simulated Exploration of IMU Placement Across the Human Body for Designing Smarter Wearable. In *Proceedings of the 2025 ACM International Symposium on Wearable Computers*. 170–176.
- [27] Jeba Rezwana and Mary Lou Maher. 2023. Designing creative AI partners with COFI: A framework for modeling interaction in human-AI co-creative systems. *ACM Transactions on Computer-Human Interaction* 30, 5 (2023), 1–28.
- [28] Giovanni Saggio, Francesco Riillo, Laura Sbernini, and Lucia Rita Quitadamo. 2016. Resistive flex sensors: a survey. *Smart Materials and Structures* 25, 1 (2016), 013001.
- [29] Seyed Yahya Shirazi et al. 2024. A Standardized Framework for Sensor Placement in Human Motion Capture and Wearable Applications. *arXiv preprint arXiv:2412.21159* (2024).
- [30] Matteo Stoppa and Alessandro Chiolerio. 2014. Wearable electronics and smart textiles: A critical review. *Sensors* 14, 7 (2014), 11957–11992.
- [31] Corrin P Walmsley, Sian A Williams, Tiffany Grisbrook, Catherine Elliott, Christine Imms, and Amity Campbell. 2018. Measurement of upper limb range of motion using wearable sensors: a systematic review. *Sports medicine-open* 4, 1 (2018), 53.
- [32] Ge Wu, Frans CT Van der Helm, HEJ DirkJan Veeger, Mohsen Makhsous, Peter Van Roy, Carolyn Anglin, Jochem Nagels, Andrew R Karduna, Kevin McQuade, Xuguang Wang, et al. 2005. ISB recommendation on definitions of joint coordinate systems of various joints for the reporting of human joint motion—Part II: shoulder, elbow, wrist and hand. *Journal of biomechanics* 38, 5 (2005), 981–992.

- [33] Huatao Xu, Liying Han, Qirui Yang, Mo Li, and Mani Srivastava. 2024. Penetrative ai: Making llms comprehend the physical world. In *Proceedings of the 25th International Workshop on Mobile Computing Systems and Applications*. 1–7.
- [34] Wanqi Yin, Zhongang Cai, Ruisi Wang, Ailing Zeng, Chen Wei, Qingping Sun, Haiyi Mei, Yanjun Wang, Hui En Pang, Mingyuan Zhang, Lei Zhang, Chen Change Loy, Atsushi Yamashita, Lei Yang, and Ziwei Liu. 2025. SMPLeSt-X: Ultimate Scaling for Expressive Human Pose and Shape Estimation. *IEEE Transactions on Pattern Analysis and Machine Intelligence* (2025). arXiv:2501.09782.
- [35] Ailing Zeng, Lei Yang, Xuan Ju, Jiefeng Li, Jianyi Wang, and Qiang Xu. 2022. SmoothNet: A Plug-and-Play Network for Refining Human Poses in Videos. In *European Conference on Computer Vision (ECCV)*. Springer, 625–642.
- [36] Runhua Zhang, Yuanda Hu, Yuxuan He, Shiwen Fang, Bin Yu, Xiaohua Sun, and Qi Wang. 2023. A Tailored Textile Sensor-based Wrap for Shoulder Complex Angles Monitoring. In *Adjunct Proceedings of the 2023 ACM International Joint Conference on Pervasive and Ubiquitous Computing & the 2023 ACM International Symposium on Wearable Computing*. 137–141.
- [37] Ziyin Zhang, Chaoyu Chen, Bingchang Liu, Cong Liao, Zi Gong, Hang Yu, Jianguo Li, and Rui Wang. 2023. Unifying the perspectives of nlp and software engineering: A survey on language models for code. *arXiv preprint arXiv:2311.07989* (2023).
- [38] Yu Meng Zhou, Cameron J Hohimer, Harrison T Young, Connor M McCann, David Pont-Esteban, Umut S Civici, Yichu Jin, Patrick Murphy, Diana Wagner, Tazzy Cole, et al. 2024. A portable inflatable soft wearable robot to assist the shoulder during industrial work. *Science Robotics* 9, 91 (2024), eadi2377.

## A Prompt Template

### SYSTEM ROLE

You are an expert in biomechanics, wearable sensors, and e-textile design. I need your help with a sensor placement design task, but before we proceed to the actual design, I want to understand your internal knowledge and reasoning process.

### TASK CONTEXT

I am designing a wearable garment with strain sensors to capture human motion. Specifically, I need to track the movement of the **Shoulder Joint Complex** using **SpectraFlex Flex Sensors (95mm, Male Pins)** sensors embedded in a tight-fitting garment.

### TASK VARIABLES

- **Body Part:** **Shoulder Joint Complex**
- **Sensor Type:** **SpectraFlex Flex Sensors (95mm, Male Pins)**
- **Target Angles:** **Shoulder Clinical Joint Angles (Shoulder Flexion/Extension, Abduction/Adduction, Internal/External Rotation)**
- **Sensor Count (K):** **4**

### YOUR TASK (PART 1: KNOWLEDGE ELICITATION)

Before proposing any specific sensor layout, please provide a comprehensive analysis covering the following aspects:

#### SECTION 1 — Biomechanical Foundations

- What are the key anatomical structures of the **Shoulder Joint Complex** that are relevant to motion capture?
- What are the primary degrees of freedom (DOF) and types of movements this body part can perform?
- Which specific movements or angles are we trying to capture? (e.g., **Shoulder Clinical Joint Angles (Shoulder Flexion/Extension, Abduction/Adduction, Internal/External Rotation)**)

#### SECTION 2 — Skin Deformation & Strain Patterns

- During the movements mentioned above, which areas of the skin experience the most significant stretching or deformation?
- **CRITICAL:** What is the specific **direction of principal strain** (e.g., lines of non-extension vs. lines of maximum extension) in these hotspot regions?
- How does the direction of skin stretch correlate with the sensor's longitudinal axis? (Remember: the sensors are uni-directional).

#### SECTION 3 — Sensor Placement Principles

- What are the general principles or heuristics for placing **SpectraFlex Flex Sensors (95mm, Male Pins)** sensors on the **Shoulder Joint Complex**?
- What biomechanical or physiological factors should guide sensor positioning?
- Are there any anatomical landmarks that serve as reliable reference points?

#### SECTION 4 — Design Trade-offs and Constraints

Given that I can only use **4** sensors (this is a hard constraint), what are the key trade-offs I should consider?

- **Coverage vs. Redundancy:** How do I balance capturing multiple DOFs versus having redundant sensors for robustness?
- **Signal Quality vs. Comfort:** Which body regions might provide strong signals but may be uncomfortable or unstable?
- **Inter-sensor Correlation:** Should I avoid placing sensors too close together? Why or why not?
- **Practical Wearability:** Are there regions I should avoid due to garment construction issues?

#### SECTION 5 — Potential Challenges

- What are common failure modes or challenges in sensor-based motion capture for the **Shoulder Joint Complex**?
- How might individual anatomical variations affect sensor performance (assuming a "general purpose" design)?

### OUTPUT FORMAT

Please structure your response as a clear, analytical report. Use headings for each section (1–5 above). Be specific and technical where appropriate, but ensure your reasoning is transparent and well-justified.

- *Do NOT propose a specific sensor layout yet. This step is purely about articulating the knowledge and principles that will guide the design.*

Fig. 11. Prompt for divergent phase (step 1). This prompt extracts the LLM's internal knowledge prior to any design proposal

### CONTEXT LINK

Thank you for the comprehensive analysis in your previous response. I now have a clear understanding of the biomechanical principles and design considerations you've outlined.

### YOUR TASK (PART 2: DESIGN APPLICATION)

Based **strictly and explicitly** on the principles, trade-offs, and knowledge you articulated in your previous response, please now design a specific sensor layout.

### DESIGN REQUIREMENTS (MANDATORY CONSTRAINTS)

- **Number of Sensors:** Exactly 4 sensors (no more, no less).
- **Target Body Part:** *Shoulder Joint Complex*
- **Sensor Type:** *SpectraFlex Flex Sensors (95mm, Male Pins)* sensors (95mm length).
- **Target Outputs:** The layout should optimally predict *Shoulder Clinical Joint Angles (Shoulder Flexion/Extension, Abduction/Adduction, Internal/External Rotation)*.
- **Garment Type:** Sensors will be embedded in a tight-fitting upper-body garment.

### OUTPUT FORMAT (STRICT — USE THIS STRUCTURE)

Please provide your design in the following structured format:

#### Design Overview

*[Provide a 2–3 sentence summary of your overall design strategy and how it reflects the principles from Part 1]*

#### Sensor Layout Specification

For each of the 4 sensors, provide:

- **Sensor [Number]:**
  - **Anatomical Location:** [Precise description using anatomical landmarks]
  - **Orientation:** [Direction of sensor's longitudinal axis, e.g., "Vertical", "Horizontal", "Oblique at 45°"]
  - **Primary Target Movement(s):** [Which specific angle(s) or DOF this sensor is designed to capture]
  - **Rationale:** [2–3 sentences explicitly linking this placement to the principles you stated in Part 1. Reference specific points from your previous analysis.]

#### Design Trade-offs Made

*[Explain the key trade-offs you made given the 4 constraint. What did you prioritize? What did you sacrifice? How does this reflect your Section 4 analysis from Part 1?]*

#### Machine-Readable Output

Please also provide your design in the following JSON format for data extraction.

### JSON SCHEMA (KNEE EXAMPLE — ANTI-PRIMING)

**IMPORTANT EXAMPLE:** The example below shows a layout for a **KNEE**. Use this format, but apply it to the **Shoulder Joint Complex**.

```
{
  "design_id": "LLM_Only_v1",
  "sensor_count": 4,
  "sensors": [
    {
      "id": 1,
      "anatomical_location": "EXAMPLE: Distal Rectus Femoris (Knee)",
      "orientation": "Vertical",
      "primary_targets": ["Knee Flexion"],
      "coordinates_description": "EXAMPLE: 5cm proximal to patella, midline"
    },
    {
      "id": 2,
      "anatomical_location": "...",
      "orientation": "...",
      "primary_targets": [...],
      "coordinates_description": "..."
    }
  ]
}
```

### CRITICAL INSTRUCTIONS

- ① **Consistency Check:** Ensure your design choices are directly traceable to the principles you stated in Part 1.
- ② **No New Knowledge:** Do NOT introduce new principles that were not mentioned in Part 1.
- ③ **Precision:** Be as specific as possible in anatomical descriptions.

— Begin your design now. —

Fig. 12. Prompt for divergent phase (step 1). Conditioned on the knowledge elicited by P1, this prompt requests a structured sensor layout. The JSON example uses a knee scenario to prevent misleading.

### SYSTEM ROLE

You are a **Lead Design Engineer** and **Meta-Analyzer**. Your task is to synthesize the work of five junior designers into a single, robust, and final "master design."

These five designers (who are all instances of yourself) were given the exact same design brief (Task: **Design a k=4 sensor layout for shoulder motion capture using stretch strain sensors on a tight-fitting upper-body garment to optimally predict shoulder clinical joint angles**) and they each produced a plausible, independent design.

Your task is to analyze these 5 designs, identify common patterns (convergence) and unique ideas (divergence), and then use your expert judgment to consolidate them into **one, final, superior design**.

### INPUT: THE 5 INDEPENDENT DESIGNS

Here are the 5 designs provided in JSON format, along with their core rationale:

#### Design 1:

[Design 1 rationale and JSON blob inserted programmatically from Phase A outputs]

#### Design 2:

[Design 2 rationale and JSON blob inserted programmatically from Phase A outputs]

#### Design 3:

[Design 3 rationale and JSON blob inserted programmatically from Phase A outputs]

#### Design 4:

[Design 4 rationale and JSON blob inserted programmatically from Phase A outputs]

#### Design 5:

[Design 5 rationale and JSON blob inserted programmatically from Phase A outputs]

### YOUR TASK (PART 3: META-ANALYSIS & SYNTHESIS)

Please provide your final master design in the following structured format:

#### SECTION 1 — Meta-Analysis of Input Designs

[First, briefly analyze the 5 designs:]

- **Convergence:** What key anatomical "hotspots" appear repeatedly (e.g., "Designs 1, 3, and 5 all placed a sensor on Location X")?
- **Divergence:** What were the main differences or disagreements?
- **Outliers:** Did any design propose something radically different? Is it genius or a hallucination?

#### SECTION 2 — Final "Master Design" Rationale

[Explain your final design strategy:]

- **Synthesis Logic:** How did you select the best sensors? (e.g., "I adopted the consensus placement for Sensor 1 and 2, but chose Design 3's unique approach for Sensor 3 because...")
- **Conflict Resolution:** Did you identify any **spatial conflicts** (e.g., two proposed locations overlapping)? How did you resolve them?
- **Constraint Check:** Confirm that your final set of 4 sensors covers the target angles efficiently.

#### SECTION 3 — Final "Master Design" Specification (STRICT FORMAT)

Provide the single, consolidated design using the *exact same* format as the inputs (Sensor Specification + JSON). This design must also contain exactly 4 sensors.

#### Sensor Layout Specification (FINAL)

- **Sensor [Number]:**
  - **Anatomical Location:** [...]
  - **Orientation:** [...]
  - **Primary Target Movement(s):** [...]
  - **Rationale:** [Justify this *final* placement, referencing the input designs if relevant]

... (repeat for all 4 sensors) ...

#### Machine-Readable Output (FINAL)

```
{
  "design_id": "LLM_Only_FINAL",
  "sensor_count": 4,
  "sensors": [
    {
      "id": 1,
      "anatomical_location": "...",
      "orientation": "...",
      "primary_targets": ["..."],
      "coordinates_description": "..."
    }
  ]
}
```

Fig. 13. Prompt for convergent phase. This prompt synthesizes  $N = 5$  independent designs from Phase A into a single consolidated master design.

### SYSTEM ROLE

You are the Lead Sensor Layout Designer for an advanced wearable motion-tracking system. Your mission is to develop an optimal sensor topology using a **SpectraFlex Flex Sensors (95mm, Male Pins)** specifically engineered for the **Shoulder Joint Complex**. The success of your design will be measured by its ability to achieve the lowest possible Mean Per-Joint Angular Error (MPJAE) for the critical motions: **Flexion, Abduction, and Rotation**, while accounting for the sensor's inherent bending-aware characteristics.

### THE DATA CONTEXT

- ① **Current Design (Iteration N)**

*[JSON of the current sensor layout inserted programmatically]*

- ② **Quantitative Metrics (The Signal Reality)**

(Performance data from the hardware validation loop)

*[Per-angle MPJAE, signal variance, SNR, etc. inserted programmatically]*

- ③ **Human Expert Feedback (The Physical Reality)**

(Observational notes from the domain expert regarding fit, mechanics, and artifacts)

*[Per-sensor observational notes on fit, mechanics, motion artifacts, comfort inserted programmatically]*

### YOUR TASK: ROOT CAUSE ANALYSIS

You need to diagnose why the current design is not performing perfectly.

You must synthesize the **Quantitative Metrics** with the **Human Expert Feedback** to find the root causes of error.

■ **Output Format:** Provide a clear, professional engineering report. The diagnosis will directly condition the next design iteration (P5).

Fig. 14. Prompt for Diagnostic Integration. The LLM receives the current design, quantitative performance metrics, and qualitative human designer feedback, then diagnoses failure modes.

**CONTEXT LINK**

Thank you for the analysis. I now have a clear understanding of the root causes.

**YOUR TASK (PART 2: DESIGN APPLICATION)**

Based **strictly** on the diagnosis and strategy you just provided, please generate the specific sensor layout for **Iteration N+1**.

**DESIGN REQUIREMENTS**

- **Number of Sensors:** Exactly 4 sensors.
- **Target Body Part:** Shoulder Joint Complex
- **Sensor Type:** SpectraFlex Flex Sensors (95mm, Male Pins) (95mm length).
- **Target Outputs:** The layout should optimally predict Flexion, Abduction, Rotation.
- **Garment Type:** Tight-fitting upper-body garment.

**OUTPUT FORMAT (STRICT)**

Please provide your design in the following structured format:

**Design Overview**

*[A concise summary of the changes made and the rationale.]*

**Sensor Layout Specification**

For each of the 4 sensors, provide:

- **Sensor [Number]:**
  - **Anatomical Location:** [Precise description]
  - **Orientation:** [Vertical / Horizontal / Oblique]
  - **Primary Target Movement(s):** [Which angle(s) this sensor captures]
  - **Rationale:** [Link this decision to your Step 1 diagnosis.]

**Machine-Readable Output**

Provide the design in JSON format.

**JSON SCHEMA (KNEE EXAMPLE — ANTI-PRIMING)**

**IMPORTANT:** The example below is for a **KNEE** layout. Use this structure, but apply it to the **Shoulder Joint Complex**.

```
{
  "design_id": "LH_Iteration_Next",
  "sensor_count": 4,
  "sensors": [
    {
      "id": 1,
      "anatomical_location": "EXAMPLE: Distal Rectus Femoris (Knee)",
      "orientation": "Vertical",
      "primary_targets": ["Knee Flexion"],
      "coordinates_description": "EXAMPLE: 5cm proximal to patella, midline. (Adjusted to improve stability)"
    },
    {
      "id": 2,
      "anatomical_location": "...",
      "orientation": "...",
      "primary_targets": ["..."],
      "coordinates_description": "..."
    }
  ]
}
```

**CRITICAL INSTRUCTIONS**

- ① **Consistency Check:** Ensure your design choices are directly traceable to your Step 1 diagnosis.
- ② **No New Knowledge:** Do NOT introduce new analysis that was not mentioned in Part 1.
- ③ **Precision:** Be as specific as possible in anatomical descriptions.

— *Begin your design now.* —

Fig. 15. Prompt for synthesis and refinement. Conditioned on the diagnosis, this prompt generates the next-iteration sensor layout.

## B LLM Initial Design Outputs

### C1 — Run 1 — Knowledge Elicitation

#### 2. Skin Deformation & Strain Patterns

##### Areas of Significant Skin Stretch/Deformation

During large-amplitude shoulder movements, **skin stretch is not uniform** across the region. Key zones of deformation:

- **Anterior Shoulder (Deltopectoral Groove):** Stretches during flexion, horizontal adduction, and internal rotation.
- **Lateral Deltoid Region:** Stretches during abduction and flexion.
- **Posterior Shoulder (Over Infraspinatus/Teres Minor):** Stretches during extension, horizontal abduction, and external rotation.
- **Superior Shoulder (Over Acromion):** Experiences less stretch due to bony prominence—usually a line of non-extension.
- **Axillary (Underarm) Region:** Stretches during abduction; complex deformation due to folding and sliding of skin.

##### Direction of Principal Strain (Critical)

**Principal strain directions** align with the underlying muscle fiber orientation and the direction of segment movement:

- **Flexion:** Maximum stretch is along the anterior deltoid, running from the clavicle/acromion toward the humeral shaft.
- **Abduction:** Maximum stretch is from the lateral acromion down the deltoid toward the midshaft humerus.
- **Internal Rotation:** Principal strain appears diagonally from the anterior shoulder (pectoralis major/deltoid) toward the posterior axilla.
- **External Rotation:** Principal strain runs from the posterior deltoid/infraspinatus toward the anterior axilla.

**Lines of non-extension** (i.e., skin folds or regions overlying bony prominences like the acromion or clavicle) experience minimal strain and are less informative for sensor placement.

##### Correlation of Skin Stretch with Sensor Orientation

- **Strain sensors are most effective when their longitudinal axis aligns with the direction of principal skin stretch.**
- For **uni-directional sensors**, off-axis placement (not parallel to principal strain) will reduce sensitivity and may introduce artifacts.
- Therefore, identifying and matching the principal strain direction for each movement/region is crucial for optimal signal acquisition.

#### 3. Sensor Placement Principles

##### General Principles and Heuristics

- **Align with Principal Strain:** Place sensors along skin regions that exhibit maximal and consistent strain for the target joint angles, matching the sensor axis to the principal strain direction.
- **Cover Multiple DOFs:** Distribute sensors to capture independent information about the three primary movements, minimizing overlap of strain patterns.
- **Avoid Lines of Non-Extension:** Placing sensors over bony prominences or skin folds reduces signal quality and may increase noise.
- **Stable Attachment:** Select regions where the garment remains in close, stable contact with the skin to avoid motion artifacts.
- **Reference to Anatomical Landmarks:** Use landmarks such as the acromion, lateral epicondyle, clavicle, and scapular spine for consistent and reproducible placement.

##### Biomechanical and Physiological Factors

- **Muscle Bulk and Movement:** Consider regions where muscle contraction changes local skin tension (e.g., over the deltoid).
- **Scapular Movement:** Scapular motion can confound readings if sensors are placed too medially or over the scapula itself.
- **Soft Tissue Displacement:** Areas with significant overlying soft tissue may dampen or distort strain signals.

##### Anatomical Landmarks for Reference

- **Acromion Process**
- **Clavicle (lateral third)**
- **Deltoid Tuberosity (mid-humerus, lateral)**
- **Scapular Spine**
- **Axillary Folds (anterior/posterior)**

These points aid in reproducible placement and alignment with principal movement axes.

#### 4. Design Trade-offs and Constraints

Given **K = 4 sensors** (hard constraint), the following trade-offs and considerations are critical:

Fig. 16. C1 Run 1 — Knowledge Elicitation (Part 1).

**Coverage vs. Redundancy**

- **Coverage:** With only four sensors, prioritizing maximum independent coverage of the three DOFs is generally preferred over redundancy.
- **Redundancy:** Adding overlapping sensors improves robustness to noise or garment slippage but reduces the number of distinct movement directions captured.
- **Optimal Strategy:** Assign at least one sensor to capture the principal strain for each DOF, and use the fourth sensor to either enhance information on a complex movement or provide minimal redundancy for the most critical DOF.

**Signal Quality vs. Comfort**

- **Optimal Signal Locations:** Regions of greatest stretch (e.g., anterior/lateral/posterior deltoid) often provide the best signals but may be over bony or highly mobile areas, leading to discomfort or garment instability.
- **Comfort Considerations:** Avoid axilla (can chafe), upper trapezius (garment may slip), or areas prone to excessive garment motion.

**Inter-sensor Correlation**

- **Spacing:** Placing sensors too close together can cause redundant signals and increased correlation (i.e., limited independent information).
- **Distribution:** Sensors should be spaced to maximize coverage of the different principal strain directions and minimize redundancy, unless intentional for robustness.

**Practical Wearability**

- **Garment Construction:** Avoid placing sensors across seams, or areas prone to wrinkling or poor contact (e.g., under the arm, over the scapula).
- **User Variability:** Choose locations that are reproducible across users and body types, and that do not interfere with arm movement or garment donning/doffing.

**5. Potential Challenges**

**Common Failure Modes**

- **Garment Slippage or Misalignment:** Movement of the garment relative to the skin reduces data reliability.
- **Sensor Detachment or Wrinkling:** Poor adhesion or garment fit can cause sensors to lift or fold, corrupting the signal.
- **Cross-talk:** Movement at adjacent joints (e.g., elbow, scapula) may produce strain signals unrelated to intended shoulder movements.
- **Non-linear Skin Behavior:** Skin does not always deform linearly with underlying joint motion, especially at extremes of motion or with muscle contraction.
- **Sweat or Moisture:** Can affect sensor conductivity and adhesive properties.

**Individual Anatomical Variation**

- **Body Shape:** Variations in muscle mass, adiposity, or bone prominence affect skin stretch patterns.
- **Sex/Age Differences:** Affect skin elasticity and soft tissue distribution.
- **Scapular Kinematics:** Variability in scapulothoracic rhythm can lead to inconsistent strain patterns.
- **Sensor Placement Repeatability:** Difficulty in reproducing exact placement across users or sessions can impact calibration and accuracy.

**Summary Table**

Aspect	Key Points/Guidelines
**Anatomy**	Glenohumeral joint, scapula, deltoid, acromion, clavicle
**Movement DOFs**	Flexion/Extension, Abduction/Adduction, Internal/External Rotation
**Skin Strain Hotspots**	Anterior, lateral, posterior deltoid regions; avoid bony prominences
**Strain Direction**	Align with principal movement directions (sagittal, coronal, diagonal)
**Landmarks**	Acromion, clavicle, deltoid tuberosity, axillary folds
**Design Trade-offs**	Maximize DOF coverage, minimize redundancy, balance comfort and stability
**Constraints**	Only 4 sensors: prioritize coverage, avoid high-correlation placements
**Failure Modes**	Slippage, non-linear skin strain, garment fit issues, anatomical variability

This knowledge base will inform the subsequent sensor layout strategy, focusing on maximizing biomechanical relevance, signal quality, and practical usability given the sensor count constraint.

Fig. 17. C1 Run 1 – Knowledge Elicitation (Part 2).

**C1 — Run 1 — Design Application**

**Design Trade-offs Made**

With only four sensors, the design prioritizes maximal independent coverage of the three clinical DOFs (flexion/extension, abduction/adduction, internal/external rotation), aligning each sensor with the principal strain direction of one movement axis (Part 1, Section 4: Coverage vs. Redundancy). The fourth sensor is placed obliquely, targeting compound/diagonal movement patterns (especially internal rotation), rather than providing redundancy for robustness. This sacrifices redundancy for movements most susceptible to garment shift or individual anatomical variation. Placement avoids high-discomfort zones (axilla, upper trapezius), and sensors are distributed to minimize inter-sensor correlation (Part 1, Section 4: Inter-sensor Correlation). All placements use clear and reproducible anatomical landmarks, reflecting the importance of consistency and practical wearability stated in Part 1.

**Machine-Readable Output**

```
{
  "design_id": "LLM_Shoulder_v1",
  "sensor_count": 4,
  "sensors": [
    {
      "id": 1,
      "anatomical_location": "Anterior shoulder, from just lateral to the coracoid process (inferior to the distal clavicle) down along the anterior deltoid to the deltoid tuberosity (mid-humerus).",
      "orientation": "Vertical (sagittal plane, parallel to humeral shaft)",
      "primary_targets": ["Shoulder Flexion", "Shoulder Extension"],
      "coordinates_description": "Start: 2cm lateral to the coracoid process at the distal clavicle; End: anterior midline of the humerus at the level of the deltoid tuberosity (-12cm below acromion).",
    },
    {
      "id": 2,
      "anatomical_location": "Lateral shoulder, from the lateral tip of the acromion down over the midline of the lateral deltoid to the deltoid tuberosity.",
      "orientation": "Vertical (coronal plane, parallel to humeral shaft)",
      "primary_targets": ["Shoulder Abduction", "Shoulder Adduction"],
      "coordinates_description": "Start: lateral acromion process; End: lateral midline of the humerus at the deltoid tuberosity (-12cm below acromion).",
    },
    {
      "id": 3,
      "anatomical_location": "Posterior shoulder, from just inferior and lateral to the scapular spine (posterior deltoid origin) obliquely downward and laterally toward the posterior humerus above the triceps insertion.",
      "orientation": "Oblique (-45°, posterolateral to inferolateral)",
      "primary_targets": ["Shoulder Extension", "Shoulder External Rotation"],
      "coordinates_description": "Start: 2cm inferior to the scapular spine, posterior deltoid origin; End: posterior humerus, 4cm above the triceps insertion.",
    },
    {
      "id": 4,
      "anatomical_location": "Anterior axillary fold, starting at the lateral-inferior border of the pectoralis major running obliquely upward and laterally toward the mid-lateral humerus.",
      "orientation": "Oblique (-45°, anterolateral to superolateral)",
      "primary_targets": ["Shoulder Internal Rotation", "Shoulder Horizontal Adduction"],
      "coordinates_description": "Start: anterior axillary line at the inferior border of the deltoid; End: mid-lateral humerus, -8cm below acromion."
    }
  ]
}
```

Fig. 18. C1 Run 1 — Design Application.

## C1 — Run 2 — Knowledge Elicitation

### 2. Skin Deformation & Strain Patterns

#### Skin Stretch During Shoulder Movements

The skin overlying the Shoulder Joint Complex deforms significantly during arm motion, with **localized regions of maximum strain**. Key observations:

- **Flexion/Extension:**
- **Flexion:** Significant stretch occurs over the posterior shoulder (posterior deltoid, scapular region).
- **Extension:** Anterior shoulder (anterior deltoid, pectoral region) stretches.
- **Abduction/Adduction:**
- **Abduction:** Skin over the lateral deltoid and axillary (armpit) region stretches; inferior axillary fold may experience compression.
- **Adduction:** Less skin stretch, more compression.
- **Internal/External Rotation:**
- **Internal Rotation:** Anterior upper arm and chest skin stretches.
- **External Rotation:** Posterior/lateral shoulder (over infraspinatus/teres minor) stretches.
- **Scapular Motion:** Elevation/depression and protraction/retraction of the scapula further complicate local skin strain patterns, especially near the scapular spine and upper back.

#### Direction of Principal Strain

- **Lines of Maximum Extension (Principal Strain):** Skin stretches most along lines **parallel to the underlying muscle fiber direction** and movement vector.
- For **flexion**, principal strain is roughly **inferior–superior** direction over posterior shoulder.
- For **abduction**, principal strain is **medial–lateral** over the deltoid region.
- For **rotation**, the strain direction is **oblique**, following an **anterolateral–posteromedial** path for internal rotation and **posterolateral–anteromedial** for external rotation.
- **Lines of Non-Extension:** Perpendicular to principal strain lines; minimal sensor response if placed along these.

#### Correlation with Sensor Axis

- **Sensor Sensitivity:** Uni-directional stretch sensors are maximally responsive when their **longitudinal axis is aligned with the direction of principal strain**.
- **Placement Implication:** Sensors must be oriented **along lines of maximum expected skin stretch** for each target movement to yield strong, movement-specific signals.

### 3. Sensor Placement Principles

#### General Principles & Heuristics

- **Alignment with Principal Strain:** Place sensors along the predicted lines of maximum skin extension for each movement/DOF.
- **Non-interference:** Avoid regions with excessive garment wrinkling, folding, or anatomical occlusion (e.g., axillary fold).
- **Anatomical Landmark Referencing:** Use palpable bony landmarks (acromion, clavicle, spine of scapula, humeral shaft) for repeatable, anatomically meaningful placement.
- **Functional Coverage:** Distribute sensors to cover all desired DOFs, minimizing redundancy unless needed for robustness.

#### Biomechanical/Physiological Factors

- **Muscle Bulk & Skin Mobility:** Overlying muscles (deltoid, pectoralis) provide both prominent skin movement and stable surface.
- **Scapular Movement:** Scapular region is essential for capturing complex shoulder kinematics but can be affected by garment fit and movement artifacts.
- **Axilla (Armpit):** High skin strain but problematic for sensor adhesion and comfort.

#### Reliable Anatomical Landmarks

- **Acromion Process:** Lateral tip of the shoulder; reference for deltoid region.
- **Clavicle:** Easily palpable, guides anterior sensor placement.
- **Scapular Spine:** Posterior reference for scapular sensors.
- **Mid-humerus:** Landmark for upper arm sensor alignment.

### 4. Design Trade-offs and Constraints

Given a **hard constraint of 4 sensors**, several trade-offs arise:

Fig. 19. C1 Run 2 — Knowledge Elicitation (Part 1).

### Coverage vs. Redundancy

- **Coverage:** Maximize the number of distinct DOFs captured (ideally mapping each sensor to a unique principal strain line for a specific movement).
- **Redundancy:** Adding redundant sensors (e.g., two for the same movement) increases robustness (e.g., in case of signal loss, fit variation) but reduces DOF coverage.

With only 4 sensors, coverage of all 3 DOFs is possible, with one additional sensor for redundancy or cross-validation.

### Signal Quality vs. Comfort

- **Strong Signal Regions:** Overlying major muscles (deltoid, pectoralis) provide reliable skin stretch but may be subject to garment slippage or user discomfort.
- **Uncomfortable/Unstable Regions:** Axilla, scapular border (due to bony prominence, skin folds), and areas near garment seams can yield unreliable signals or irritate the wearer.

### Inter-sensor Correlation

- **Sensor Spacing:** Avoid clustering sensors too closely; high spatial correlation yields redundant data and wastes sensor resources.
- **Functional Independence:** Sensors should be spatially and functionally distinct (i.e., respond preferentially to different movements/DOFs) unless redundancy is an explicit design goal.

### Practical Wearability

- **Garment Construction:** Seams, stitching, and fabric stretch properties influence sensor placement feasibility.
- **User Comfort:** Avoid high-friction or high-mobility zones (e.g., directly in axilla).
- **Attachment Security:** Sensors need stable, non-slipping substrate for consistent readings.

## 5. Potential Challenges

### Common Failure Modes & Challenges

- **Sensor Slippage/Displacement:** Sensor may move relative to anatomical landmarks during high-motion activities, degrading signal fidelity.
- **Non-uniform Skin Stretch:** Skin does not always move uniformly with the underlying bone; effects vary with subcutaneous fat, skin elasticity, and muscle tone.
- **Garment Fit Variation:** Loose or wrinkled garments reduce strain transfer from skin to sensor.
- **Crosstalk:** A single sensor may respond to multiple movements due to overlapping strain fields (e.g., abduction and flexion).
- **Artifact from Garment Construction:** Seams, folds, or sensor encapsulation can introduce noise or dampen true strain.
- **Sweat & Moisture:** Can affect sensor adhesion and signal quality.

### Anatomical Variations & General-Purpose Design

- **Body Shape Differences:** Variation in muscle bulk, adiposity, and bone prominence can alter both skin strain patterns and garment fit.
- **Landmark Palpation:** Consistent placement is harder on individuals with higher adiposity or less defined bony landmarks.
- **Movement Amplitude:** Range of motion varies across individuals (age, injury history, flexibility), affecting strain magnitude.
- **Skin Properties:** Differences in skin elasticity, thickness, and hydration can alter strain transmission.

### Summary

Designing an effective sensor layout for the shoulder joint complex with only four stretch strain sensors requires deep understanding of joint biomechanics, skin strain patterns, sensor alignment, and practical garment constraints. The priority should be maximizing DOF coverage by aligning sensors along distinct principal strain lines for each clinical movement, referenced to reliable anatomical landmarks, while balancing comfort, repeatability, and robustness against individual anatomical variation. Potential challenges include garment fit, sensor slippage, and anatomical variability, all of which must inform placement strategy and overall system robustness.

**No specific sensor layout is proposed here, per instructions.**

Fig. 20. C1 Run 2 – Knowledge Elicitation (Part 2).

## C1 — Run 2 — Design Application

### Design Overview

This sensor layout strategically places four stretch strain sensors along the principal lines of skin extension corresponding to the three clinical shoulder joint angles (flexion/extension, abduction/adduction, internal/external rotation), with one sensor providing redundancy and cross-talk mitigation. Each placement is referenced to reliable anatomical landmarks and aligns the sensor axis with the predicted principal strain direction for each movement, maximizing signal quality, distinctiveness, and garment wearability as established in Part 1.

### Sensor Layout Specification

#### Sensor 1:

- **Anatomical Location:** Posterior-lateral shoulder, spanning from the midpoint of the acromion process diagonally toward the spine of the scapula.
- **Orientation:** Oblique at  $-45^\circ$ , running from superolateral (acromion) to inferomedial (scapular spine).
- **Primary Target Movement(s):** Shoulder Flexion/Extension (emphasis on flexion)
- **Rationale:** As noted, posterior shoulder skin experiences maximum stretch during shoulder flexion. Placing the sensor obliquely across the deltoid and scapular region aligns with the principal strain for flexion, leveraging the stable muscle mass for strong signal and referencing the acromion and scapular spine for repeatability (see Section 2 and 3, Part 1).

#### Sensor 2:

- **Anatomical Location:** Lateral aspect of the upper arm, over the mid-deltoid muscle, from just below the acromion process down the lateral humerus.
- **Orientation:** Vertical (parallel to the humeral shaft)
- **Primary Target Movement(s):** Shoulder Abduction/Adduction
- **Rationale:** The lateral deltoid region exhibits significant longitudinal skin stretch during abduction. This placement targets the principal strain line for abduction, using the acromion and humeral shaft as landmarks, and avoids the axilla for comfort and garment stability (see Section 2 and 3, Part 1).

#### Sensor 3:

- **Anatomical Location:** Anterior shoulder, spanning from the lateral third of the clavicle diagonally down across the anterior deltoid toward the proximal third of the humerus.
- **Orientation:** Oblique at  $-45^\circ$ , running from superomedial (clavicle) to inferolateral (anterior deltoid/humerus)
- **Primary Target Movement(s):** Shoulder Internal/External Rotation (emphasis on internal rotation)
- **Rationale:** Internal rotation creates an oblique extension of the anterior shoulder skin. This sensor's alignment matches the predicted principal strain direction for internal rotation, with placement guided by the clavicle and humeral landmarks for consistency (see Section 2 and 3, Part 1).

#### Sensor 4:

- **Anatomical Location:** Posterior upper arm, midline over the triceps, from the posterior edge of the deltoid (just below acromion) down the humeral shaft.
- **Orientation:** Vertical (parallel to the humeral shaft)
- **Primary Target Movement(s):** Shoulder External Rotation (secondary: flexion/extension cross-talk)
- **Rationale:** This region experiences principal skin stretch during external rotation and also contributes to flexion/extension signal as a cross-check. Placing the sensor here achieves partial redundancy (for flexion) and robust external rotation detection, while using anatomical landmarks for reproducibility (see Section 2, 3, and 4, Part 1).

### Design Trade-offs Made

Given the strict 4-sensor constraint, the design prioritizes coverage of all three primary shoulder DOFs by dedicating one sensor to each clinical angle, with the fourth sensor providing redundancy and cross-validation for movements that may involve overlapping strain fields (notably flexion and external rotation). Sensor placement avoids high-wrinkle and high-motion garment regions (e.g., axilla, garment seams), and leverages regions of high skin stretch over muscle mass for signal quality and user comfort (Section 4, Part 1). This sacrifices some redundancy for abduction/adduction and limits direct scapular tracking, but maximizes functional independence, anatomical repeatability, and practical wearability.

Fig. 21. C1 Run 2 — Design Application (Part 1).

**Machine-Readable Output**

```
{
  "design_id": "LLM_Shoulder_v1",
  "sensor_count": 4,
  "sensors": [
    {
      "id": 1,
      "anatomical_location": "Posterior-lateral shoulder, from midpoint of acromion process to spine of scapula",
      "orientation": "Oblique at 45°, superolateral (acromion) to inferomedial (scapular spine)",
      "primary_targets": ["Shoulder Flexion/Extension"],
      "coordinates_description": "Place sensor diagonally across the posterior deltoid, starting at the midpoint of the acromion process and ending at the superior border of the scapular spine"
    },
    {
      "id": 2,
      "anatomical_location": "Lateral upper arm, mid-deltoid, just below acromion to mid-humerus",
      "orientation": "Vertical (parallel to humerus)",
      "primary_targets": ["Shoulder Abduction/Adduction"],
      "coordinates_description": "Place sensor vertically along the lateral deltoid from just below the acromion process to approximately 95mm down the lateral humerus"
    },
    {
      "id": 3,
      "anatomical_location": "Anterior shoulder, from lateral third of clavicle across anterior deltoid to proximal humerus",
      "orientation": "Oblique at 45°, superomedial (clavicle) to inferolateral (anterior deltoid/humerus)",
      "primary_targets": ["Shoulder Internal/External Rotation"],
      "coordinates_description": "Place sensor diagonally across the anterior deltoid, starting from the lateral third of the clavicle to the proximal third of the humerus"
    },
    {
      "id": 4,
      "anatomical_location": "Posterior upper arm, midline over triceps, from posterior deltoid edge (below acromion) down humeral shaft",
      "orientation": "Vertical (parallel to humerus)",
      "primary_targets": ["Shoulder External Rotation", "Shoulder Flexion/Extension (secondary)"],
      "coordinates_description": "Place sensor vertically along the posterior upper arm, starting from the posterior edge of the deltoid just below the acromion and running down the midline over the triceps"
    }
  ]
}
```

Fig. 22. C1 Run 2 – Design Application (Part 2).

## C1 — Run 3 — Knowledge Elicitation

### 2. Skin Deformation & Strain Patterns

#### Key Skin Stretch/Deformation Regions During Movement

- **Flexion/Extension:**
  - *Flexion:* Anterior deltoid region (over clavicle and top of pectoralis major) stretches most as the arm lifts forward; posterior axillary fold compresses.
  - *Extension:* Posterior deltoid and triceps region stretches.
- **Abduction/Adduction:**
  - *Abduction:* Lateral deltoid area stretches as the arm moves away from the body; axillary arch and superior-lateral chest skin also deform.
  - *Adduction:* Medial upper arm and lower pectoral region stretch as the arm moves toward the torso.
- **Internal/External Rotation:**
  - *Internal:* Anterior aspect of upper arm and chest stretch (pecs and anterior deltoid).
  - *External:* Posterior/lateral shoulder region (posterior deltoid, infraspinatus area) stretches.

#### Direction of Principal Strain

- **Lines of Non-extension:** Often run perpendicular to the axis of joint movement (e.g., horizontal across the deltoid for abduction).
- **Lines of Maximum Extension:** Typically align with muscle fiber direction for the acting muscle (e.g., vertical or oblique over the anterior deltoid for flexion).

#### Example:

- During abduction, the *lateral deltoid* skin stretches superiorly-inferiorly (vertical).
- During flexion, the *anterior deltoid/clavicular* skin stretches in an oblique direction from the clavicle toward the lateral humerus.
- For internal/external rotation, the principal strain follows a spiral or helical path around the upper arm and shoulder.

#### Correlation with Sensor Axis

- Stretch strain sensors are most sensitive when their longitudinal axis aligns with the direction of maximum tissue stretch.
- Misalignment reduces sensitivity and may yield ambiguous signals.
- Placing sensors along the predicted path of principal strain for each movement optimizes signal quality.

### 3. Sensor Placement Principles

#### General Principles/Heuristics

- **Alignment:** Place sensors along predicted axes of principal strain for target movements.
- **Coverage:** Distribute sensors to capture distinct DOFs (e.g., one each for flexion/extension, abduction/adduction, rotation, and a redundant or composite axis).
- **Non-interference:** Avoid regions prone to excessive garment wrinkling, skin folding, or sensor crumpling.
- **Stability:** Select areas with minimal skin slippage over muscle bulk (e.g., over deltoid apex rather than axillary pouch).
- **Landmarking:** Anchor sensor endpoints to anatomical landmarks for consistency in placement and interpretation.

#### Biomechanical/Physiological Factors Guiding Placement

- **Muscle Bulk/Movement:** Overlying muscle bellies (deltoid, pecs, triceps) provide robust, repeatable deformation patterns.
- **Joint Center Proximity:** Sensors should span across the axis of rotation where possible, not directly over bony prominences (e.g., acromion) which may not deform significantly.
- **Tendon/Bone Regions:** Avoid areas with minimal soft tissue, as skin stretch may be limited.

#### Reliable Anatomical Landmarks

- Acromion (lateral shoulder tip)
- Clavicle (anterior superior)
- Deltoid tuberosity (lateral upper arm)
- Axillary fold
- Inferior angle of scapula (posterior, for reference)

These points can be consistently located and used as anchoring or reference positions for sensor placement.

### 4. Design Trade-offs and Constraints

Given  $K = 4$  sensors, the following trade-offs and considerations arise:

Fig. 23. C1 Run 3 — Knowledge Elicitation (Part 1).

### Coverage vs. Redundancy

- **Max Coverage:** Assign each sensor to a unique movement axis to capture all three main DOFs, with one extra for a composite or diagonal axis.
- **Redundancy:** Adding a second sensor along the same axis can improve robustness (e.g., averaging signals, error detection), but reduces the number of unique DOFs covered.
- **Trade-off:** With only 4 sensors, maximizing coverage is usually preferred unless one movement is clinically more important.

### Signal Quality vs. Comfort

- **Strong Signals:** Lateral and anterior deltoid, upper arm, and chest provide strong deformation signals, but sensors here may intersect axillary or pectoral regions, leading to chafing or discomfort.
- **Comfortable Regions:** Over muscle bellies tend to be more comfortable than over bony prominences or in the axilla.
- **Trade-off:** Some optimal signal regions may be less comfortable or more prone to motion artifacts; balance is needed.

### Inter-sensor Correlation

- **Spacing:** Sensors placed too close together may capture redundant information due to correlated skin deformation.
- **Orthogonality:** Placing sensors along orthogonal axes (e.g., anterior-posterior, superior-inferior, oblique) reduces inter-sensor correlation and maximizes independent information.
- **Trade-off:** Overlapping sensor regions may improve accuracy for a single DOF but at the cost of overall system coverage.

### Practical Wearability

- **Garment Construction:** Avoid seams, high-stress garment areas, or regions subject to bunching/wrinkling (e.g., axilla, underarm).
- **Donning/Doffing:** Sensors crossing high-mobility regions (e.g., axilla) may be stressed or damaged during putting on/taking off.
- **Aesthetics/Discretion:** Bulky or visible sensors may reduce user acceptance.

## 5. Potential Challenges

### Common Failure Modes/Challenges

- **Sensor Slippage:** Relative motion between garment and skin can cause misregistration of strain signals.
- **Skin Wrinkling/Folding:** In some ranges of motion, skin may fold or wrinkle, producing ambiguous or noisy signals.
- **Garment Fit Variability:** Looser garments reduce strain transfer; overly tight garments may restrict motion or cause discomfort.
- **Signal Nonlinearity:** Strain sensors may have nonlinear responses to large deformations, complicating calibration.
- **Sweat/Moisture:** May affect sensor performance, especially in axillary and upper chest regions.
- **Cross-talk:** Adjacent sensors may experience correlated stretch if not properly spaced/aligned.

### Anatomical Variation Effects

- **Body Shape Differences:** Variability in shoulder width, muscle bulk, fat distribution, and scapular positioning impacts skin deformation patterns.
- **Sex/Age Effects:** Differences in tissue composition and skin elasticity can alter strain transfer.
- **Landmark Identification:** Consistent placement across users can be challenging due to anatomical diversity.
- **General Purpose Design Implication:** Placement must account for the "average" anatomy, possibly sacrificing optimal signal for universality.

### Summary:

Designing a 4-sensor stretch strain system for the shoulder requires careful consideration of anatomical structure, movement biomechanics, skin strain patterns, and practical garment constraints. Optimal sensor placement aligns with principal strain directions for the target DOFs, uses reliable anatomical landmarks, and balances coverage, comfort, and robustness. Awareness of common challenges and individual variability is critical to developing a general-purpose, wearable system.

Fig. 24. C1 Run 3 – Knowledge Elicitation (Part 2).

## C1 — Run 3 — Design Application

### Design Trade-offs Made

With only four sensors, the design prioritizes maximal independent coverage of each clinical DOF (flexion/extension, abduction/adduction, internal/external rotation), as recommended in Part 1, Section 4 (Coverage vs. Redundancy). This means each sensor is primarily dedicated to a unique movement axis, sacrificing redundancy for robustness. Placement targets regions of strong, repeatable skin stretch, but avoids the axilla and areas prone to garment wrinkling (Signal Quality vs. Comfort, Practical Wearability). Sensors are spaced to minimize inter-sensor correlation and maximize orthogonality of information. Some secondary or subtle scapular contributions may not be fully captured due to sensor count constraints, but the chosen layout balances biomechanical fidelity with practical garment integration, as per the principles in Part 1.

### Machine-Readable Output

```
{
  "design_id": "LLM_Shoulder_v1",
  "sensor_count": 4,
  "sensors": [
    {
      "id": 1,
      "anatomical_location": "Anterior shoulder, spanning from the lateral third of the clavicle to the mid-humerus (over anterior deltoid)",
      "orientation": "Oblique (approx. 30-45° from horizontal, running inferolaterally)",
      "primary_targets": ["Shoulder Flexion/Extension"],
      "coordinates_description": "Origin at lateral third of clavicle, terminating at mid-humerus anterior surface, directly over anterior deltoid muscle belly"
    },
    {
      "id": 2,
      "anatomical_location": "Lateral shoulder, from acromion to deltoid tuberosity of the humerus (over mid-deltoid)",
      "orientation": "Vertical (superior-inferior)",
      "primary_targets": ["Shoulder Abduction/Adduction"],
      "coordinates_description": "Origin at acromion (lateral tip of shoulder), terminating at deltoid tuberosity (midpoint on lateral humerus)"
    },
    {
      "id": 3,
      "anatomical_location": "Posterior shoulder, from spine of the scapula (just medial to the acromion) to posterior mid-humerus (over posterior deltoid)",
      "orientation": "Oblique (approx. 30-45° from horizontal, running inferolaterally)",
      "primary_targets": ["Shoulder Extension", "Shoulder External Rotation"],
      "coordinates_description": "Origin at spine of scapula (proximal to acromion), terminating at posterior mid-humerus, overlying posterior deltoid bulk"
    },
    {
      "id": 4,
      "anatomical_location": "Upper arm, spiral path from medial bicipital groove (proximal, near axilla) anteriorly, diagonally across humerus to lateral mid-humerus",
      "orientation": "Oblique/Spiral (approx. 45° from vertical, anterior-medial to lateral)",
      "primary_targets": ["Shoulder Internal/External Rotation"],
      "coordinates_description": "Origin at proximal medial bicipital groove (near anterior axilla), wrapping diagonally over anterior upper arm to lateral mid-humerus"
    }
  ]
}
```

Fig. 25. C1 Run 3 — Design Application.

## C1 — Run 4 — Knowledge Elicitation

### 1. Biomechanical Foundations

#### 1.1 Anatomical Structures Relevant to Motion Capture

The **Shoulder Joint Complex** is among the most mobile and biomechanically intricate regions of the body. It consists of several articulating components:

- **Glenohumeral (GH) Joint:** Ball-and-socket joint between the humeral head and the glenoid fossa of the scapula. Primary contributor to arm movement.
- **Scapulothoracic (ST) Articulation:** Functional joint where the scapula glides over the posterior thoracic cage; essential for full range of motion.
- **Acromioclavicular (AC) Joint:** Junction between the clavicle and the acromion of the scapula; allows scapular rotation and tilting.
- **Sternoclavicular (SC) Joint:** Connects the clavicle to the sternum; allows clavicular elevation, protraction, and rotation.

#### Key Supporting Tissues:

- **Muscles:** Deltoid, rotator cuff group (supraspinatus, infraspinatus, teres minor, subscapularis), pectoralis major, latissimus dorsi, trapezius, serratus anterior.
- **Ligaments:** GH ligaments, coracoacromial ligament, AC and SC ligaments.
- **Skin and Superficial Fascia:** Overlies these structures, mediates strain transmission to wearable sensors.

#### 1.2 Primary Degrees of Freedom (DOF) and Movements

The shoulder complex offers a high degree of mobility, with three principal DOFs at the GH joint, augmented by scapular and clavicular movements:

- **Flexion/Extension:** Movement of the arm in the sagittal plane (forward/backward).
- **Abduction/Adduction:** Movement in the coronal plane (away from/toward the body midline).
- **Internal/External Rotation:** Rotation about the humeral axis (turning the arm inward/outward).
- **Secondary SC and ST Contributions:** Scapular upward/downward rotation, elevation/depression, protraction/retraction.

#### 1.3 Target Movements/Angles

For clinical motion capture, the **Shoulder Clinical Joint Angles** of interest are:

- **Flexion/Extension:** Raising/lowering the arm in front of the body.
- **Abduction/Adduction:** Raising/lowering the arm out to the side.
- **Internal/External Rotation:** Rotating the arm along its long axis with the elbow flexed at 90°, typically with the arm at the side or abducted to 90°.

## 2. Skin Deformation & Strain Patterns

### 2.1 Regions of Maximum Skin Stretch/Deformation

Shoulder movements produce complex skin deformations, influenced by underlying muscle contraction, joint articulation, and sliding of the scapula:

- **Anterior Shoulder (Deltoid/Clavicle Region):** Significant stretch during flexion and abduction.
- **Lateral Aspect (Over Deltoid):** Stretched during abduction, flexion, and external rotation.
- **Posterior Shoulder (Scapular Spine, Infraspinatus Region):** Stretched during horizontal abduction, extension, and internal rotation.
- **Axillary Fold (Inferior Border of Deltoid):** Notable stretch during abduction/adduction.
- **Upper Trapezius/Clavicle:** Stretches during scapular elevation and protraction.

### 2.2 Principal Strain Directions

- **Flexion:** Skin stretches in an anteroposterior direction over the anterior deltoid and upper arm.
- **Abduction:** Stretch is maximal over the lateral deltoid, running superior-inferiorly (shoulder-to-arm).
- **Internal/External Rotation:** Torsional or helical strain patterns around the upper arm, with the greatest skin movement over the lateral and posterior deltoid.
- **Lines of Non-Extension:** Typically align with the axis of the humerus and the acromion-clavicular region; minimal skin stretch.

Fig. 26. C1 Run 4 — Knowledge Elicitation (Part 1).

### 2.3 Correlation with Sensor Longitudinal Axis

- For **optimal sensitivity**, sensors should be aligned with the direction of principal skin stretch for the targeted movement.
- **Uni-directional sensors**: If the principal strain is along the longitudinal axis of the sensor, signal amplitude is maximized.
- If placed perpendicular to the main strain direction, the sensor's output will be minimized and less informative.

## 3. Sensor Placement Principles

### 3.1 General Principles/Heuristics

- **Alignment to Strain**: Place sensors along the lines of maximum extension for each movement/DOF to maximize signal-to-noise ratio.
- **Coverage of DOFs**: Distribute sensors to uniquely capture the strain signatures associated with each clinical angle/movement.
- **Avoid Lines of Non-Extension**: These areas will yield minimal sensor output.
- **Minimize Crosstalk**: Avoid placements where multiple DOFs generate similar strain signals in the same sensor.

### 3.2 Biomechanical/Physiological Factors

- **Muscle Bulk and Movement**: Sensors over large, mobile muscles (e.g., deltoid) capture substantial strain but are also more susceptible to artifacts from muscle bulging.
- **Skin Mobility**: Regions where the skin slides significantly over underlying tissue (e.g., over scapula) may introduce noise.
- **Joint Proximity**: Closer placement to the GH joint captures more direct joint-related strain but may be limited by garment fit.

### 3.3 Reference Anatomical Landmarks

- **Acromion Process**: Key superior bony landmark for repeatable placement.
- **Deltoid Tuberosity**: Distal lateral humerus, for anchoring sensor ends.
- **Clavicle**: For anterior placements.
- **Scapular Spine and Inferior Angle**: Posterior reference points.
- **Axillary Line**: Useful for tracking abduction/adduction.

## 4. Design Trade-offs and Constraints

### 4.1 Coverage vs. Redundancy

- **Coverage**: With only 4 sensors, maximizing the unique capture of each DOF is critical. Prioritize placements that provide complementary information for different movements.
- **Redundancy**: Some redundancy improves robustness to signal loss or noise but sacrifices the ability to capture all DOFs distinctly.

### 4.2 Signal Quality vs. Comfort

- **Strong Signal Regions**: Overlying the deltoid or upper lateral arm produce strong signals but may be uncomfortable, especially near the axilla or where the skin is highly mobile.
- **Comfort**: Avoid placing sensors where they may cause chafing (e.g., inside axilla), impede joint motion, or where they are subject to frequent garment slippage.

### 4.3 Inter-sensor Correlation

- **Proximity**: Closely placed sensors may experience highly correlated strains, reducing the effective number of independent signals.
- **Spacing**: Distribute sensors to maximize information diversity, unless aiming for redundancy for error correction.

### 4.4 Practical Wearability

- **Garment Construction**: Avoid regions with seams, high stretch, or where sensors could delaminate due to constant motion.
- **Attachment**: Ensure sensor ends can be securely anchored to stable garment regions (e.g., at or near bony landmarks).
- **User Variability**: Placement should be robust to differences in body size, shape, and garment fit.

## 5. Potential Challenges

### 5.1 Common Failure Modes

- **Sensor Slippage**: Movement of the garment relative to the skin leads to signal artifacts.
- **Signal Saturation**: Excessive strain may drive sensors beyond their operational range, especially during large movements.
- **Crosstalk**: Sensors may respond to multiple DOFs, confounding interpretation.
- **Wear-and-Tear**: Frequent motion and washing may degrade sensor performance.

Fig. 27. C1 Run 4 – Knowledge Elicitation (Part 2).

### 5.2 Individual Anatomical Variation

- **Muscle Mass and Fat Distribution:** Varies greatly, affecting strain transfer from skin to sensor.
- **Bone Landmark Palpability:** Difficult in users with high adiposity, complicating repeatable placement.
- **Arm Length and Circumference:** Alters strain profiles and effective sensor coverage.
- **Scapular Kinematics:** Vary widely between individuals, especially with different shoulder pathologies or postures.

#### Summary:

Designing a 4-sensor stretch strain wearable for the shoulder requires careful mapping of anatomical landmarks, alignment with principal skin strain directions for each clinical DOF, and balancing coverage against comfort and redundancy. The complexity of the shoulder complex, high inter-individual variability, and practical garment constraints are major challenges. Sensor placement should maximize unique, informative strain signals corresponding to flexion/extension, abduction/adduction, and internal/external rotation, while ensuring wearability and robustness.

Fig. 28. C1 Run 4 – Knowledge Elicitation (Part 3).

## C1 — Run 4 — Design Application

### Design Trade-offs Made

Given the strict limit of four sensors, the design prioritizes unique coverage of each major shoulder DOF (flexion/extension, abduction/adduction, internal/external rotation), as recommended in Part 1, Section 4.1. Full redundancy was sacrificed in favor of maximizing information diversity. Sensors are spaced to minimize inter-sensor correlation (Part 1, 4.3) while avoiding skin regions prone to garment slippage or discomfort, particularly the axilla (Part 1, 4.2, 4.4). All placements use palpable anatomical landmarks for repeatability and robustness against anatomical variation (Part 1, 3.3, 5.2). The spiral sensor for rotation reflects a compromise: while not as robust as dual redundant sensors for DOFs, it aligns with skin strain and garment practicality. Overall, the layout favors high-quality, interpretable signals for each clinical angle, consistent with the principles articulated earlier.

### Machine-Readable Output

```
{
  "design_id": "Shoulder_4Sensor_v1",
  "sensor_count": 4,
  "sensors": [
    {
      "id": 1,
      "anatomical_location": "Anterior shoulder, spanning from just lateral to the sternoclavicular joint (clavicle) to the mid-anterior deltoid belly",
      "orientation": "Oblique (inferolateral, 30-45° from vertical)",
      "primary_targets": ["Shoulder Flexion/Extension"],
      "coordinates_description": "Starts ~2cm lateral to sternoclavicular joint on the clavicle, ending at the center of the anterior deltoid, above the axillary fold"
    },
    {
      "id": 2,
      "anatomical_location": "Lateral shoulder, from acromion process to deltoid tuberosity on the humerus",
      "orientation": "Vertical (superior-inferior)",
      "primary_targets": ["Shoulder Abduction/Adduction"],
      "coordinates_description": "Anchored at the tip of the acromion, running straight down the midline of the lateral deltoid to the deltoid tuberosity (~10cm below acromion)"
    },
    {
      "id": 3,
      "anatomical_location": "Posterior shoulder, from spine of scapula (just medial to acromion) to posterior deltoid insertion",
      "orientation": "Oblique (inferolateral, 30-45° from vertical)",
      "primary_targets": ["Shoulder Extension", "Horizontal Abduction", "Internal/External Rotation (secondary)"],
      "coordinates_description": "Starts at the midpoint of the scapular spine (medial to acromion), ending at the posterior deltoid insertion, above the triceps"
    },
    {
      "id": 4,
      "anatomical_location": "Proximal upper arm, spiraling from lateral just below deltoid insertion toward anterior-medial biceps region",
      "orientation": "Oblique spiral (approximately 45°)",
      "primary_targets": ["Shoulder Internal/External Rotation"],
      "coordinates_description": "Begins on lateral upper arm about 3cm below deltoid insertion, wraps obliquely around the arm toward the medial biceps"
    }
  ]
}
```

Fig. 29. C1 Run 4 — Design Application.

## C1 — Run 5 — Knowledge Elicitation

### 2. Skin Deformation & Strain Patterns

#### Skin Stretch During Movements

The **skin overlying the shoulder** undergoes complex deformation due to multi-axial joint movement, sliding of underlying tissues, and muscle contraction. Key observations:

- **Flexion/Extension:**
  - During flexion (arm forward), skin over the anterior deltoid and upper chest stretches, while posterior skin (scapular region) compresses/folds.
  - During extension, the opposite occurs: posterior skin stretches, anterior skin compresses.
- **Abduction/Adduction:**
  - Abduction (arm out to side) stretches the lateral deltoid and superior axillary skin, with some stretch over the upper trapezius.
  - Adduction relaxes these regions.
- **Internal/External Rotation:**
  - Internal rotation stretches posterior skin (over infraspinatus/teres minor), compresses anterior skin.
  - External rotation stretches anterior skin (over subscapularis/pectoralis major), compresses posterior skin.

#### Directions of Principal Strain

- **Lines of Maximum Extension:** Run approximately **parallel to the direction of the underlying muscle fibers** and the axis of movement.
- **Flexion:** Principal strain runs longitudinally over the anterior deltoid/pectoralis region.
- **Abduction:** Strain is mainly along the lateral aspect of the shoulder, between the deltoid tuberosity and the acromion.
- **Rotation:** Strain occurs diagonally across the shoulder, from the anterior upper arm to the posterior scapular region (and vice versa), depending on rotation direction.

**Lines of non-extension** (or minimal strain) are often along skin folds or close to bony prominences (e.g., over the acromion or spine of scapula).

#### Correlation with Sensor Axis

- **Sensor Sensitivity:** Stretch sensors are most sensitive to elongation **along their longitudinal axis**.
- **Alignment Principle:** For maximal signal, sensor axis should be **aligned with the principal strain direction** in the region of interest.
- **Orthogonal Placement:** If placed perpendicular to strain direction, signal amplitude is minimized.

### 3. Sensor Placement Principles

#### General Principles/Heuristics

1. **Anatomical Alignment:** Sensors should be placed along lines of expected maximum skin stretch for each desired movement/DOF.
2. **Functional Coverage:** Each sensor should ideally capture a unique aspect of shoulder motion, aligned with a particular DOF or a combination, given the shared movement axes.
3. **Landmark-Based Reference:** Use palpable, stable bony landmarks (acromion, clavicle, deltoid tuberosity, scapular spine) to ensure consistent placement across users and donning events.
4. **Surface Stability:** Place sensors on areas with sufficient underlying tissue to avoid artifacts from garment shifting or bone prominence.

#### Biomechanical/Physiological Factors Guiding Positioning

- **Muscle Bulk:** Regions over large muscles (deltoid, pectoralis major) can provide strong, interpretable strain signals.
- **Joint Center Proximity:** Sensors should straddle or be adjacent to the axes of rotation but not directly over highly mobile, unstable skin.
- **Skin Mobility:** Avoid highly mobile or loose skin regions (e.g., axilla), as these may introduce non-representative strain.

#### Anatomical Landmarks for Reference

- **Acromion (shoulder tip):** Consistent and palpable.
- **Clavicle (collarbone):** Easily located.
- **Deltoid Tuberosity (lateral upper arm):** Distal anchor for shoulder sensors.
- **Spine of Scapula:** Posterior reference, especially for rotation sensors.
- **Sternal Notch:** For midline reference (especially in multi-sensor arrays).

Fig. 30. C1 Run 5 — Knowledge Elicitation (Part 1).

#### 4. Design Trade-offs and Constraints

##### Coverage vs. Redundancy

- **With only 4 sensors, maximizing coverage is usually preferable:** Each sensor should ideally provide unique information about a different plane/axis of movement.
- **Redundancy (overlapping sensors):** Generally avoided unless targeting robustness for a critical DOF or compensating for expected signal loss.

##### Signal Quality vs. Comfort

- **Strong Signals:** Achievable over large, mobile muscle bellies (deltoid, pectoralis), but these regions may experience garment slippage or discomfort due to bulk.
- **Comfort/Practicality:** Avoid underarm (axilla), bony prominences (acromion, clavicle), and high-movement skin regions (where repetitive folding or bunching occurs).

##### Inter-sensor Correlation

- **Spacing:** Sensors placed too close together may measure highly correlated strains, reducing overall information content.
- **Decorrelation:** Space sensors to cover different axes or mechanical lines of action.
- **Overlap:** Some partial overlap may help with sensor fusion, but full redundancy should be avoided due to the sensor count constraint.

##### Practical Wearability

- **Garment Construction:** Avoid major seams, closure zones (e.g., zippers), and high-stretch panels designed for donning.
- **Sensor Durability:** Avoid high-wear areas (under shoulder straps, backpack contact zones).
- **Fit Consistency:** Ensure sensors are placed where the garment fits snugly and reproducibly.

#### 5. Potential Challenges

##### Common Failure Modes

- **Sensor Slippage:** Garment or sensor migration during movement leads to variable signal quality.
- **Signal Artifacts:** Due to skin folding, garment wrinkling, or sweat/moisture.
- **Sensor Saturation:** Large movements may exceed the sensor's dynamic range.
- **Cross-talk:** Adjacent movements (e.g., scapular motion) may induce strain unrelated to target DOF.
- **Interference from Clothing/Equipment:** Straps or external devices compressing sensors.

##### Individual Anatomical Variations

- **Shoulder Shape:** Differences in muscle bulk, fat distribution, and skeletal morphology affect strain patterns.
- **Skin Mobility:** Older adults or those with higher BMI may have more mobile skin, reducing signal specificity.
- **Landmark Variability:** Palpation accuracy and garment alignment may vary between users.

**General Purpose Design Implication:** Placement should be robust to inter-individual variation—favoring easily located landmarks and regions with consistent skin strain patterns across populations.

##### Summary:

Designing a 4-sensor layout to capture shoulder clinical angles with stretch strain sensors requires careful anatomical and biomechanical consideration. Sensor alignment with principal strain directions for each movement, reference to stable anatomical landmarks, avoidance of regions prone to noise or discomfort, and maximizing information content per sensor are key principles to guide the forthcoming sensor placement design.

Fig. 31. C1 Run 5 — Knowledge Elicitation (Part 2).

## C1 — Run 5 — Design Application

### Design Trade-offs Made

Given the strict limit of four sensors, the design prioritizes **maximal DOF coverage** (one sensor per principal movement axis, with the fourth capturing the complex skin strain of rotation) over redundancy. This sacrifices robustness to signal loss and limits the ability to correct for garment migration or anatomical variability, but ensures that each clinical angle is directly addressed (Part 1, Section 4). Sensors are spaced to minimize inter-sensor correlation and are placed on regions with reliable signal and high comfort, avoiding the axilla, bony prominences, and garment seams, as specified in Part 1. This approach reflects a calculated balance between coverage, signal quality, and practical wearability, directly referencing the design principles and trade-off analysis previously articulated.

### Machine-Readable Output

```
{
  "design_id": "Shoulder_Strains_v1",
  "sensor_count": 4,
  "sensors": [
    {
      "id": 1,
      "anatomical_location": "Anterior shoulder, spanning from lateral third of clavicle (just medial to acromion) to mid-humerus along the anterior deltoid",
      "orientation": "Vertical (slightly oblique, -10-15° medial to lateral)",
      "primary_targets": ["Shoulder Flexion", "Shoulder Extension"],
      "coordinates_description": "From the lateral third of the clavicle (2-3 cm medial to the acromion) down the anterior deltoid to a point halfway between the acromion and the deltoid tuberosity on the humerus"
    },
    {
      "id": 2,
      "anatomical_location": "Lateral shoulder, from acromion to deltoid tuberosity along the midline of the lateral deltoid",
      "orientation": "Vertical",
      "primary_targets": ["Shoulder Abduction", "Shoulder Adduction"],
      "coordinates_description": "From the acromion process vertically down the lateral midline of the deltoid to the deltoid tuberosity"
    },
    {
      "id": 3,
      "anatomical_location": "Posterior shoulder, from the spine of the scapula (just medial to the acromion) to mid-posterior deltoid/humerus",
      "orientation": "Vertical (slightly oblique, -10-15° lateral to medial)",
      "primary_targets": ["Shoulder Extension", "Shoulder External Rotation", "Shoulder Internal Rotation"],
      "coordinates_description": "From the spine of the scapula (1-2 cm medial to acromion) down the posterior deltoid to the mid-posterior humerus"
    },
    {
      "id": 4,
      "anatomical_location": "Oblique across anterior upper arm, from coracoid process/clavicular intersection to mid-humerus (over upper biceps)",
      "orientation": "Oblique (-45° medial-superior to lateral-inferior)",
      "primary_targets": ["Shoulder Internal Rotation", "Shoulder External Rotation", "Horizontal Adduction/Abduction"],
      "coordinates_description": "From the coracoid process/clavicular junction diagonally across the anterior upper arm to the midpoint between the biceps belly and the deltoid tuberosity"
    }
  ]
}
```

Fig. 32. C1 Run 5 — Design Application.

## C1 — Phase B — Meta-Analysis & Synthesis

### 3. Final "Master Design" Specification (STRICT FORMAT)

#### Sensor Layout Specification (FINAL)

##### Sensor 1:

- **Anatomical Location:** Anterior shoulder, spanning from the lateral third of the clavicle (just medial to the acromion) down over the anterior deltoid to the midline of the humerus.
- **Orientation:** Oblique (approx. 30–45° from horizontal, running superomedial to inferolateral).
- **Primary Target Movement(s):** Shoulder Flexion/Extension.
- **Rationale:** This placement is universally present in all designs (1–5), targeting the principal skin stretch during flexion/extension. The oblique orientation maximizes signal for flexion while minimizing overlap with the lateral sensor.

##### Sensor 2:

- **Anatomical Location:** Lateral shoulder, from the acromion process vertically down the midline of the lateral deltoid to the deltoid tuberosity.
- **Orientation:** Vertical (superior-inferior, parallel to humeral shaft).
- **Primary Target Movement(s):** Shoulder Abduction/Adduction.
- **Rationale:** All designs converge on this placement, which aligns with the axis of maximal skin stretch during abduction/adduction and uses clear, repeatable landmarks.

##### Sensor 3:

- **Anatomical Location:** Posterior shoulder, from the spine of the scapula (just medial to the acromion) obliquely down over the posterior deltoid to the posterior mid-humerus.
- **Orientation:** Oblique (approx. 30–45° from horizontal, superomedial to inferolateral).
- **Primary Target Movement(s):** Shoulder Extension, Shoulder External Rotation.
- **Rationale:** All designs include this sensor, with consensus on its oblique path to best capture extension and external rotation, using robust bony landmarks.

##### Sensor 4:

- **Anatomical Location:** Proximal upper arm, spiral path from the medial bicipital groove (proximal, near anterior axilla) diagonally across the anterior upper arm to the lateral mid-humerus.
- **Orientation:** Oblique/spiral (approx. 45° from vertical, anterior-medial to lateral).
- **Primary Target Movement(s):** Shoulder Internal/External Rotation, Horizontal Adduction/Abduction.
- **Rationale:** Synthesizing Designs 1, 3, 4, and 5, this spiral/oblique path best captures the complex skin strain during internal/external rotation, while avoiding the axilla and maximizing garment practicality.

Fig. 33. C1 Phase B — Meta-Analysis & Synthesis (Part 1).

**Machine-Readable Output (FINAL)**

```

{
  "design_id": "LLM_Only_FINAL",
  "sensor_count": 4,
  "sensors": [
    {
      "id": 1,
      "anatomical_location": "Anterior shoulder, spanning from the lateral third of the clavicle (just medial to the acromion) down over the anterior deltoid to the midline of the humerus.",
      "orientation": "Oblique (approx. 30-45° from horizontal, running superomedial to inferolateral)",
      "primary_targets": [
        "Shoulder Flexion",
        "Shoulder Extension"
      ],
      "coordinates_description": "Origin: lateral third of clavicle (2-3 cm medial to acromion); Termination: midline of anterior humerus at the level of the deltoid tuberosity."
    },
    {
      "id": 2,
      "anatomical_location": "Lateral shoulder, from acromion process vertically down the midline of the lateral deltoid to the deltoid tuberosity.",
      "orientation": "Vertical (superior-inferior, parallel to humeral shaft)",
      "primary_targets": [
        "Shoulder Abduction",
        "Shoulder Adduction"
      ],
      "coordinates_description": "Origin: tip of acromion; Termination: deltoid tuberosity on lateral humerus (~10-12 cm below acromion)."
    },
    {
      "id": 3,
      "anatomical_location": "Posterior shoulder, from the spine of the scapula (just medial to the acromion) obliquely down over the posterior deltoid to the posterior mid-humerus.",
      "orientation": "Oblique (approx. 30-45° from horizontal, superomedial to inferolateral)",
      "primary_targets": [
        "Shoulder Extension",
        "Shoulder External Rotation"
      ],
      "coordinates_description": "Origin: spine of scapula (1-2 cm medial to acromion); Termination: posterior mid-humerus, overlying posterior deltoid."
    },
    {
      "id": 4,
      "anatomical_location": "Proximal upper arm, spiral path from the medial bicipital groove (proximal, near anterior axilla) diagonally across the anterior upper arm to the lateral mid-humerus.",
      "orientation": "Oblique/spiral (approx. 45° from vertical, anterior-medial to lateral)",
      "primary_targets": [
        "Shoulder Internal Rotation",
        "Shoulder External Rotation",
        "Horizontal Adduction",
        "Horizontal Abduction"
      ],
      "coordinates_description": "Origin: proximal medial bicipital groove (near anterior axilla); Path: diagonally over anterior upper arm; Termination: lateral mid-humerus, just below deltoid insertion."
    }
  ]
}

```

Fig. 34. C1 Phase B — Meta-Analysis &amp; Synthesis (Part 2).

**C Iteration Layouts**

Figure 35 presents the complete set of sensor layouts evaluated across both experiments, providing a visual reference for the iteration trajectories summarized in Table 4.

Several spatial trends are visible. In the H-Series, Designers A and B progressively shifted sensors toward the posterior shoulder and scapular regions across iterations, converging on similar coverage despite different starting configurations. Designer C's H-Series regression in iteration 2 ( $H_1^C: 10.08^\circ \rightarrow H_2^C: 13.03^\circ$ ) corresponds to a visible repositioning that reduced posterior coverage. In the LH-Series, Designer C's monotonic improvement is accompanied by gradual anterior-to-posterior migration and alignment of sensors along muscle fiber directions, while Designer A's single-round modification resulted in a substantially different spatial distribution that increased error. Designer B's LH-Series shows moderate spatial adjustments in iteration 1 followed by a redistribution in iteration 2 that did not sustain the initial improvement.

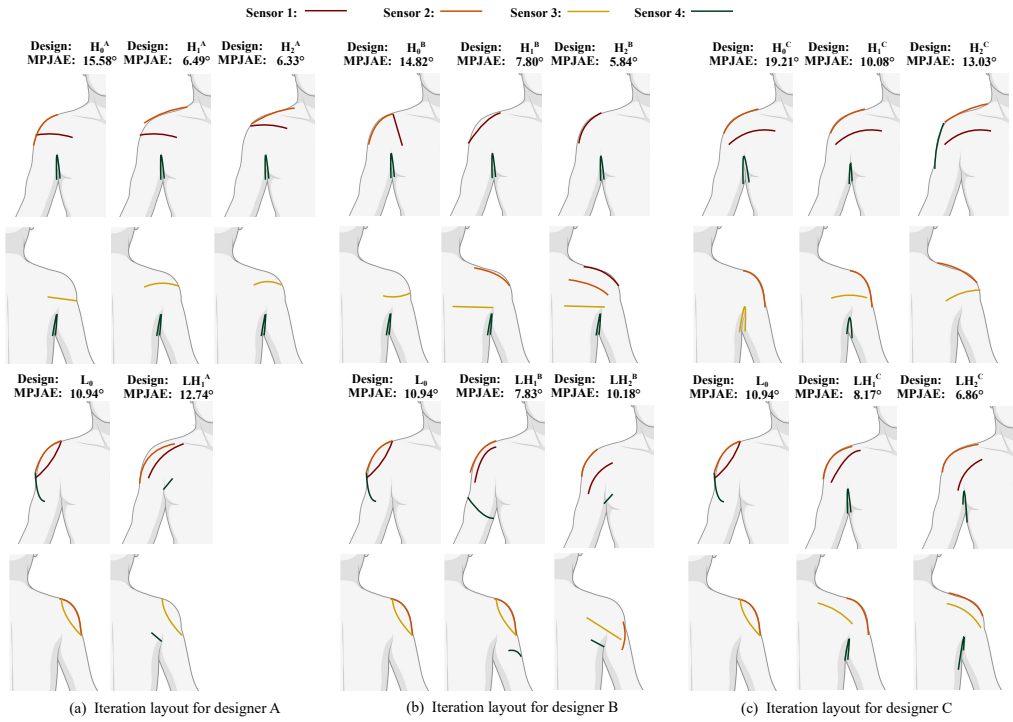


Fig. 35. Complete sensor layout evolution across all experimental conditions. Each sub-figure corresponds to one designer: (a) Designer A (kinesiology), (b) Designer B (e-textile engineering), (c) Designer C (electrical engineering). Within each sub-figure, the top row shows the H-Series (human-only iteration from  $H_0$ ) and the bottom row shows the LH-Series (human-AI collaboration from  $L_0$ ), each depicted in anterior and posterior views. Sensors are color-coded: Sensor 1 (red), Sensor 2 (orange), Sensor 3 (yellow), Sensor 4 (teal). MPJAE values are annotated for each layout.

## D Performance Feedback Dashboard

Figures 36–41 present the performance feedback dashboards provided to each designer after every iteration cycle, showing global metrics (MPJAE, AMPE, PCC, RMSE), per-joint error decomposition, angle prediction curves, and sensor contribution rankings.

**C4 WORKSHOP PROTOCOL - ITERATION METRICS REPORT**

---

**GLOBAL METRICS**

MPJAE: 18.943°  
 AMPE: 4.75%  
 RMSE: 17.025°  
 PCC: 0.9702  
 MAE\_S4E: 13.842°  
 MAE\_S7E: 188.851°

---

**PER-JOINT METRICS**

**FLEXION:**  
 MPJAE: 18.413°  
 AMPE: 5.98%  
 RMSE: 25.784°  
 PCC: 0.8796  
 ROM: 181.84°

**ABDUCTION:**  
 MPJAE: 9.418°  
 AMPE: 15.39%  
 RMSE: 12.649°  
 PCC: 0.6223  
 ROM: 62.52°

**ROTATION:**  
 MPJAE: 5.197°  
 AMPE: 4.89%  
 RMSE: 7.266°  
 PCC: 0.8791  
 ROM: 190.27°

---

**SENSOR IMPORTANCE**

Rank	Sensor	Importance	Contribution %
#1	S1	0.2748	27.48%
#2	S2	0.2355	23.55%
#3	S4	0.2333	23.33%
#4	S3	0.2372	23.72%

Mean: 0.2580  
 Std: 0.0388  
 Max: 0.2748  
 Min: 0.2172

---

**END OF REPORT**

---

**C4 WORKSHOP PROTOCOL - ITERATION METRICS REPORT**

---

**GLOBAL METRICS**

MPJAE: 18.943°  
 AMPE: 4.75%  
 RMSE: 17.025°  
 PCC: 0.9702  
 MAE\_S4E: 13.842°  
 MAE\_S7E: 188.851°

---

**PER-JOINT METRICS**

**FLEXION:**  
 MPJAE: 18.413°  
 AMPE: 5.98%  
 RMSE: 25.784°  
 PCC: 0.8796  
 ROM: 181.84°

**ABDUCTION:**  
 MPJAE: 9.418°  
 AMPE: 15.39%  
 RMSE: 12.649°  
 PCC: 0.6223  
 ROM: 62.52°

**ROTATION:**  
 MPJAE: 5.197°  
 AMPE: 4.89%  
 RMSE: 7.266°  
 PCC: 0.8791  
 ROM: 190.27°

---

**SENSOR IMPORTANCE**

Rank	Sensor	Importance	Contribution %
#1	S1	0.2748	27.48%
#2	S2	0.2416	24.16%
#3	S4	0.2333	23.33%
#4	S3	0.2372	23.72%

Mean: 0.2580  
 Std: 0.0388  
 Max: 0.2748  
 Min: 0.2172

---

**END OF REPORT**

---

**C4 WORKSHOP PROTOCOL - ITERATION REPORT**

---

**GLOBAL METRICS**

Global MPJAE: 6.334°  
 Global AMPE: 4.75%  
 Global RMSE: 15.457°  
 Global PCC: 0.8368

---

**PER-JOINT BREAKDOWN**

**Flexion:**  
 MPJAE: 8.762°  
 AMPE: 2.52%  
 RMSE: 23.954°  
 PCC: 0.8173  
 ROM: 345.04°

**Abduction:**  
 MPJAE: 4.824°  
 AMPE: 6.80%  
 RMSE: 6.878°  
 PCC: 0.9312  
 ROM: 78.31°

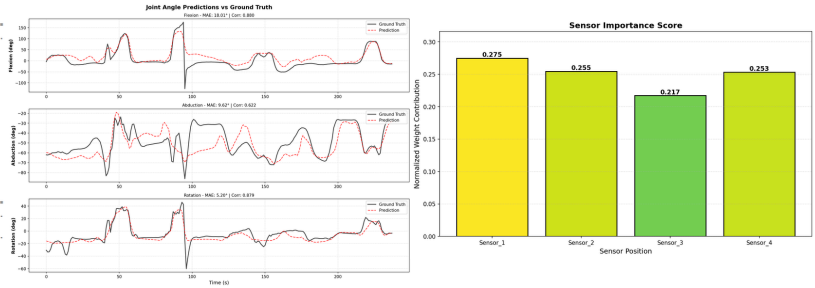
**Rotation:**  
 MPJAE: 5.476°  
 AMPE: 4.80%  
 RMSE: 9.779°  
 PCC: 0.7621  
 ROM: 112.76°

---

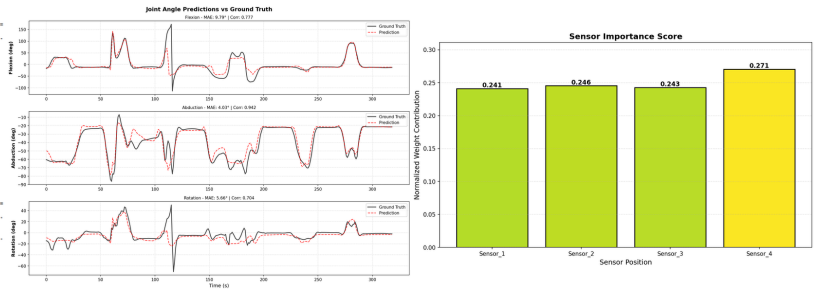
**ADDITIONAL STATISTICS**

MAE Std Dev: 14.899°  
 Max Error: 247.523°

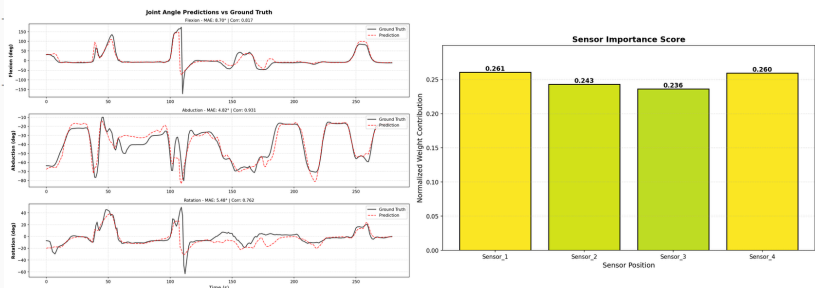
Performance feedback dashboard for  $H_0^A$



Performance feedback dashboard for  $H_1^A$



Performance feedback dashboard for  $H_2^A$



(a) Metrics report

(b) Angle prediction curve

(c) Sensor importance

Fig. 36. Performance feedback dashboard for Designer A, H-Series.

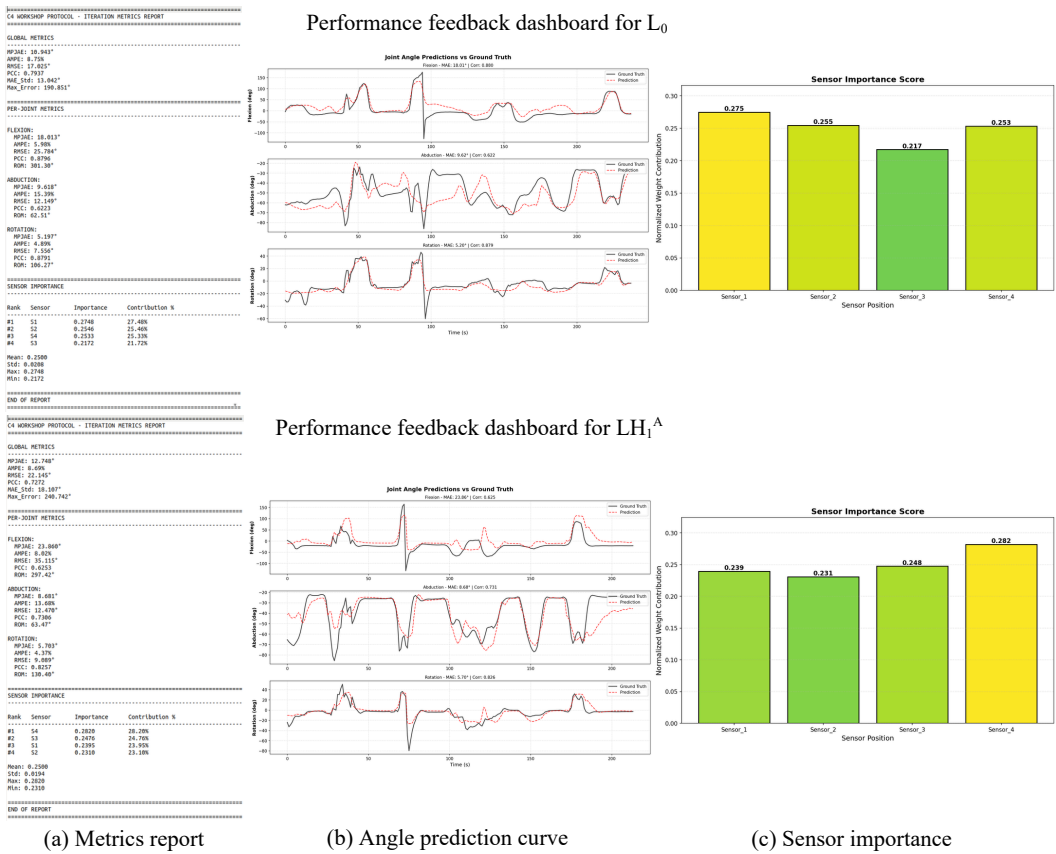


Fig. 37. Performance feedback dashboard for Designer A, LH-Series.

CA WORKSHOP PROTOCOL - ITERATION METRICS REPORT

---

GLOBAL METRICS

RMSE: 14.823°  
 AMPE: 6.50%  
 RMSE: 21.424°  
 PCCI: 0.1972  
 MAE\_S4D: 29.658°  
 MAE\_FF10F: 128.885°

---

PER-JOINT METRICS

FLEXION:  
 RMSE: 25.355°  
 AMPE: 7.45%  
 RMSE: 39.434°  
 PCCI: 0.2192  
 MAE: 589.23°

ABDUCTION:  
 RMSE: 9.811°  
 AMPE: 14.62%  
 RMSE: 14.477°  
 PCCI: 0.0153  
 MAE: 19.75°

ROTATION:  
 RMSE: 9.288°  
 AMPE: 7.53%  
 RMSE: 14.290°  
 PCCI: 0.3361  
 MAE: 157.27°

---

SENSOR IMPORTANCE

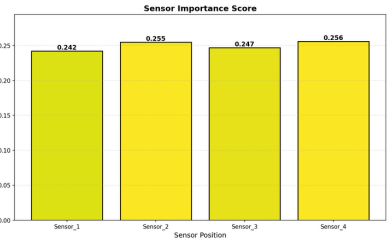
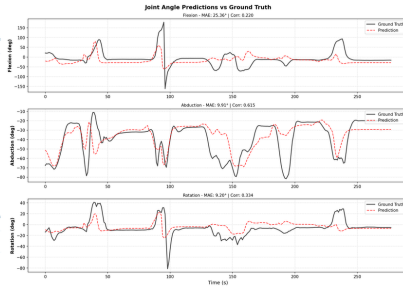
Rank	Sensor	Importance	Contribution %
#1	S4	0.2568	25.68%
#2	S2	0.2548	25.48%
#3	S1	0.2489	24.89%
#4	S3	0.2423	24.23%

Mean: 0.2500  
 Std: 0.0057  
 Max: 0.2568  
 Min: 0.2423

---

END OF REPORT

Performance feedback dashboard for  $H_0^B$



CA WORKSHOP PROTOCOL - ITERATION METRICS REPORT

---

GLOBAL METRICS

RMSE: 9.796°  
 AMPE: 6.16%  
 RMSE: 15.156°  
 PCCI: 0.0157  
 MAE\_S4D: 15.995°  
 MAE\_FF10F: 219.218°

---

PER-JOINT METRICS

FLEXION:  
 RMSE: 9.877°  
 AMPE: 3.62%  
 RMSE: 21.465°  
 PCCI: 0.0329  
 MAE: 527.45°

ABDUCTION:  
 RMSE: 7.438°  
 AMPE: 18.19%  
 RMSE: 19.118°  
 PCCI: 0.0494  
 MAE: 67.75°

ROTATION:  
 RMSE: 6.896°  
 AMPE: 6.12%  
 RMSE: 11.223°  
 PCCI: 0.7468  
 MAE: 135.68°

---

SENSOR IMPORTANCE

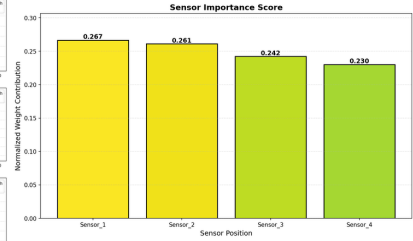
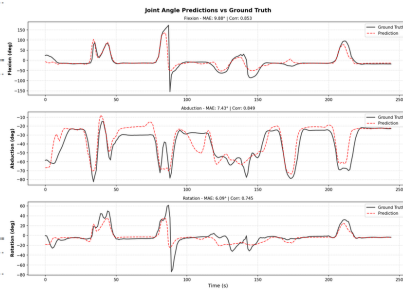
Rank	Sensor	Importance	Contribution %
#1	S2	0.2670	26.70%
#2	S1	0.2610	26.10%
#3	S3	0.2423	24.23%
#4	S4	0.2392	23.92%

Mean: 0.2500  
 Std: 0.0100  
 Max: 0.2670  
 Min: 0.2392

---

END OF REPORT

Performance feedback dashboard for  $H_1^B$



CA WORKSHOP PROTOCOL - ITERATION METRICS REPORT

---

GLOBAL METRICS

RMSE: 5.838°  
 AMPE: 6.06%  
 RMSE: 12.115°  
 PCCI: 0.0462  
 MAE\_S4D: 16.615°  
 MAE\_FF10F: 76.844°

---

PER-JOINT METRICS

FLEXION:  
 RMSE: 6.384°  
 AMPE: 3.12%  
 RMSE: 17.581°  
 PCCI: 0.0620  
 MAE: 596.51°

ABDUCTION:  
 RMSE: 6.197°  
 AMPE: 6.26%  
 RMSE: 7.251°  
 PCCI: 0.9840  
 MAE: 66.46°

ROTATION:  
 RMSE: 5.817°  
 AMPE: 3.98%  
 RMSE: 6.851°  
 PCCI: 0.8259  
 MAE: 132.46°

---

SENSOR IMPORTANCE

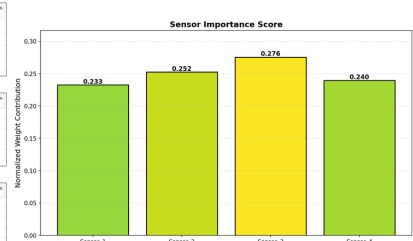
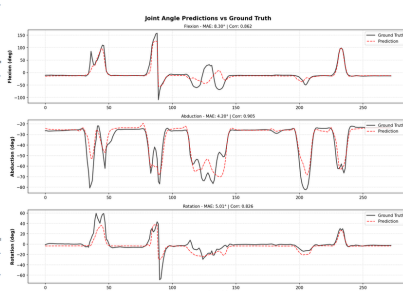
Rank	Sensor	Importance	Contribution %
#1	S3	0.2755	27.55%
#2	S2	0.2529	25.29%
#3	S4	0.2396	23.96%
#4	S1	0.2325	23.25%

Mean: 0.2500  
 Std: 0.0168  
 Max: 0.2755  
 Min: 0.2325

---

END OF REPORT

Performance feedback dashboard for  $H_2^B$



(a) Metrics report

(b) Angle prediction curve

(c) Sensor importance

Fig. 38. Performance feedback dashboard for Expert B, H-Series.

=====

CA WORKSHOP PROTOCOL - ITERATION METRICS REPORT

=====

GLOBAL METRICS

MPAE: 18.941°  
 RMSE: 6.776°  
 RMSE: 17.023°  
 PCC: 0.71146°  
 MAE\_S40: 13.464°  
 MAE\_Error: 198.851°

=====

PER-JOINT METRICS

=====

FLEXION:

MPAE: 18.613°  
 RMSE: 5.966°  
 RMSE: 25.784°  
 PCC: 0.8786°  
 RM: 381.38°

ABDUCTION:

MPAE: 9.518°  
 RMSE: 15.396°  
 RMSE: 32.149°  
 PCC: 0.8223°  
 RM: 62.51°

ROTATION:

MPAE: 5.137°  
 RMSE: 4.896°  
 RMSE: 7.564°  
 PCC: 0.8792°  
 RM: 106.17°

=====

SENSOR IMPORTANCE

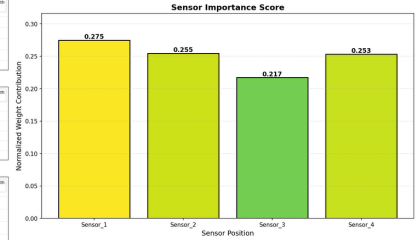
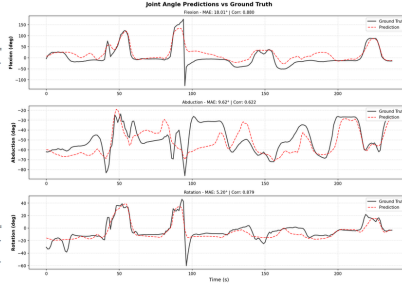
Rank	Sensor	Importance	Contribution %
#1	S1	0.2748	27.48%
#2	S2	0.2455	24.55%
#3	S3	0.2172	21.72%
#4	S4	0.2625	26.25%

Mean: 0.2489  
 Std: 0.0208  
 Max: 0.2748  
 Min: 0.2172

=====

END OF REPORT

Performance feedback dashboard for L<sub>0</sub>



=====

CA WORKSHOP PROTOCOL - ITERATION METRICS REPORT

=====

GLOBAL METRICS

MPAE: 7.829°  
 RMSE: 6.378°  
 RMSE: 17.667°  
 PCC: 0.7667°  
 MAE\_S40: 13.389°  
 MAE\_Error: 209.535°

=====

PER-JOINT METRICS

=====

FLEXION:

MPAE: 18.178°  
 RMSE: 5.125°  
 RMSE: 22.559°  
 PCC: 0.7745°  
 RM: 319.76°

ABDUCTION:

MPAE: 7.279°  
 RMSE: 11.546°  
 RMSE: 11.513°  
 PCC: 0.7784°  
 RM: 68.96°

ROTATION:

MPAE: 6.838°  
 RMSE: 6.396°  
 RMSE: 9.260°  
 PCC: 0.7663°  
 RM: 131.58°

=====

SENSOR IMPORTANCE

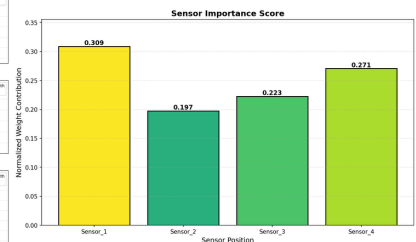
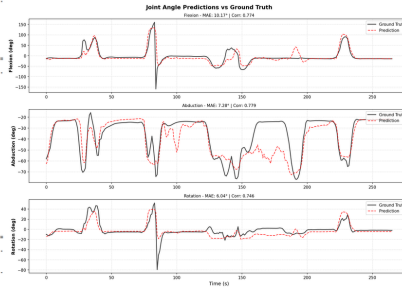
Rank	Sensor	Importance	Contribution %
#1	S1	0.3099	30.99%
#2	S4	0.2769	27.69%
#3	S2	0.2227	22.27%
#4	S3	0.1974	19.74%

Mean: 0.2580  
 Std: 0.0463  
 Max: 0.3099  
 Min: 0.1974

=====

END OF REPORT

Performance feedback dashboard for LH<sub>1</sub><sup>B</sup>



=====

CA WORKSHOP PROTOCOL - ITERATION METRICS REPORT

=====

GLOBAL METRICS

MPAE: 18.181°  
 RMSE: 7.428°  
 RMSE: 17.254°  
 PCC: 0.7076°  
 MAE\_S40: 13.391°  
 MAE\_Error: 137.999°

=====

PER-JOINT METRICS

=====

FLEXION:

MPAE: 13.688°  
 RMSE: 5.988°  
 RMSE: 23.447°  
 PCC: 0.6824°  
 RM: 386.28°

ABDUCTION:

MPAE: 8.891°  
 RMSE: 18.988°  
 RMSE: 18.942°  
 PCC: 0.8759°  
 RM: 74.147°

ROTATION:

MPAE: 6.817°  
 RMSE: 5.316°  
 RMSE: 20.789°  
 PCC: 0.7377°  
 RM: 124.19°

=====

SENSOR IMPORTANCE

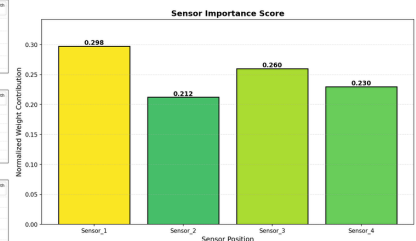
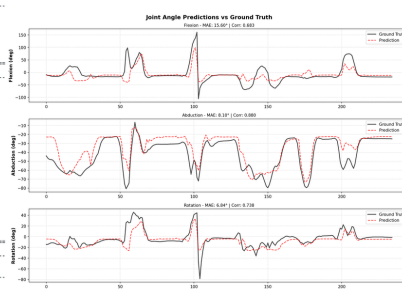
Rank	Sensor	Importance	Contribution %
#1	S1	0.2975	29.75%
#2	S2	0.2661	26.61%
#3	S4	0.2389	23.89%
#4	S3	0.2123	21.23%

Mean: 0.2580  
 Std: 0.0323  
 Max: 0.2975  
 Min: 0.2123

=====

END OF REPORT

Performance feedback dashboard for LH<sub>2</sub><sup>B</sup>



(a) Metrics report

(b) Angle prediction curve

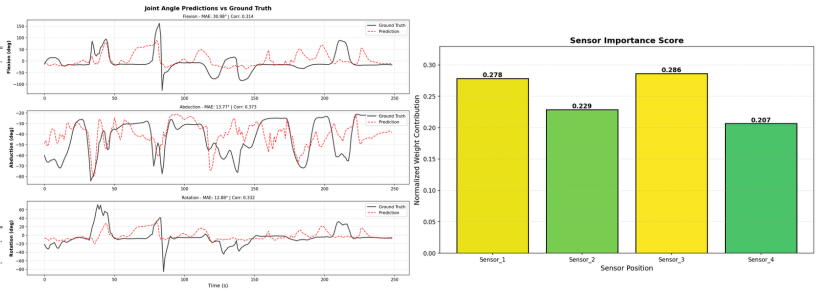
(c) Sensor importance

Fig. 39. Performance feedback dashboard for Designer B, LH-Series.

```

=====
CA WORKSHOP PROTOCOL - ITERATION METRICS REPORT
=====
GLOBAL METRICS
.....
MPJAE: 19.2807
MPSE: 15.208
RMSE: 28.8152
PCCI: 0.3296
RMSE_Sqr: 28.2847
RMSE_Error: 145.8644
=====
PER-30SNT METRICS
.....
FLEXION:
MPJAE: 26.6764
MPSE: 18.704
RMSE: 41.5517
PCCI: 0.3143
RMSE_Sqr: 28.2847
ABDUCTION:
MPJAE: 13.7617
MPSE: 11.624
RMSE: 16.4837
PCCI: 0.3727
RMSE_Sqr: 61.1647
ROTATION:
MPJAE: 12.8718
MPSE: 8.1294
RMSE: 12.566
PCCI: 0.3328
RMSE_Sqr: 157.2957
=====
SENSOR IMPORTANCE
.....
Rank  Sensor  Importance  Contribution %
#1  S3  0.2863  28.47%
#2  S1  0.2786  27.86%
#3  S2  0.2287  22.87%
#4  S4  0.2066  20.66%
Mean: 0.2588
Std: 0.0334
Min: 0.2066
Max: 0.2863
=====
END OF REPORT
=====
    
```

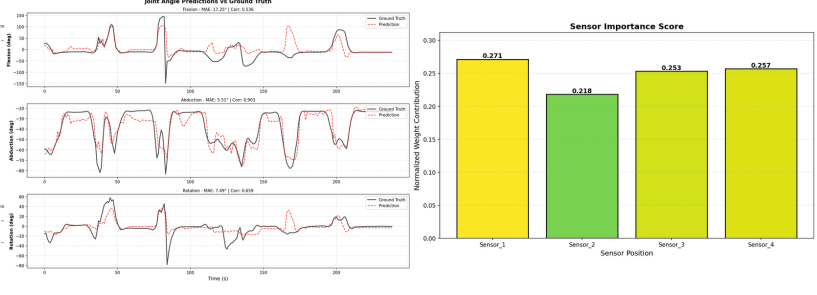
Performance feedback dashboard for  $H_0^C$



```

=====
CA WORKSHOP PROTOCOL - ITERATION METRICS REPORT
=====
GLOBAL METRICS
.....
MPJAE: 16.9857
MPSE: 6.1776
RMSE: 5.1475
PCCI: 0.3867
RMSE_Sqr: 16.3967
RMSE_Error: 244.2887
=====
PER-30SNT METRICS
.....
FLEXION:
MPJAE: 5.2807
MPSE: 0.326
RMSE: 7.3279
PCCI: 0.3928
RMSE_Sqr: 61.5137
ABDUCTION:
MPJAE: 7.4897
MPSE: 5.561
RMSE: 11.8117
PCCI: 0.4088
RMSE_Sqr: 136.1597
ROTATION:
MPJAE: 5.5807
MPSE: 3.1776
RMSE: 4.1776
PCCI: 0.4088
RMSE_Sqr: 136.1597
=====
SENSOR IMPORTANCE
.....
Rank  Sensor  Importance  Contribution %
#1  S3  0.2776  27.76%
#2  S4  0.2378  23.78%
#3  S2  0.2188  21.88%
#4  S1  0.2188  21.88%
Mean: 0.2368
Std: 0.0325
Min: 0.2188
Max: 0.2776
=====
END OF REPORT
=====
    
```

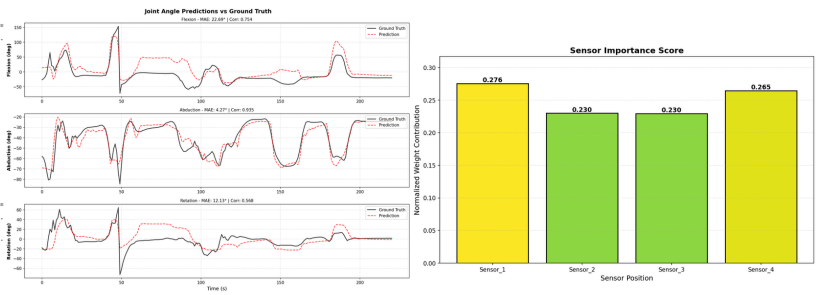
Performance feedback dashboard for  $H_1^C$



```

=====
CA WORKSHOP PROTOCOL - ITERATION METRICS REPORT
=====
GLOBAL METRICS
.....
MPJAE: 13.0271
MPSE: 6.598
RMSE: 26.1217
PCCI: 0.3725
RMSE_Sqr: 15.3567
RMSE_Error: 94.1297
=====
PER-30SNT METRICS
.....
FLEXION:
MPJAE: 22.4887
MPSE: 18.466
RMSE: 40.347
PCCI: 0.3738
RMSE_Sqr: 125.3557
ABDUCTION:
MPJAE: 4.2657
MPSE: 0.726
RMSE: 5.4887
PCCI: 0.3947
RMSE_Sqr: 61.8277
ROTATION:
MPJAE: 12.1267
MPSE: 9.476
RMSE: 16.3827
PCCI: 0.3679
RMSE_Sqr: 137.3377
=====
SENSOR IMPORTANCE
.....
Rank  Sensor  Importance  Contribution %
#1  S1  0.2786  27.86%
#2  S4  0.2647  26.47%
#3  S2  0.2382  23.82%
#4  S3  0.2295  22.95%
Mean: 0.2588
Std: 0.0285
Min: 0.2295
Max: 0.2786
=====
END OF REPORT
=====
    
```

Performance feedback dashboard for  $H_2^C$

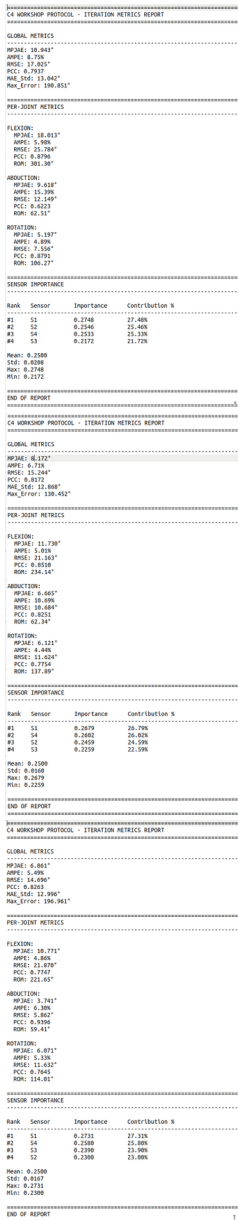


(a) Metrics report

(b) Angle prediction curve

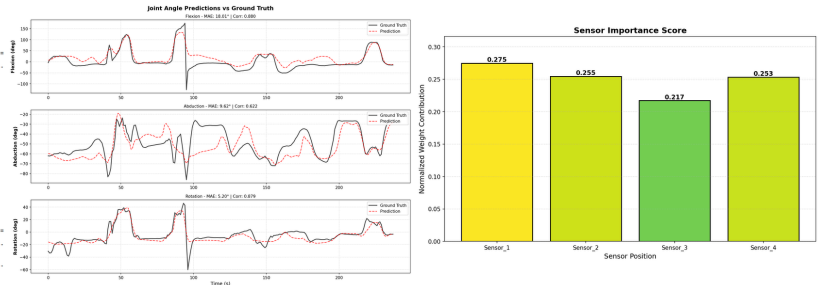
(c) Sensor importance

Fig. 40. Performance feedback dashboard for Designer C, H-Series.

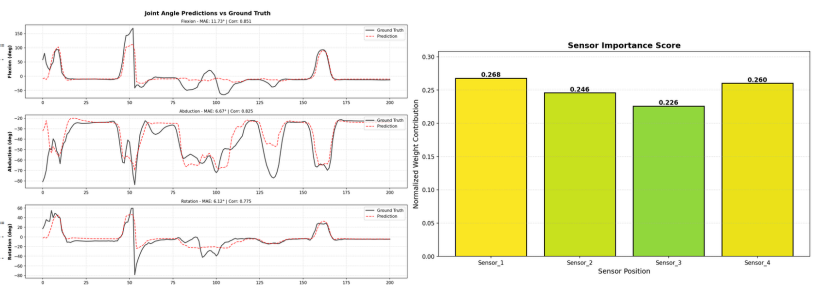


(a) Metrics report

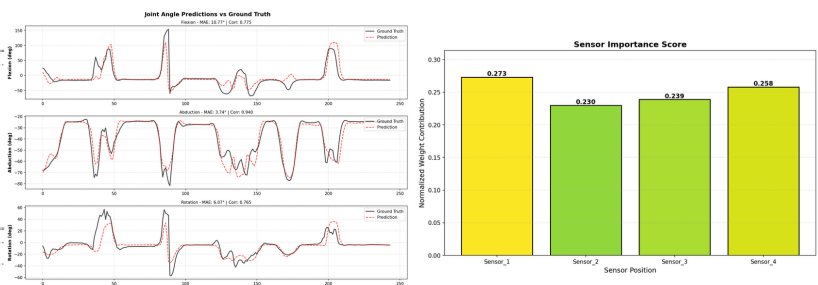
Performance feedback dashboard for L<sub>0</sub>



Performance feedback dashboard for LH<sub>1</sub><sup>C</sup>



Performance feedback dashboard for LH<sub>2</sub><sup>C</sup>



(b) Angle prediction curve

(c) Sensor importance

Fig. 41. Performance feedback dashboard for Designer C, LH-Series.

## E LH-Series Human Designer Structured Feedbacks

### Metadata

- **Expert ID:** expert\_A
- **Domain:** [not provided]
- **Iteration:** 1
- **Base Design:** L0
- **Date:** 2025-11-28
- **Time:** [not provided]

### Sensor Feedback

#### S1

if the sensor is placed like in the description (and pictured), there will be curves (waves) that the sensor will make, which will not align with the human body surface, during flexion and abduction movement. This sensor position mimics the m.deltoides anterior part placement/location in the body. The flex sensor should touch or pass the GH joint.

#### S2

if the sensor is placed like in the description (and pictured), there will be curves (waves) that the sensor will make, which will not align with the human body surface, during flexion and abduction movement. This sensor position mimics the m.deltoides middle part placement/location in the body. The flex sensor should touch or pass the GH joint.

#### S3

if the sensor is placed like in the description (and pictured), there will be curves (waves) that the sensor will make, which will not align with the human body surface, during flexion and abduction movement. This sensor position mimics the m.deltoides posterior part placement/location in the body. The flex sensor should touch or pass the GH joint. This position will not detect IR/ER rotations of the shoulder.

#### S4

the sensor does not cross the GH joint, so, as a flex sensor flexing nature, during movement, the sensor should flex. If the sensor is positioned on a flat surface of the human body segment, like the upper arm, then the sensor will not flex or bend, so the sensor should be closer to the GH joint, where bending occurs.

### Global Observations

It is a good starting point that needs to be slightly adjusted. But anatomical landmarks are precisely named.

### Suggested Focus

[No focus suggested]

Fig. 42. Designer A – Round 1 structured feedback.

#### Metadata

- Expert ID: [not provided]
- Domain: [not provided]
- Iteration: 1
- Base Design: [not provided]
- Date: [not provided]
- Time: 15:29 – 15:39

#### Sensor Feedback

S1 [No comment provided]

S2 [No comment provided]

S3 [No comment provided]

S4 [No comment provided]

#### Global Observations

The detection results have a lot of error. Move it so that the sensors better moves with the joint. Also note that the sensors bend only on one direction, so orient the sensors accordingly.

#### Suggested Focus

The current suggestion seems to be based on the muscle&joint movements however we place the sensors on clothes, can you compensate for that in your next sensor iteration.

Fig. 43. Designer B – Round 1 structured feedback.

#### Metadata

- Expert ID: [not provided]
- Domain: [not provided]
- Iteration: 1
- Base Design: [not provided]
- Date: [not provided]
- Time: 16:28 – 16:38

#### Sensor Feedback

S1 [No comment provided]

S2 [No comment provided]

S3 [No comment provided]

S4 [No comment provided]

#### Global Observations

S2 importance is quite low, this may be because the orientation of the sensor is not aligned well enough to the direction of bending of the joints. Also currently the three sensors are placed quite close to one another, maybe distributing them a bit wider would capture different movements around the shoulder seam of the jacket. Rotation detection got worse

#### Suggested Focus

move sensor location slightly to optimise for where the shoulder seams of the jacket would move most, move sensor 2 to a place that would improve rotation detection. note that these are bending sensors and bend in only one direction, so place the sensors where they will bend when the shoulder moves.

Fig. 44. Designer B – Round 2 structured feedback.

### Metadata

- Expert ID: expert\_C
- Domain: [not provided]
- Iteration: 1
- Base Design: L0
- Date: 2025-12-04
- Time: 16:58 - 17:14

### Sensor Feedback

#### S1

Maybe can be move a bit to chest side so that some of the sensing are touch chest. Flexion could maybe be improved. During arm movement, arm muscle may also affect on chest muscle. This suggestion is especially based on my own testing results.

#### S2

This is good position. Shoulder is critical position to detect arm movements.

#### S3

This is quite good position, or maybe slightly more back side due to the same reason mentioned for sensor 1 (also affect on back muscle).

#### S4

This is maybe not so useful postion as we already have a sensor on the shoulder in a pretty similar direction (sensor 1, which is also more sensitive based on my own testing). I would consider moving it under the arm and also try to connect it to chest (opposite direction, from arm to to ribs as a down u shape)

### Global Observations

Overall result is good, but the focus is mainly on shoulder. Maybe it is also essential to pay attention on the area close to it. as they also have notable impactions.

### Suggested Focus

Flexion performance seems worse than other two, it is worth to consider how to improve it better.

Fig. 45. Designer C – Round 1 structured feedback.

#### Metadata

- **Expert ID:** [not provided]
- **Domain:** [not provided]
- **Iteration:** 1
- **Base Design:** [not provided]
- **Date:** [not provided]
- **Time:** 17:40 – 17:59

#### Sensor Feedback

S1

This updated position is much better. I am wondering would it be even better if we place the sensor even more to the chest area? Maybe we could place the sensor to be more following the muscle direction instead of just a straight line.

S2

This position is also very good now. I am still wondering the neck area, because it also has impaction. Maybe it would be even better, if we place sensor so that it touches areas from all neck, shoulder and arm.

S3

The importance of this sensor is less than sensors 1 and 2. Maybe we can still try to improve the position. I am wondering similar positioning possibilities than for sensor 1. Maybe try to follow muscle direction and try to find the best balance of touching back and arm. And also what if we try to include a bit shoulder area too?

S4

The importance of this sensor is the worst but I still think that the position under arm is a good idea. Maybe try to find a more optimal position. Again, try to follow muscle direction under arm to chest side and also consider how much should we touch arm area and how much chest/ or even ribs area.

#### Global Observations

The flexion has improved and is much better now. The importance of sensors are more equal and balanced.

#### Suggested Focus

We can still try to optimise the flexion and also try to find the balance between flexion, abduction and rotation. Currently, MPJAE is around 11.7, 6.7 and 6.1 for flexion, abduction and rotation.

Fig. 46. Designer C – Round 2 structured feedback.

## F LH-Series LLM Outputs

### Session Metadata

- Expert: expert\_A
- Iteration: 1
- Timestamp: 2025-12-04T18:08:51.078278
- Model: gpt-4.1-2025-04-14
- Cost: €0.0374

### Engineering Report: Root Cause Analysis of SpectraFlex Flex Sensor Topology for Shoulder Joint Complex

Prepared by: Lead Sensor Layout Designer

System: Advanced Wearable Motion-Tracking (SpectraFlex Flex Sensor, 95mm, Male Pins)

Target: Shoulder Joint Complex (Flexion, Abduction, Rotation)

Date: 2024-06

#### 1. Executive Summary

The current 4-sensor topology for the SpectraFlex-based shoulder tracker demonstrates moderate performance, with a **global MPJAE of 10.714°**, but shows significant error in flexion (MPJAE: 19.140°) and moderate error in abduction (MPJAE: 8.435°). Rotation is tracked with high accuracy (MPJAE: 4.567°). Human expert feedback highlights critical issues related to sensor-to-anatomy conformance, especially regarding the glenohumeral (GH) joint, and the bending mechanics of the flex sensors. This report synthesizes quantitative and qualitative data to diagnose the root causes of error and inform future design iterations.

#### 2. Quantitative Metrics Analysis

##### 2.1. Global and Per-Joint Performance

Metric	Global	Flexion	Abduction	Rotation
MPJAE (°)	10.714	19.140	8.435	4.567
RMSE (°)	16.935	26.082	11.284	7.267
PCC	0.8279	0.8760	0.7232	0.8844
ROM (°)	—	301.3	62.51	106.27

- **Flexion:** Largest error (MPJAE: 19.140°), indicating poor tracking of this movement.
- **Abduction:** Moderate error (MPJAE: 8.435°).
- **Rotation:** Best performance (MPJAE: 4.567°).

##### 2.2. Sensor Importance

Sensor	Contribution (%)
S1	27.90
S4	26.26
S2	23.50
S3	22.34

- S1 (anterior) and S4 (spiral/rotation) are most influential.
- S2 (lateral) and S3 (posterior) are less influential, but still significant.

#### 3. Human Expert Feedback Synthesis

- **S1, S2, S3:** All three deltoid-mimicking sensors create "curves (waves)" that do not align with the human body surface during flexion and abduction. These sensors do **not cross the GH joint**, which is the anatomical pivot for shoulder motion.
- **S4:** Placed on the upper arm, does **not cross the GH joint**; thus, during movement, the sensor does **not flex** as expected, leading to poor signal.
- **Global:** Anatomical landmarks are correctly identified, but sensor paths do **not conform to the dynamic curvature and pivot points** of the shoulder, especially at the GH joint.

Fig. 47. LLM output for Designer A, Iteration 1 (Part 1).

4. Root Cause Analysis

4.1. Sensor Placement Relative to Joint Kinematics

- **Flex Sensors Require Bending:** The SpectraFlex sensor is designed to transduce mechanical bending into electrical signals. If the sensor is placed on a region that remains flat or only minimally deforms during motion, its output is insensitive to joint movement.
- **Sensors Do Not Cross the GH Joint:** All four sensors are placed such that they **do not pass over the GH joint** (the true axis of rotation for the shoulder). As a result, during flexion and abduction, the sensor either does not bend, or bends in a non-linear/unpredictable manner due to surface "waves."
- **Surface Conformance Issues:** The sensors, when placed as described, experience "waves"—areas where the sensor lifts off or buckles away from the skin, especially during large ROM movements. This introduces artifacts and non-physiological bending, corrupting the sensor signal.

4.2. Movement-Specific Implications

- **Flexion (High Error):** S1 (anterior) is intended to track flexion but does not cross the GH joint, and thus fails to capture the true angular change. The "waves" further degrade signal fidelity.
- **Abduction (Moderate Error):** S2 (lateral) is similarly misaligned relative to the GH joint, leading to moderate error.
- **Rotation (Low Error):** S4 (spiral) and S3 (posterior) partially capture rotation due to their oblique/spiral placement, but S4's placement on the upper arm (not crossing GH) limits its effectiveness. However, the overall rotational movement may still produce enough bending in these sensors to yield lower error, possibly due to compensation by S3/S4.

4.3. Sensor Redundancy and Contribution

- The sensor importance scores are relatively balanced, but the highest contributors (S1, S4) are still suboptimal due to placement errors.
- The current configuration lacks a sensor that **directly bridges the proximal scapula/clavicle and the distal humerus across the GH joint**, which is essential for accurate joint angle measurement.

5. Root Causes Summary Table

Root Cause	Evidence (Quantitative)	Evidence (Qualitative)	Impact
Sensors do not cross GH joint	High MPJAE for flexion/abd.	Expert: "should touch or pass GH"	Major (all motions)
Sensors experience "waves"/buckling	High RMSE, Max Error	Expert: "curves (waves) appear"	Major (flexion/abd.)
Flat placement on non-bending regions	Low sensor output in S4	Expert: "sensor will not flex/bend"	Major (rotation)
Lack of anatomical conformance	High error variance	Expert: "does not align with surface"	Moderate

6. Conclusion

The primary root cause of suboptimal performance is the failure to align sensor placement and orientation with the true biomechanical axes and pivot points of the shoulder, specifically the GH joint. The current sensor paths do not cross the joint center, resulting in poor bending response during primary motions (flexion, abduction). Additionally, the physical conformance of the sensors to the dynamic surface of the shoulder is inadequate, causing artifacts and non-physiological signal behavior.

7. Recommendations for Next Iteration

1. **Redesign sensor paths to cross the GH joint** directly, ensuring that each sensor bridges the anatomical axis of rotation relevant to the target motion.
2. **Improve surface conformance** by selecting sensor paths that remain in contact with the skin throughout full ROM, avoiding regions prone to buckling or lifting.
3. **Optimize sensor orientation** to maximize bending for the intended motion (e.g., align longitudinal axis of sensor with the axis of maximal curvature during movement).
4. **Validate with dynamic anatomical modeling** to predict sensor deformation and signal output prior to prototyping.

Prepared by:

Lead Sensor Layout Designer  
Advanced Wearable Motion-Tracking Project

Part 2: Design Synthesis & Optimization (JSON Spec)

Design Overview

This revised sensor layout for Iteration N+1 directly addresses the root causes identified in the previous analysis. All sensor paths are now designed to **cross the glenohumeral (GH) joint**, ensuring that each SpectraFlex sensor bends in direct relation to the primary axis of movement. Sensor placements have been optimized for anatomical conformance, maximizing skin contact and minimizing buckling or lifting throughout the full range of motion. Sensor orientations are chosen to maximize bending for the specific target movement (flexion, abduction, or rotation), with each sensor bridging the dynamic curvature associated with its primary joint action.

Fig. 48. LLM output for Designer A, Iteration 1 (Part 2).

**Sensor Layout Specification****Sensor 1:**

- **Anatomical Location:** Anterior shoulder, spanning from the mid-clavicle (just medial to the acromion) diagonally across the GH joint to the mid-anterior humerus (over the deltoid insertion).
- **Orientation:** Oblique (superomedial to inferolateral,  $\sim 45^\circ$  from horizontal)
- **Primary Target Movement(s):** Shoulder Flexion / Extension
- **Rationale:** This path ensures the sensor crosses the GH joint, directly capturing flexion-related bending and maintaining contact throughout the motion, addressing the previous issue of non-crossing and "waves."

**Sensor 2:**

- **Anatomical Location:** Lateral shoulder, from the superior acromion process, vertically over the GH joint, terminating on the lateral mid-humerus (over the deltoid tuberosity).
- **Orientation:** Vertical (superior-inferior, parallel to humeral shaft)
- **Primary Target Movement(s):** Shoulder Abduction / Adduction
- **Rationale:** By running directly over the GH joint, this sensor maximizes bending during abduction, correcting the prior misalignment and ensuring signal fidelity.

**Sensor 3:**

- **Anatomical Location:** Posterior shoulder, from the spine of the scapula (just medial to the acromion), diagonally across the GH joint to the posterior mid-humerus (over the posterior deltoid insertion).
- **Orientation:** Oblique (superolateral to inferomedial,  $\sim 45^\circ$  from horizontal)
- **Primary Target Movement(s):** Shoulder Extension / External Rotation
- **Rationale:** This placement ensures the sensor crosses the GH joint and tracks posterior movement, eliminating prior issues of flat placement and lack of rotational sensitivity.

**Sensor 4:**

- **Anatomical Location:** Spiral path starting at the anterior axillary fold (just medial to the GH joint), wrapping obliquely and laterally over the GH joint to the posterior lateral humerus (just below the deltoid insertion).
- **Orientation:** Oblique/Spiral ( $\sim 45^\circ$  from vertical, anterior-medial to posterior-lateral)
- **Primary Target Movement(s):** Shoulder Internal/External Rotation, Horizontal Abduction/Adduction
- **Rationale:** This sensor now crosses the GH joint, maximizing bending during rotational movements and addressing the previous flat upper arm placement, ensuring the sensor is active during all relevant motions.

Fig. 49. LLM output for Designer A, Iteration 1 (Part 3).

Machine-Readable Output

```
{
  "design_id": "LH_iteration_Next",
  "sensor_count": 4,
  "sensors": [
    {
      "id": 1,
      "anatomical_location": "Anterior shoulder, spanning from the mid-clavicle (just medial to the acromion) diagonally across the glenohumeral (GH) joint to the mid-anterior humerus (over the deltoid insertion).",
      "orientation": "Oblique (superomedial to inferolateral, ~45° from horizontal)",
      "primary_targets": ["Shoulder Flexion", "Shoulder Extension"],
      "coordinates_description": "Origin: mid-clavicle (2-3 cm medial to acromion); Path: diagonally over anterior GH joint; Termination: mid-anterior humerus at the level of the deltoid insertion."
    },
    {
      "id": 2,
      "anatomical_location": "Lateral shoulder, from the superior acromion process vertically over the GH joint to the lateral mid-humerus (over the deltoid tuberosity).",
      "orientation": "Vertical (superior-inferior, parallel to humeral shaft)",
      "primary_targets": ["Shoulder Abduction", "Shoulder Adduction"],
      "coordinates_description": "Origin: tip of acromion; Path: vertically over lateral GH joint; Termination: deltoid tuberosity on lateral humerus (~10-12 cm below acromion)."
    },
    {
      "id": 3,
      "anatomical_location": "Posterior shoulder, from the spine of the scapula (just medial to the acromion), diagonally across the GH joint to the posterior mid-humerus (over the posterior deltoid insertion).",
      "orientation": "Oblique (superolateral to inferomedial, ~45° from horizontal)",
      "primary_targets": ["Shoulder Extension", "Shoulder External Rotation"],
      "coordinates_description": "Origin: spine of scapula (1-2 cm medial to acromion); Path: diagonally over posterior GH joint; Termination: posterior mid-humerus, over posterior deltoid insertion."
    },
    {
      "id": 4,
      "anatomical_location": "Spiral path starting at the anterior axillary fold (just medial to the GH joint), wrapping obliquely and laterally over the GH joint to the posterior lateral humerus (just below the deltoid insertion).",
      "orientation": "Oblique/Spiral (~45° from vertical, anterior-medial to posterior-lateral)",
      "primary_targets": ["Shoulder Internal Rotation", "Shoulder External Rotation", "Horizontal Adduction", "Horizontal Abduction"],
      "coordinates_description": "Origin: anterior axillary fold (just medial to GH joint); Path: spirals over anterior-lateral GH joint; Termination: posterior lateral humerus, just below deltoid insertion."
    }
  ]
}
```

Fig. 50. LLM output for Designer A, Iteration 1 (Part 4).

Session Metadata

- Expert: expert\_B
- Iteration: 1
- Timestamp: 2025-12-03T15:41:54.179855
- Model: gpt-4.1-2025-04-14
- Cost: €0.0319

Engineering Root Cause Analysis Report

Project: High-Performance Wearable Sensor Array (Shoulder & Upper Arm)

Design Iteration: LLM\_Only\_FINAL (4-sensor array)

Date: [Auto-generated]

Lead Sensor Architect: [Your Name]

Executive Summary

The current 4-sensor wearable array for shoulder kinematics demonstrates suboptimal performance, with a global Mean Per-Joint Angular Error (MPJAE) of 10.943° and notably high error in shoulder flexion (MPJAE: 18.013°). Quantitative sensor importance is relatively balanced, but human expert feedback highlights issues with sensor placement relative to joint motion and mechanical bending constraints. This report synthesizes hardware metrics and expert observations to identify root causes and recommend targeted improvements.

1. Quantitative Metrics Analysis

1.1 Global Performance

- MPJAE: 10.943° (High for precision applications)
- AMPE: 8.75%
- RMSE: 17.025°
- PCC: 0.7937 (Moderate correlation)
- Max Error: 190.851° (Indicates occasional catastrophic failure)

1.2 Per-Joint Breakdown

Joint	MPJAE (°)	RMSE (°)	PCC	ROM (°)
Flexion	18.013	25.784	0.8796	301.30
Abduction	9.618	12.149	0.6223	62.51
Rotation	5.197	7.556	0.8791	106.27

- Flexion is the worst-performing DOF, with both the highest MPJAE and RMSE.
- Abduction shows moderate error and lower correlation.
- Rotation is relatively well-captured.

1.3 Sensor Importance

- All sensors contribute significantly (21.7%–27.5%), indicating no single sensor is redundant.
- S1 (Anterior shoulder) is most important, followed by S2 (Lateral), S4 (Proximal spiral), and S3 (Posterior).
- Importance is balanced (Std: 0.0208), suggesting all sensors are needed, but none are optimal.

2. Human Expert Feedback Synthesis

- Global:
  - "Detection results have a lot of error."
  - "Move [the sensors] so that the sensors better move with the joint."
  - "Sensors bend only in one direction, so orient the sensors accordingly."
- Sensor-specific notes:
  - No specific feedback per sensor, but global comments imply issues with sensor placement, orientation, and mechanical compliance.

Fig. 51. LLM output for Expert B, Iteration 1 (Part 1).

**3. Root Cause Analysis**

**3.1 Sensor Placement Relative to Joint Kinematics**

- **Misalignment with Joint Axes:**
  - Sensors may not be optimally aligned with the axes of rotation or muscle bulges for each DOF.
  - Particularly, S1 (targeting flexion/extension) may not track the true axis of shoulder flexion, leading to high flexion error.
- **Insufficient Coupling to Segment Motion:**
  - Sensors may shift or not deform congruently with the underlying bones/muscles during movement, especially in complex DOFs like flexion.

**3.2 Sensor Mechanical Constraints**

- **Unidirectional Bending:**
  - Hardware can only bend in one direction, but current placements/orientations may not exploit this, reducing sensitivity to certain joint motions.
  - Oblique/spiral placements (e.g., S4) may not align with the principal strain direction during key movements.

**3.3 Array Sparsity and Coverage**

- **Sparse Array Limitations:**
  - Four sensors may not provide sufficient spatial coverage for complex, multi-axial movements of the shoulder, especially for flexion which involves substantial scapulothoracic contribution.

**3.4 Sensor Importance Distribution**

- **No Dominant Sensor:**
  - The relatively uniform importance suggests that no sensor is optimally placed to capture a principal movement axis, especially for high-error DOFs.

**4. Key Failure Modes Identified**

Root Cause	Evidence (Metrics)	Evidence (Expert)
Misalignment with joint axes	High flexion MPJAE, RMSE	"Move sensors to better move with the joint"
Suboptimal sensor orientation (bending axis)	High error, no dominant sensor	"Sensors bend only in one direction..."
Insufficient mechanical coupling	High max error, moderate PCC	"Detection results have a lot of error"
Sparse coverage of complex kinematics	High flexion error, low abduction PCC	Implicit in "move with the joint"

**5. Conclusions**

The primary root causes of error in the current design are:

1. **Sensor Placement and Orientation Misalignment:**
  - Sensors are not optimally positioned or oriented to track the true axes of major shoulder movements, especially flexion/extension.
2. **Mechanical Mismatch:**
  - The unidirectional bending property of the sensors is not being leveraged; current orientations may not align with the principal strain directions during key movements.
3. **Sparse Array Coverage:**
  - Four sensors are insufficient to robustly capture the complex, multi-planar motion of the shoulder, particularly for flexion.
4. **Lack of Sensor-Joint Coupling:**
  - Sensors may not deform congruently with the underlying anatomy, leading to poor signal fidelity.

**6. Recommendations (Preview)**

- **Reevaluate sensor anatomical placement** to ensure alignment with primary axes of rotation.
- **Reorient sensors** so their bending axes align with the direction of maximal strain for each targeted movement.
- **Consider increasing sensor count** or repositioning for better spatial coverage, especially for flexion.
- **Enhance mechanical coupling** (e.g., better fixation, improved substrate compliance) to reduce artifacts.

Prepared by:

[Your Name]

Lead Sensor Architect

**Part 2: Design Synthesis & Optimization (JSON Spec)**

Fig. 52. LLM output for Designer B, Iteration 1 (Part 2).

### Design Overview

This revised 4-sensor shoulder array directly addresses the root causes identified in the previous analysis:

- **Alignment with Joint Axes:** Sensors are repositioned and reoriented to align with the anatomical axes of flexion, abduction, and rotation, maximizing strain signal during target movements.
- **Leveraging Unidirectional Bending:** Each sensor is oriented such that its primary bending axis matches the principal strain direction for its target movement.
- **Improved Mechanical Coupling:** Sensors are placed over regions with minimal soft-tissue artifact and maximal congruence with underlying bone movement.
- **Optimized Coverage:** Sensor locations are chosen to ensure each major degree of freedom is robustly captured, with special attention to flexion (previously the highest-error DOF).

### Sensor Layout Specification

#### Sensor 1:

- **Anatomical Location:** Superior anterior shoulder, spanning from the coracoid process (just medial to the humeral head) down the midline of the anterior deltoid to the deltoid tuberosity.
- **Orientation:** Vertical (superior-inferior, parallel to the humeral shaft)
- **Primary Target Movement(s):** Shoulder Flexion/Extension
- **Rationale:** Directly aligns with the axis of flexion/extension, maximizing strain signal during these movements and correcting the previous oblique misalignment.

#### Sensor 2:

- **Anatomical Location:** Lateral shoulder, from the acromion process vertically down the midline of the lateral deltoid to the deltoid tuberosity.
- **Orientation:** Vertical (superior-inferior)
- **Primary Target Movement(s):** Shoulder Abduction/Adduction
- **Rationale:** Maintains vertical orientation for optimal detection of abduction/adduction, ensuring the sensor bends maximally with lateral arm elevation.

#### Sensor 3:

- **Anatomical Location:** Posterior shoulder, from the spine of the scapula (just medial to the acromion) vertically down the midline of the posterior deltoid to the posterior mid-humerus.
- **Orientation:** Vertical (superior-inferior)
- **Primary Target Movement(s):** Shoulder Extension, External Rotation
- **Rationale:** Vertical placement over the posterior deltoid maximizes sensitivity to extension and external rotation, leveraging the sensor's unidirectional bending.

#### Sensor 4:

- **Anatomical Location:** Proximal upper arm, spiral path starting at the anterior axillary fold, wrapping obliquely (45°) across the anterior upper arm to the lateral mid-humerus.
- **Orientation:** Oblique (approx. 45° from vertical, anterior-medial to lateral)
- **Primary Target Movement(s):** Shoulder Internal/External Rotation, Horizontal Abduction/Adduction
- **Rationale:** Oblique orientation matches the principal strain direction during rotational and horizontal plane movements, improving signal for these DOFs and addressing prior mechanical mismatch.

Fig. 53. LLM output for Designer B, Iteration 1 (Part 3).

**Machine-Readable Output**

```
{
  "design_id": "Shoulder_Iteration_Nplus1",
  "sensor_count": 4,
  "sensors": [
    {
      "id": 1,
      "anatomical_location": "Superior anterior shoulder, spanning from the coracoid process (just medial to the humeral head) down the midline of the anterior deltoid to the deltoid tuberosity.",
      "orientation": "Vertical (superior-inferior, parallel to humeral shaft)",
      "primary_targets": ["Shoulder Flexion", "Shoulder Extension"],
      "coordinates_description": "Origin: coracoid process (just medial to humeral head); Termination: deltoid tuberosity on anterior humerus."
    },
    {
      "id": 2,
      "anatomical_location": "Lateral shoulder, from the acromion process vertically down the midline of the lateral deltoid to the deltoid tuberosity.",
      "orientation": "Vertical (superior-inferior)",
      "primary_targets": ["Shoulder Abduction", "Shoulder Adduction"],
      "coordinates_description": "Origin: tip of acromion; Termination: deltoid tuberosity on lateral humerus (-10-12 cm below acromion)."
    },
    {
      "id": 3,
      "anatomical_location": "Posterior shoulder, from the spine of the scapula (just medial to the acromion) vertically down the midline of the posterior deltoid to the posterior mid-humerus.",
      "orientation": "Vertical (superior-inferior)",
      "primary_targets": ["Shoulder Extension", "Shoulder External Rotation"],
      "coordinates_description": "Origin: spine of scapula (1-2 cm medial to acromion); Termination: posterior mid-humerus, overlying posterior deltoid."
    },
    {
      "id": 4,
      "anatomical_location": "Proximal upper arm, spiral path starting at the anterior axillary fold, wrapping obliquely (45°) across the anterior upper arm to the lateral mid-humerus.",
      "orientation": "Oblique (approx. 45° from vertical, anterior-medial to lateral)",
      "primary_targets": ["Shoulder Internal Rotation", "Shoulder External Rotation", "Horizontal Adduction", "Horizontal Abduction"],
      "coordinates_description": "Origin: anterior axillary fold; Path: oblique across anterior upper arm; Termination: lateral mid-humerus, just below deltoid insertion."
    }
  ]
}
```

Fig. 54. LLM output for Designer B, Iteration 1 (Part 4).

Session Metadata

- Expert: expert\_B
- Iteration: 2
- Timestamp: 2025-12-03T16:49:33.078839
- Model: gpt-4.1-2025-04-14
- Cost: €0.0340

Engineering Root Cause Analysis Report

System: SpectraFlex Flex Sensor Array (95mm, Male Pins) – Shoulder Joint Complex

Design Iteration: Shoulder\_Iteration\_Nplus1

Date: [Auto-generated]

1. Executive Summary

The current four-sensor topology for the shoulder joint complex achieves moderate performance (Global MPJAE: 7.829°), but exhibits suboptimal accuracy for critical motions, especially Flexion (MPJAE: 10.170°). Quantitative metrics and expert feedback both indicate that sensor placement and orientation—particularly for S2 (lateral shoulder)—are not fully exploiting the sensor’s bending-aware properties, resulting in underutilization and increased error. This report identifies the root causes and provides actionable insights for improvement.

2. Quantitative Metrics Synthesis

Global Performance:

- MPJAE: 7.829° (moderate; not at state-of-the-art)
- AMPE: 6.57%
- RMSE: 15.509°
- PCC: 0.7667 (moderate correlation)
- Max Error: 269.535° (outliers present)

Per-Joint Breakdown:

Motion	MPJAE (°)	AMPE (%)	RMSE (°)	PCC	ROM (°)
Flexion	10.170	3.18	22.559	0.7745	319.76
Abduction	7.279	11.94	11.313	0.7794	60.96
Rotation	6.038	4.59	9.206	0.7463	131.50

Sensor Importance (Contribution to Signal Quality):

Sensor	Importance	Contribution (%)
S1	0.3090	30.90
S4	0.2708	27.08
S3	0.2227	22.27
S2	0.1974	19.74

- Observation: S2 (lateral shoulder) is the least important sensor, with the lowest contribution to overall signal quality.

3. Expert Feedback Synthesis

• S2 (Lateral Shoulder):

- Issue: Low importance, likely due to suboptimal orientation relative to the primary axis of abduction/adduction.
- Hypothesis: Sensor may not be aligned with the direction of maximal bending during abduction, reducing sensitivity and signal amplitude.
- Sensor Distribution:
  - Issue: Sensors are "placed quite close to one another."
  - Hypothesis: Overlapping sensing regions may cause redundant data and under-sampling of the full shoulder kinematic envelope.
- Rotation Detection:
  - Issue: "Rotation detection got worse."
  - Hypothesis: Sensor orientations and placements may not adequately capture the complex, multiplanar nature of shoulder rotation, especially internal/external rotation.

Fig. 55. LLM output for Designer B, Iteration 2 (Part 1).

4. Root Cause Analysis

4.1. Sensor Placement and Orientation

• S2 (Lateral Shoulder):

- **Root Cause:** The vertical (superior-inferior) orientation may not align with the axis of maximal bending during abduction. The deltoid muscle and overlying skin stretch more along an oblique or lateral axis during abduction, not strictly vertical.
- **Effect:** Reduced sensor deformation, lower signal amplitude, and diminished contribution to abduction angle estimation.
- **Evidence:** S2 has the lowest importance (0.1974), and abduction MPJAE is still high (7.279°).

• S1, S3, S4 (Anterior, Posterior, Oblique):

- **Root Cause:** Placement "quite close to one another" may lead to correlated signals, reducing the effective dimensionality of captured motion.
- **Effect:** Overlapping sensitivity fields, less unique information per sensor, and increased error in complex or multiplanar motions.

4.2. Sensor Coverage and Distribution

- **Root Cause:** The current topology does not sufficiently cover the full circumferential range of the shoulder, especially along the scapular and axillary lines, which are critical for capturing multi-axis rotation and complex movements.
- **Effect:** Incomplete motion capture, especially for internal/external rotation and horizontal ab/adduction.

4.3. Sensor Bending Characteristics

- **Root Cause:** Flex sensors are maximally sensitive when the primary axis of bending is perpendicular to the sensor's length. Misalignment reduces bending-induced resistance change, degrading signal quality.
- **Effect:** Inaccurate mapping of joint angles, especially for motions where the sensor is not optimally aligned.

4.4. Signal Artifacts and Outliers

- **Root Cause:** High max error (269.535°) and large RMSE suggest occasional misreadings, possibly due to sensor lift-off, skin movement, or mechanical artifacts.
- **Effect:** Large, sporadic errors that degrade overall performance metrics.

5. Summary Table: Root Causes and Effects

Issue	Root Cause	Effect on Metrics
S2 Low Importance	Poor orientation vs. abduction bending axis	High abduction MPJAE, low S2 contribution
Sensors too close	Redundant coverage, correlated signals	Lower unique info, higher MPJAE
Poor rotation detection	Inadequate multiplanar coverage, suboptimal S4 path	Higher rotation MPJAE, lower PCC
High max error	Sensor artifacts, lift-off, skin motion	Outliers, increased RMSE

6. Recommendations (Preview)

- **Reorient S2** to better match the direction of deltoid stretching during abduction (consider more oblique/lateral alignment).
- **Increase spatial distribution** of sensors to cover more of the shoulder circumference, especially posterior and axillary regions.
- **Adjust S4 path** to better capture multiplanar rotation.
- **Review attachment method** to minimize sensor lift-off and skin artifact.

7. Conclusion

The current sensor topology underperforms due to **suboptimal sensor orientation (especially S2), insufficient spatial separation, and incomplete coverage of the shoulder's full motion envelope**. These factors reduce the system's sensitivity to critical motions, particularly abduction and rotation, and introduce redundant or low-value data. Addressing these root causes will be essential to achieve lower MPJAE and higher reliability in subsequent design iterations.

Prepared by:

Lead Sensor Layout Designer

[Your Name]

[Date]

Part 2: Design Synthesis & Optimization (JSON Spec)

Fig. 56. LLM output for Designer B, Iteration 2 (Part 2).

### Design Overview

This revised four-sensor shoulder layout directly addresses the root causes identified in the previous analysis. The main changes are:

- **S2 (Lateral Sensor) is reoriented obliquely** to better align with the deltoid's stretch during abduction, maximizing bending signal.
- **Sensors are distributed more widely** around the shoulder circumference, especially posteriorly and along the axillary line, to reduce redundancy and improve multiplanar coverage.
- **S4 (Rotation Sensor) is shifted to a more circumferential path** to better capture internal/external rotation and horizontal motions.
- **All sensors are placed to minimize overlap and maximize unique kinematic information**, in line with garment fit constraints.

### Sensor Layout Specification

#### Sensor 1:

- **Anatomical Location:** Superior anterior shoulder, spanning from the coracoid process (just medial to the humeral head) down the midline of the anterior deltoid to the deltoid tuberosity.
- **Orientation:** Vertical (superior-inferior, parallel to humeral shaft)
- **Primary Target Movement(s):** Shoulder Flexion, Shoulder Extension
- **Rationale:** Retained from prior design as S1 had highest importance; vertical placement here optimally captures anterior deltoid stretch during flexion/extension.

#### Sensor 2:

- **Anatomical Location:** Lateral shoulder, from the anterior edge of the acromion, running obliquely (approx. 30° posterior to vertical) across the lateral deltoid toward the posterior-lateral mid-humerus.
- **Orientation:** Oblique (approx. 30° posterior to vertical)
- **Primary Target Movement(s):** Shoulder Abduction, Shoulder Adduction
- **Rationale:** Reoriented to align with the primary axis of deltoid muscle stretch during abduction, directly addressing prior low importance and improving sensitivity.

#### Sensor 3:

- **Anatomical Location:** Posterior shoulder, from the medial edge of the scapular spine (about 2 cm medial to acromion) obliquely downward and laterally to the posterior mid-humerus, just above the triceps insertion.
- **Orientation:** Oblique (approx. 45° from vertical, medial-superior to lateral-inferior)
- **Primary Target Movement(s):** Shoulder Extension, Shoulder External Rotation
- **Rationale:** Distributed more posteriorly and obliquely to reduce overlap with S1/S2 and enhance sensitivity to extension and external rotation.

#### Sensor 4:

- **Anatomical Location:** Circumferential path starting at the anterior axillary fold, wrapping horizontally (transverse plane) across the mid-upper arm to terminate at the posterior axillary fold.
- **Orientation:** Horizontal (transverse, perpendicular to humeral shaft)
- **Primary Target Movement(s):** Shoulder Internal Rotation, Shoulder External Rotation, Horizontal Abduction/Adduction
- **Rationale:** Circumferential placement maximizes bending during internal/external rotation and horizontal movements, improving rotation detection as per prior diagnosis.

Fig. 57. LLM output for Designer B, Iteration 2 (Part 3).

**Machine-Readable Output**

```
{
  "design_id": "Shoulder_Iteration_Nplus2",
  "sensor_count": 4,
  "sensors": [
    {
      "id": 1,
      "anatomical_location": "Superior anterior shoulder, spanning from the coracoid process (just medial to the humeral head) down the midline of the anterior deltoid to the deltoid tuberosity.",
      "orientation": "Vertical (superior-inferior, parallel to humeral shaft)",
      "primary_targets": ["Shoulder Flexion", "Shoulder Extension"],
      "coordinates_description": "Origin: coracoid process (just medial to humeral head); Termination: deltoid tuberosity on anterior humerus."
    },
    {
      "id": 2,
      "anatomical_location": "Lateral shoulder, from the anterior edge of the acromion, running obliquely (approx. 30° posterior to vertical) across the lateral deltoid toward the posterior-lateral mid-humerus.",
      "orientation": "Oblique (approx. 30° posterior to vertical)",
      "primary_targets": ["Shoulder Abduction", "Shoulder Adduction"],
      "coordinates_description": "Origin: anterior edge of acromion; Path: oblique across lateral deltoid; Termination: posterior-lateral mid-humerus."
    },
    {
      "id": 3,
      "anatomical_location": "Posterior shoulder, from the medial edge of the scapular spine (about 2 cm medial to acromion) obliquely downward and laterally to the posterior mid-humerus, just above triceps insertion.",
      "orientation": "Oblique (approx. 45° from vertical, medial-superior to lateral-inferior)",
      "primary_targets": ["Shoulder Extension", "Shoulder External Rotation"],
      "coordinates_description": "Origin: medial edge of scapular spine (2 cm medial to acromion); Path: oblique to posterior mid-humerus, just above triceps insertion."
    },
    {
      "id": 4,
      "anatomical_location": "Circumferential path starting at the anterior axillary fold, wrapping horizontally (transverse plane) across the mid-upper arm to terminate at the posterior axillary fold.",
      "orientation": "Horizontal (transverse, perpendicular to humeral shaft)",
      "primary_targets": ["Shoulder Internal Rotation", "Shoulder External Rotation", "Horizontal Abduction", "Horizontal Adduction"],
      "coordinates_description": "Origin: anterior axillary fold; Path: horizontal around mid-upper arm; Termination: posterior axillary fold."
    }
  ]
}
```

Fig. 58. LLM output for Designer B, Iteration 2 (Part 4).

Session Metadata

- Expert: expert\_C
- Iteration: 1
- Timestamp: 2025-12-04T17:15:49.879052
- Model: gpt-4.1-2025-04-14
- Cost: €0.0367

Root Cause Analysis Report

Subject: Suboptimal MPJAE in SpectraFlex-Based Shoulder Joint Sensor Topology

Prepared by: Lead Sensor Layout Designer

Date: 2024-06-13

1. Executive Summary

The current 4-sensor SpectraFlex layout for the shoulder joint complex achieves a global MPJAE of 10.714°, with joint-specific errors of 19.140° (Flexion), 8.435° (Abduction), and 4.567° (Rotation). While overall system performance is strong, Flexion accuracy is notably suboptimal, and there are opportunities to further reduce error in Abduction. This report synthesizes quantitative metrics and expert feedback to identify root causes and guide future design iterations.

2. Quantitative Metrics Analysis

2.1. Global and Per-Joint Performance

Metric	Flexion	Abduction	Rotation
**MPJAE (°)**	**19.140**	8.435	4.567
AMPE (%)	6.35	13.49	4.30
RMSE (°)	26.082	11.284	7.267
PCC	0.8760	0.7232	0.8844

- Flexion: Highest MPJAE and RMSE, though correlation (PCC) remains strong.
- Abduction: Moderate error, but relatively high AMPE and lower PCC.
- Rotation: Lowest error and highest correlation.

2.2. Sensor Importance

Sensor	Importance	Contribution (%)
S1	0.2790	27.90
S4	0.2626	26.26
S2	0.2350	23.50
S3	0.2234	22.34

- S1 (Anterior Shoulder): Most critical for system output.
- S4 (Proximal Upper Arm, Spiral): Second most important, but criticized in expert feedback.
- S2 (Lateral Shoulder): Strong position for abduction.
- S3 (Posterior Shoulder): Least important, but still significant.

Fig. 59. LLM output for Designer C, Iteration 1 (Part 1).

**3. Human Expert Feedback Synthesis**

**3.1. Sensor-Specific Observations**

- **S1 (Anterior Shoulder):**
  - *Feedback:* Should be shifted more medially, possibly onto the chest, to better capture flexion. Current placement may miss synergistic movement between chest and shoulder during flexion.
  - *Implication:* Suboptimal flexion sensing due to anatomical misalignment.
- **S2 (Lateral Shoulder):**
  - *Feedback:* Good placement; critical for abduction.
  - *Implication:* No immediate issues; supports abduction accuracy.
- **S3 (Posterior Shoulder):**
  - *Feedback:* Good, but could be shifted further back to better capture posterior muscle activity.
  - *Implication:* Potential to improve extension/external rotation accuracy.
- **S4 (Proximal Upper Arm, Spiral):**
  - *Feedback:* Overlaps with S1; not as useful. Suggests moving under the arm, connecting to chest in a "U" shape (from arm to ribs).
  - *Implication:* Current placement may be redundant and not optimally leveraging sensor capabilities for rotation/horizontal movements.

**3.2. Global Observations**

- The design is shoulder-centric; adjacent regions (chest, back, ribs) may contribute significantly to joint kinematics and should be considered for sensor placement.

**4. Root Cause Identification**

**4.1. Flexion Error (MPJAE: 19.140°)**

- **Primary Cause:**
  - **S1's current placement** does not adequately capture the complex motion of the shoulder during flexion, particularly the contribution of the chest (pectoralis major) and anterior deltoid. The lack of sensor coverage on the chest side reduces sensitivity to the full range of flexion motion.
- **Secondary Cause:**
  - **S4's redundancy** with S1 may limit the diversity of motion capture, failing to provide unique data for flexion.

**4.2. Abduction Error (MPJAE: 8.435°)**

- **Primary Cause:**
  - While S2 is well-placed, the **lack of complementary sensors on the superior-lateral thorax or below the axilla** may reduce abduction tracking fidelity, especially at higher ranges of motion where scapulothoracic movement is involved.

**4.3. Rotation Error (MPJAE: 4.567°)**

- **Primary Cause:**
  - **Current sensor configuration is generally effective** for rotation, but S4's spiral path may not be optimally oriented for pure rotational movements, especially internal rotation.

**4.4. General Systemic Issues**

- **Redundancy in Sensor Placement:**
  - S1 and S4 cover similar anatomical paths, reducing the effective diversity of motion capture.
- **Insufficient Coverage of Adjacent Regions:**
  - No sensors directly monitor the chest or rib area, which are critical for capturing complex shoulder kinematics, especially during flexion and horizontal movements.

**5. Summary Table: Error Source Mapping**

Error Type	Root Cause(s)	Evidence (Metrics/Feedback)
Flexion (High)	S1 misplacement; lack of chest coverage; S4 overlap	High MPJAE; expert S1/S4 feedback
Abduction (Mod.)	No inferior/axillary coverage; S2 only	Moderate MPJAE; S2 feedback
Rotation (Low)	S4 suboptimal spiral; S3 could be further posterior	Low MPJAE; S3/S4 feedback
General	Redundant sensor paths; lack of thoracic/rib sensors	Sensor importance; expert feedback

Fig. 60. LLM output for Designer C, Iteration 1 (Part 2).

## 6. Recommendations for Next Iteration

1. **Reposition S1:** Shift medially to include chest (pectoral) region, capturing more of the flexion arc.
2. **Reorient S4:** Move under the arm, connecting to the chest/ribs in a "U" shape, as per expert suggestion, to better capture horizontal and rotational movements.
3. **Consider S3 Adjustment:** Shift slightly more posterior to better sense extension and external rotation.
4. **Explore Additional Sensor Diversity:** If possible, introduce coverage to the upper rib cage or scapular region to capture complex 3D shoulder kinematics.
5. **Reduce Redundancy:** Ensure each sensor provides unique, non-overlapping biomechanical information.

## 7. Conclusion

The main limitation of the current design is **insufficient anatomical diversity in sensor placement**, particularly for **flexion and horizontal movements**. By **realigning S1 to include the chest**, **repositioning S4 for underarm/chest coverage**, and **optimizing S3's posterior placement**, the system can achieve lower MPJAE and improved robustness across all critical motions.

### End of Report

## Part 2: Design Synthesis & Optimization (JSON Spec)

### Design Overview

This iteration realigns the sensor topology to maximize anatomical diversity and minimize redundancy, directly addressing the root causes identified in the previous analysis.

- **S1** is shifted medially to span the anterior shoulder and upper chest, enhancing flexion capture by including pectoral movement.
- **S4** is repositioned to a U-shaped path under the axilla, connecting the medial upper arm to the lower lateral chest/ribs, optimizing sensitivity for internal/external rotation and horizontal movements.
- **S3** is moved slightly further posterior to better capture extension and external rotation.
- **S2** remains on the lateral shoulder, as it already provides optimal abduction sensing.

### Sensor Layout Specification

#### Sensor 1:

- **Anatomical Location:** Anterior shoulder, spanning from the medial third of the clavicle (just lateral to the sternoclavicular joint) diagonally over the upper pectoralis major to the anterior midline of the humerus (at deltoid tuberosity level).
- **Orientation:** Oblique (superomedial to inferolateral,  $\sim 35^\circ$  from horizontal)
- **Primary Target Movement(s):** Shoulder Flexion, Shoulder Extension
- **Rationale:** Medial shift includes chest musculature, directly addressing flexion underestimation from previous design.

#### Sensor 2:

- **Anatomical Location:** Lateral shoulder, from the acromion process vertically down the midline of the lateral deltoid to the deltoid tuberosity.
- **Orientation:** Vertical (superior-inferior, parallel to humeral shaft)
- **Primary Target Movement(s):** Shoulder Abduction, Shoulder Adduction
- **Rationale:** Retained as-is, as expert feedback and metrics confirm optimal abduction tracking.

#### Sensor 3:

- **Anatomical Location:** Posterior shoulder, from the medial border of the scapular spine (2–3 cm medial to the acromion) obliquely down over the posterior deltoid to the posterior mid-humerus.
- **Orientation:** Oblique (superomedial to inferolateral,  $\sim 40^\circ$  from horizontal)
- **Primary Target Movement(s):** Shoulder Extension, Shoulder External Rotation
- **Rationale:** Shifted slightly more posterior to better capture posterior muscle activation, improving extension/external rotation fidelity.

#### Sensor 4:

- **Anatomical Location:** U-shaped path: from proximal medial upper arm (just below anterior axilla, near bicipital groove), curving under the axilla, terminating on the lateral lower rib cage (mid-axillary line,  $\sim 8\text{--}10$  cm below axilla).
- **Orientation:** Oblique/U-shaped (anterior-medial upper arm  $\rightarrow$  under axilla  $\rightarrow$  lateral lower ribs)
- **Primary Target Movement(s):** Shoulder Internal Rotation, Shoulder External Rotation, Horizontal Adduction, Horizontal Abduction
- **Rationale:** Repositioned for unique, non-redundant coverage of underarm and chest/rib movement, as per expert recommendation.

Fig. 61. LLM output for Designer C, Iteration 1 (Part 3).

**Machine-Readable Output**

```
{
  "design_id": "Shoulder_Iteration_Nplus1",
  "sensor_count": 4,
  "sensors": [
    {
      "id": 1,
      "anatomical_location": "Anterior shoulder, spanning from the medial third of the clavicle (just lateral to the sternoclavicular joint) diagonally over the upper pectoralis major to the anterior midline of the humerus at the level of the deltoid tuberosity.",
      "orientation": "Oblique (superomedial to inferolateral, -35° from horizontal)",
      "primary_targets": [
        "Shoulder Flexion",
        "Shoulder Extension"
      ],
      "coordinates_description": "Origin: medial third of clavicle (2-3 cm lateral to sternoclavicular joint); Path: diagonally over upper pectoralis major; Termination: anterior mid-humerus at deltoid tuberosity."
    },
    {
      "id": 2,
      "anatomical_location": "Lateral shoulder, from acromion process vertically down the midline of the lateral deltoid to the deltoid tuberosity.",
      "orientation": "Vertical (superior-inferior, parallel to humeral shaft)",
      "primary_targets": [
        "Shoulder Abduction",
        "Shoulder Adduction"
      ],
      "coordinates_description": "Origin: tip of acromion; Termination: deltoid tuberosity on lateral humerus (-10-12 cm below acromion)."
    },
    {
      "id": 3,
      "anatomical_location": "Posterior shoulder, from the medial border of the scapular spine (2-3 cm medial to acromion) obliquely down over the posterior deltoid to the posterior mid-humerus.",
      "orientation": "Oblique (superomedial to inferolateral, -40° from horizontal)",
      "primary_targets": [
        "Shoulder Extension",
        "Shoulder External Rotation"
      ],
      "coordinates_description": "Origin: medial border of scapular spine (2-3 cm medial to acromion); Path: over posterior deltoid; Termination: posterior mid-humerus."
    },
    {
      "id": 4,
      "anatomical_location": "U-shaped path: from proximal medial upper arm (just below anterior axilla, near bicipital groove), curving under the axilla, terminating on the lateral lower rib cage (mid-axillary line, -8-10 cm below axilla).",
      "orientation": "Oblique/U-shaped (anterior-medial upper arm → under axilla → lateral lower ribs)",
      "primary_targets": [
        "Shoulder Internal Rotation",
        "Shoulder External Rotation",
        "Horizontal Adduction",
        "Horizontal Abduction"
      ],
      "coordinates_description": "Origin: proximal medial upper arm (just below anterior axilla, near bicipital groove); Path: under axilla; Termination: lateral lower rib cage (mid-axillary line, -8-10 cm below axilla)."
    }
  ]
}
```

Fig. 62. LLM output for Designer C, Iteration 1 (Part 4).

Session Metadata

- Expert: expert\_C
- Iteration: 2
- Timestamp: 2025-12-04T18:00:44.078661
- Model: gpt-4.1-2025-04-14
- Cost: €0.0422

Engineering Analysis Report: Root Cause Analysis of Shoulder Sensor Topology (Iteration N+1)

**Project:** Advanced Wearable Motion-Tracking System  
**Subsystem:** Shoulder Joint Complex – SpectraFlex Flex Sensor Topology  
**Lead Sensor Layout Designer:** [Your Name]  
**Date:** [Today's Date]

1. Executive Summary

The current four-sensor design for the shoulder joint complex demonstrates improved balance in sensor importance and enhanced flexion tracking. However, the system's Mean Per-Joint Angular Error (MPJAE) remains suboptimal, with notable errors in flexion and residual issues in abduction and rotation. This report synthesizes quantitative performance metrics with expert anatomical feedback to identify the root causes of error and guide further design optimization.

2. Quantitative Metrics Analysis

2.1. Global Performance

Metric	Value
MPJAE	8.172°
AMPE	6.71%
RMSE	15.244°
PCC	0.8172
MAE_Std	12.868°
Max_Error	130.452°

Interpretation:

- The overall MPJAE is moderate; the system is functional but not precise enough for high-fidelity applications.
- The high Max\_Error and MAE\_Std indicate occasional large deviations, suggesting inconsistent tracking in certain postures or motions.

2.2. Per-Joint Breakdown

Motion	MPJAE (°)	AMPE (%)	RMSE (°)	PCC	ROM (°)
Flexion	11.730	5.01	21.163	0.8510	234.14
Abduction	6.665	10.69	10.684	0.8251	62.34
Rotation	6.121	4.44	11.624	0.7754	137.89

Interpretation:

- **Flexion:** Highest error (11.73°), with large RMSE, despite improved sensor importance balance.
- **Abduction/Rotation:** Lower errors but still above ideal thresholds for clinical/research-grade systems.

2.3. Sensor Importance

Sensor	Importance	Contribution (%)
S1	0.2679	26.79
S4	0.2602	26.02
S2	0.2459	24.59
S3	0.2259	22.59

Interpretation:

- Sensor importance is more balanced than previous iterations.
- S1 and S4 are most influential, but S3 lags in contribution.

Fig. 63. LLM output for Designer C, Iteration 2 (Part 1).

### 3. Human Expert Feedback Synthesis

#### Sensor 1 (S1) – Anterior Shoulder

- **Feedback:** Improved, but could be better if placed more on the chest and aligned with muscle direction (pectoralis major).
- **Implication:** Current path may not optimally capture the muscle deformation during flexion/extension, leading to residual error.

#### Sensor 2 (S2) – Lateral Shoulder

- **Feedback:** Good, but may benefit from extending coverage to include neck, shoulder, and arm junction.
- **Implication:** Current vertical path may miss complex scapulothoracic contributions during abduction.

#### Sensor 3 (S3) – Posterior Shoulder

- **Feedback:** Lower importance; suggest repositioning to better follow muscle direction and balance contact between back and arm, possibly including more of the shoulder area.
- **Implication:** Current placement may inadequately capture posterior deltoid and scapular movement, limiting rotation/extension accuracy.

#### Sensor 4 (S4) – Underarm/U-shaped

- **Feedback:** Importance is lowest; recommend optimizing path to better follow muscle direction under the arm, possibly increasing contact with chest/ribs and/or arm.
- **Implication:** Current path may not fully leverage the sensor's bending sensitivity for internal/external rotation and horizontal plane motions.

#### Global

- **Feedback:** Flexion tracking improved; sensor importance is now more balanced.

### 4. Root Cause Analysis

#### 4.1. Anatomical Coverage Gaps

##### • Muscle Direction Alignment:

Several sensors (notably S1 and S3) are not optimally aligned with the primary muscle fibers (pectoralis major, deltoid, and scapular muscles). This reduces sensitivity to the actual tissue deformation that correlates with joint angle changes, especially in complex compound movements.

##### • Scapulothoracic Articulation:

The shoulder complex involves significant scapular motion, especially in abduction and flexion. Current sensor placements do not adequately capture the scapula's contribution, particularly at the neck-shoulder-arm junction (S2) and posterior shoulder (S3).

#### 4.2. Sensor Path Limitations

##### • Linear vs. Curvilinear Paths:

Most sensors are placed in relatively straight lines. Human expert feedback consistently suggests following muscle paths, which are often curved, to better capture the true deformation patterns during motion.

##### • Underutilization of Sensor Length:

The 95mm sensor may not be fully utilized in some placements (e.g., S2, S3), limiting the spatial resolution and sensitivity.

#### 4.3. Insufficient Multi-Planar Coverage

##### • Flexion/Extension:

S1's current path, while improved, may not capture the full range of anterior shoulder deformation, especially at extreme ROM, leading to high flexion errors.

##### • Abduction:

S2's vertical orientation may miss contributions from the neck and upper trapezius, which are critical for accurate abduction tracking.

##### • Rotation:

S3 and S4's placements may not optimally register the complex twisting and sliding of tissues during internal/external rotation, especially if the sensors are not following the main muscle or fascial planes.

#### 4.4. Sensor Importance Imbalance

##### • S3 and S4 Underperformance:

Lower importance and contribution suggest these sensors are not optimally positioned to capture key biomechanical events, especially for extension and rotation.

#### 4.5. Artifacts and Fit Issues

##### • Attachment Artifacts:

If sensors are not well-conformed to the underlying anatomy, motion artifacts and slippage may occur, increasing error variance (evidenced by high Max\_Error and MAE\_Std).

Fig. 64. LLM output for Designer C, Iteration 2 (Part 2).

### 5. Summary Table: Root Causes

Issue	Evidence (Metrics/Feedback)	Likely Impact
S1 not fully aligned with muscle fibers	High flexion MPJAE; expert feedback	Flexion/extension error
S2 missing neck/shoulder junction	Abduction MPJAE; expert feedback	Abduction error
S3 not following muscle direction	Low importance; expert feedback	Extension/rotation error
S4 suboptimal U-shaped path	Lowest importance; expert feedback	Rotation/horizontal plane error
Sensors not following curvilinear paths	Expert feedback	All motions (reduced sensitivity)
Incomplete scapular coverage	Abduction/flexion errors	Underestimated joint ROM
Attachment artifacts	High Max_Error, MAE_Std	Inconsistent tracking

### 6. Conclusion

The current sensor topology shows meaningful progress but is limited by suboptimal anatomical alignment, insufficient multi-planar coverage, and underutilization of the sensor's bending-aware properties. The root causes are primarily:

- Incomplete alignment with muscle/tissue directions,
- Insufficient coverage of critical anatomical junctions (e.g., neck-shoulder-arm, scapula),
- Linear sensor paths that do not follow natural muscle curvature,
- Attachment and fit issues leading to artifacts.

### 7. Recommendations (For Next Iteration)

1. **Realign sensors to follow muscle fiber directions** (especially S1 and S3).
2. **Modify S2 to extend over the neck-shoulder-arm junction** to better capture scapular and clavicular motion.
3. **Reconfigure S3 and S4 to increase coverage of back, scapula, and chest/rib regions** using more curvilinear paths.
4. **Optimize sensor attachment and conformance** to minimize motion artifacts.
5. **Consider multi-planar sensor paths** to maximize sensitivity to complex shoulder kinematics.

Prepared by:

[Your Name]

Lead Sensor Layout Designer

### Part 2: Design Synthesis & Optimization (JSON Spec)

#### Design Overview

This iteration realigns all four SpectraFlex sensors to follow the primary muscle fiber directions and anatomical planes most responsible for shoulder flexion, abduction, and rotation. Sensor paths are now more curvilinear and anatomically conforming, increasing coverage of critical muscle groups and joint junctions. Placement is optimized for maximal bending response during target motions, improved scapular coverage, and minimized attachment artifacts. Each sensor is positioned to maximize its contribution to at least one key movement, as identified in the root cause analysis.

#### Sensor Layout Specification

##### Sensor 1:

- **Anatomical Location:** Anterior chest and shoulder, starting at the mid-clavicular line (just below the clavicle, ~3cm lateral to the sternoclavicular joint), curving inferolaterally over the bulk of the pectoralis major muscle belly, and terminating at the anterior mid-humerus (deltoid tuberosity region).
- **Orientation:** Oblique-curvilinear (following pectoralis major fibers, ~30–40° from horizontal).
- **Primary Target Movement(s):** Shoulder Flexion, Shoulder Extension.
- **Rationale:** Addresses prior insufficient alignment with muscle fibers and increases sensitivity to anterior tissue deformation during flexion/extension.

##### Sensor 2:

- **Anatomical Location:** Lateral shoulder, originating at the base of the neck (lateral aspect of the upper trapezius, adjacent to the acromioclavicular joint), descending vertically over the acromion and lateral deltoid, terminating at the mid-lateral humerus (deltoid tuberosity).
- **Orientation:** Vertical, slightly anterior-leaning (to capture both deltoid and trapezius deformation).
- **Primary Target Movement(s):** Shoulder Abduction, Shoulder Adduction.
- **Rationale:** Extends coverage to the neck-shoulder-arm junction, improving detection of scapulothoracic and deltoid motion during abduction.

Fig. 65. LLM output for Designer C, Iteration 2 (Part 3).

**Sensor 3:**

- **Anatomical Location:** Posterior shoulder and upper back, beginning at the medial border of the scapular spine (~2cm medial to the acromion), curving inferolaterally along the posterior deltoid and over the infraspinatus, terminating at the posterior-lateral mid-humerus.
- **Orientation:** Oblique-curvilinear (following posterior deltoid/infraspinatus fibers, ~35–45° from horizontal).
- **Primary Target Movement(s):** Shoulder Extension, Shoulder External Rotation.
- **Rationale:** Follows muscle direction and increases contact with both scapular and humeral regions, addressing prior underperformance in extension/rotation.

**Sensor 4:**

- **Anatomical Location:** U-shaped path: starting at the proximal medial upper arm (just below the anterior axilla near the bicipital groove), curving under the axilla, then sweeping laterally and superiorly to terminate on the mid-axillary line of the lower rib cage (~8–10cm below the axilla), ensuring the path closely follows the anterior border of the latissimus dorsi and serratus anterior.
- **Orientation:** Oblique/U-shaped (anterior-medial upper arm → under axilla → lateral lower ribs).
- **Primary Target Movement(s):** Shoulder Internal Rotation, Shoulder External Rotation, Horizontal Adduction, Horizontal Abduction.
- **Rationale:** Optimized to follow muscle direction under the arm, increasing contact with both chest/rib and upper arm regions, enhancing sensitivity to rotation and horizontal plane movements.

Fig. 66. LLM output for Designer C, Iteration 2 (Part 4).

**Machine-Readable Output**

```

{
  "design_id": "Shoulder_Iteration_Nplus2",
  "sensor_count": 4,
  "sensors": [
    {
      "id": 1,
      "anatomical_location": "Anterior chest and shoulder, starting at the mid-clavicular line (just below the clavicle, ~3cm lateral to the sternoclavicular joint), curving inferolaterally over the pectoralis major muscle belly, terminating at the anterior mid-humerus (deltoid tuberosity region).",
      "orientation": "Oblique-curvilinear (~30-40° from horizontal, following pectoralis major fibers)",
      "primary_targets": [
        "Shoulder Flexion",
        "Shoulder Extension"
      ],
      "coordinates_description": "Origin: mid-clavicular line (~3cm lateral to sternoclavicular joint, just below clavicle); Path: curving inferolaterally over pectoralis major; Termination: anterior mid-humerus at deltoid tuberosity."
    },
    {
      "id": 2,
      "anatomical_location": "Lateral shoulder, from the base of the neck (lateral upper trapezius, adjacent to acromioclavicular joint), vertically over acromion and lateral deltoid, terminating at mid-lateral humerus (deltoid tuberosity).",
      "orientation": "Vertical, slightly anterior-leaning",
      "primary_targets": [
        "Shoulder Abduction",
        "Shoulder Adduction"
      ],
      "coordinates_description": "Origin: base of neck (lateral upper trapezius, adjacent to acromioclavicular joint); Path: vertically over acromion and lateral deltoid; Termination: mid-lateral humerus at deltoid tuberosity."
    },
    {
      "id": 3,
      "anatomical_location": "Posterior shoulder and upper back, from medial border of scapular spine (~2cm medial to acromion), curving inferolaterally along posterior deltoid and infraspinatus, terminating at posterior-lateral mid-humerus.",
      "orientation": "Oblique-curvilinear (~35-45° from horizontal, following posterior deltoid/infraspinatus fibers)",
      "primary_targets": [
        "Shoulder Extension",
        "Shoulder External Rotation"
      ],
      "coordinates_description": "Origin: medial border of scapular spine (~2cm medial to acromion); Path: curving inferolaterally along posterior deltoid and infraspinatus; Termination: posterior-lateral mid-humerus."
    },
    {
      "id": 4,
      "anatomical_location": "U-shaped path: starting at proximal medial upper arm (just below anterior axilla, near bicipital groove), curving under axilla, then laterally and superiorly to mid-axillary line of lower rib cage (~8-10cm below axilla), following anterior border of latissimus dorsi and serratus anterior.",
      "orientation": "Oblique/U-shaped (anterior-medial upper arm → under axilla → lateral lower ribs)",
      "primary_targets": [
        "Shoulder Internal Rotation",
        "Shoulder External Rotation",
        "Horizontal Adduction",
        "Horizontal Abduction"
      ],
      "coordinates_description": "Origin: proximal medial upper arm (just below anterior axilla, near bicipital groove); Path: under axilla, curving laterally and superiorly; Termination: mid-axillary line of lower rib cage (~8-10cm below axilla)."
    }
  ]
}

```

Fig. 67. LLM output for Designer C, Iteration 2 (Part 5).

Received 20 February 2007; revised 12 March 2009; accepted 5 June 2009